

**Layered Traffic Engineering for Effective and Adaptive
Wavelength-Routed Optical Networks**

Yuki Koizumi

**Graduate School of Information Science and Technology
Osaka University**

January 2009

List of Publications

Journal Papers

1. Y. Koizumi, S. Arakawa, and M. Murata, “An integrated routing mechanism for cross-layer traffic engineering in IP over WDM networks,” *IEICE Transactions on Communications*, vol. E90-B, pp. 1142–1151, May 2007.
2. Y. Koizumi, T. Miyamura, S. Arakawa, E. Oki, K. Shiimoto, and M. Murata, “Stability of virtual network topology control for overlay routing services,” *OSA Journal of Optical Networking*, vol. 7, pp. 704–719, July 2008.
3. Y. Koizumi, T. Miyamura, S. Arakawa, E. Oki, K. Shiimoto, and M. Murata, “Adaptive virtual network topology control based on attractor selection,” re-submitted to *IEEE/OSA Journal of Lightwave Technology*, 2008.

Refereed Conference Papers

1. Y. Koizumi, S. Arakawa, and M. Murata, “On the integration of IP routing and wavelength routing in IP over WDM networks,” in *Proceedings of SPIE Asia-Pacific Optical Communications (APOC 2005) Network Architectures, Management, and Applications III*, (Shanghai, China), vol. 6022, 602205, Nov. 2005.
2. Y. Koizumi, T. Miyamura, S. Arakawa, E. Oki, K. Shiimoto, and M. Murata, “On the stability of virtual network topology control for overlay routing services,” in *Proceedings of IEEE Fourth International Conference on Broadband Communications, Networks, and Systems (IEEE Broadnets 2007)*, (Raleigh, NC, USA), pp. 810–819, Sept. 2007.

3. Y. Koizumi, T. Miyamura, S. Arakawa, E. Oki, K. Shiimoto, and M. Murata, "Application of attractor selection to adaptive virtual network topology control," in *Proceedings of ACM 3rd International Conference on Bio-Inspired Models of Network, Information, and Computing Systems (BIONETICS 2008)*, (Hyogo, Japan), Nov. 2008.
4. Y. Koizumi, T. Miyamura, S. Arakawa, E. Oki, K. Shiimoto, and M. Murata, "Robust virtual network topology control based on attractor selection," submitted to *13th Conference on Optical Network Design and Modeling (ONDM 2009)*, (Braunschweig, Germany), Feb. 2009.

Non-Refereed Technical Papers

1. Y. Koizumi, S. Arakawa, and M. Murata, "On the integration of IP routing and wavelength routing in IP over WDM networks," *Technical Report of IEICE (PN2005-24)*, vol. 105, pp. 25–30, Aug. 2005. (*in Japanese*).
2. Y. Koizumi, T. Miyamura, S. Arakawa, E. Oki, K. Shiimoto, and M. Murata, "On the stability of virtual network topology control for overlay routing services," *Technical Report of IEICE (PN2007-27)*, vol. 107, pp. 33–38, Oct. 2007.
3. N. Tsutsui, Y. Koizumi, S. Arakawa, and M. Murata, "Implementation and evaluation of integrated routing mechanism in IP over WDM networks," *Technical Report of IEICE (PN2007-80)*, vol. 107, pp. 35–40, Mar. 2008. (*in Japanese*).
4. Y. Koizumi, T. Miyamura, S. Arakawa, E. Oki, K. Shiimoto, and M. Murata, "Adaptive virtual network topology control based on attractor selection," *Technical Report of IEICE (PN2008-14)*, vol. 108, pp. 1–6, Aug. 2008.

Preface

The volume of Internet traffic has been increasing rapidly due to the growth of the population of Internet users, the popularization of high-speed access networks like Fiber To The Home, and the emergence of various application layer technologies such as peer-to-peer networks, voice over IP, video on demand, and grid computing. *Wavelength Division Multiplexing* (WDM) is the technology that carries multiple optical signals on a single fiber, and thus it is expected as a way to accommodate increasing Internet traffic. Although the WDM technology resolves the shortage of the fiber capacity, nodes connected to WDM capable fibers will still become bottlenecks because those nodes must convert received signals between the optical and the electronic format and process the signals at the speed of light. Therefore, WDM based networks are extended to *wavelength-routed networks* by installing optical cross connects, which switches optical signals within the optical domain. In such wavelength-routed networks, nodes are connected with dedicated virtual circuits called *lightpaths*. By configuring lightpaths, a *virtual network topology* (VNT) is constructed on a wavelength-routed network.

To fully utilize the large capacity offered by wavelength-routed networks, it is important to develop approaches to traffic engineering. Without traffic engineering, several links will be heavily congested while others will be underutilized. The main objective of traffic engineering in wavelength-routed networks, which we call *layered traffic engineering*, is to realize effective transportation of traffic over optical networks and efficient utilization of resources in optical networks. This objective can be achieved by appropriately designing a VNT, according to characteristics of the upper layer's traffic with considering the efficient utilization of resources in optical networks.

It is an essential objective of layered traffic engineering to accommodate traffic effectively on wavelength-routed networks. In this thesis, first, we focus on IP traffic, which is the majority of Internet traffic. To accommodate IP traffic effectively, layered traffic engineering needs to configure

a VNT on the basis of statistics of IP traffic, e.g., traffic demand matrices. However, lightpaths provided by wavelength-routed networks may not be fully utilized by IP networks even if layered traffic engineering constructs VNTs according to statistics of IP traffic. This is because the IP network and the wavelength-routed network have their own routing mechanism. Routes for forwarding IP traffic is decided by the IP routing mechanism, and thus the IP network does not always utilize lightpaths established in the wavelength-routed network. This results in the inefficient utilization of resources in the wavelength-routed networks. Hence, we propose an integrated routing mechanism for IP and wavelength-routed networks. The key idea is to first prepare a set of *virtual-links* representing the lightpaths that can be established by the WDM network, then calculate the minimum cost route on an IP network including those links. Through simulations, we show that in the case that traffic patterns do not change, the throughput of our method is almost the same as that of a VNT optimally designed for a given traffic demand. In the case that traffic patterns change, the throughput of our method is about 50% higher than that of the VNTs generated by existing heuristic approaches.

However, for achieving effective wavelength-routed networks, it is insufficient only to accommodate IP traffic effectively. Recently, a variety of emerging application layer technologies appears, and thus various traffic as well as legacy IP traffic, such as web and e-mail, flows on Internet. Among those new applications, overlay networks have received much attention as a way to achieve new functionality and enhance network performance over existing network infrastructures. One of the key technologies in overlay networks lies in overlay routing. The fundamental idea of overlay routing is to construct a logical network above the IP network and to allow routing to be controlled on that logical topology. Although overlay routing can enhance performance and resilience, it has ill effects on layered traffic engineering as discussed in many papers. Since layered traffic engineering and overlay routing make their routing decision independently on the basis of different routing objectives, interactions between layered traffic engineering and overlay routing occur. The interactions result in degradations of the performance and significant instability of layered traffic engineering. Therefore, we propose *hysteresis* based layered traffic engineering approaches to enhance the stability of layered traffic engineering. Our approaches enhance the stability by reducing reconfigurations of VNTs that make only small improvements in the performance of layered traffic engineering. Through simulations, we show that our methods improve the stability of layered traffic engineering and decrease the average maximum link utilization by about 25% compared to existing layered traffic engineering approaches.

The interaction between layered traffic engineering and overlay routing brings out not only difficulties in the effective accommodation of traffic on wavelength-routed networks but also the large fluctuations in the network environments such as traffic demand and link load. Hence, adaptability against changes in environments becomes a more important issue to achieve effective wavelength-routed networks. To realize a layered traffic engineering that is adaptive to various changes in environments, we focus on *attractor selection*, which models behaviors where living organisms adapt to unknown changes in their surrounding environments and recover their conditions. An attractor selection model uses stochastic behavior for adapting to changes in environments. Therefore, they do not guarantee optimal performance but do have capabilities for adapting to unexpected changes in environments. By appropriately incorporating the essential idea of the attractor selection model, we achieve adaptability of VNT control with achieving at least the same level of the efficiency as the existing heuristic approaches. Through simulations, we show that our method adapts to at most twice larger changes in traffic demand than existing heuristic approaches. We also show that our method can adapt to environmental changes caused by link failures in addition to changes in traffic demand.

In this thesis, we achieve above-mentioned issues, effectiveness in traffic transportation and adaptability against changes in environments, and realize effective and adaptive wavelength-routed networks.

Acknowledgments

First and foremost, I would like to express my heartfelt gratitude to Professor Masayuki Murata of Graduate School of Information Science and Technology, Osaka University for introducing me to the area of optical networking. His creative suggestions, insightful comments, and patient encouragement have been essential for my research activity. I also thank him for providing me with the opportunity to research with a talented team of researchers.

I am heartily grateful to the members of my thesis committee, Professor Koso Murakami, Professor Makoto Imase, and Professor Teruo Higashino of Graduate School of Information Science and Technology, Osaka University, and Professor Hiroataka Nakano of Cyber Media Center, Osaka University, for reviewing my dissertation and providing many valuable comments.

I am also deeply grateful to Assistant Professor Shin'ichi Arakawa of Graduate School of Information Science and Technology, Osaka University for his much appreciated comments and support. His kindness on my behalf were invaluable, and I am forever in debt.

I would like to thank Associate Professor Naoki Wakamiya, Associate Professor Go Hasegawa, and Specially Appointed Associate Professor Kenji Leibnitz of Osaka University for enlightening discussions. Their critical comments and unerring guidance are always informative and helpful.

I would also like to thank Associate Professor Eiji Oki of the University of Electro-Communications, Dr. Kohei Shiimoto and Mr. Takashi Miyamura of NTT Corporation, for their useful suggestions and fruitful discussion.

I am thankful to all the members of Advanced Network Architecture Laboratory in Graduate School of Information Science and Technology, Osaka University, for their inciting discussions and fellowship.

Last, but not least, I thank my parents for their invaluable support and constant encouragement during my doctoral studies.

Contents

List of Publications	i
Preface	iii
Acknowledgments	vii
1 Introduction	1
1.1 Background	1
1.2 Issues for Layered Traffic Engineering in Wavelength-Routed Optical Networks . .	4
1.2.1 Effectiveness in IP Traffic Transportation	5
1.2.2 Stability against Emerging Application Layer Technologies	6
1.2.3 Adaptability against Environmental Changes	8
1.3 Outline of Thesis	9
2 Integrated Routing for Effective Transport of IP Traffic over Wavelength-Routed Optical Networks	15
2.1 Routing in IP over Wavelength-Routed Optical Networks	16
2.1.1 Overlay Model	16
2.1.2 Peer Model	17
2.2 Integrated Routing for Layered Traffic Engineering	18
2.2.1 Network model	18
2.2.2 Virtual-Links	19
2.2.3 Topology Database	19
2.2.4 Route Selection	21

2.2.5	Cost Assignment to Virtual-Links	22
2.3	Flow-Level Simulation of Packets in Wavelength-Routed Networks	23
2.3.1	Difficulties in Packet-Level Simulations	23
2.3.2	Flow-Level Simulation Method	24
2.3.3	Verification of Flow-Level Simulation Method	26
2.4	Performance Evaluation	27
2.4.1	Simulation Conditions	28
2.4.2	Average End-to-End Delay	30
2.4.3	Load on Nodes	30
2.4.4	Network Throughput	34
2.5	Summary	37

3 Hysteresis Based Layered Traffic Engineering for Stable Accommodation of Overlay

	Routing Services	39
3.1	Interaction between Layered Traffic Engineering and Overlay Routing	40
3.1.1	Network Model	40
3.1.2	Overlay Routing	42
3.1.3	Layered Traffic Engineering	42
3.1.4	Model for Interaction between Layered Traffic Engineering and Overlay Routing	43
3.1.5	Simulation Conditions	44
3.1.6	Degradation of Underlay Network Performance	45
3.1.7	Instability of Underlay Network State	47
3.2	Improving Stability of Network State	49
3.2.1	Hysteresis	49
3.2.2	Performance Evaluation	52
3.3	Improving Network Performance	59
3.3.1	Two-State Utilization Hysteresis	59
3.3.2	Performance Evaluation	59
3.4	Enhancing Adaptability to Fluctuations in Traffic Demand	61
3.4.1	Filtering	61

3.4.2	Performance Evaluation	63
3.5	Summary	65
4	Adaptive Layered Traffic Engineering against Changes in Environments	67
4.1	Attractor Selection	68
4.1.1	Concept of Attractor Selection	68
4.1.2	Cell Model	68
4.1.3	Mathematical Model of Attractor Selection	70
4.2	Layered Traffic Engineering Based on Attractor Selection	72
4.2.1	Network Model	72
4.2.2	Overview of Layered Traffic Engineering Based on Attractor Selection	72
4.2.3	Dynamics of VNT Control	75
4.2.4	Regulatory Matrix	77
4.2.5	Activity	79
4.2.6	Virtual Network Topology Construction	80
4.3	Performance Evaluation	81
4.3.1	Simulation Conditions	81
4.3.2	Behaviors of Layered Traffic Engineering Based on Attractor Selection	82
4.3.3	Adaptability to Changes in Traffic Demand	86
4.3.4	Adaptability to Link Failures	88
4.4	Summary	89
5	Conclusion and Future Work	93
	Bibliography	97

List of Figures

1.1	Wavelength division multiplexing technology	2
1.2	An architecture of a wavelength-routing capable node	3
1.3	Wavelength-routed network (physical topology)	4
1.4	Wavelength-routed network (logical topology)	5
2.1	An example showing that IP routing does not always select the links provided by the WDM network	17
2.2	Node architecture	20
2.3	A network example with virtual-links	21
2.4	Congestion resulting from activating a virtual-link	23
2.5	Calculation of the number of packets at a node	25
2.6	The average end-to-end delay of flow-level and packet-level simulations	27
2.7	NSFNET topology	29
2.8	European Optical Network topology	29
2.9	Average end-to-end delay: NSFNET topology, the case of realistic traffic demand matrix	31
2.10	Average end-to-end delay: NSFNET topology, the case of random traffic demand matrix	32
2.11	Average end-to-end delay: EON topology, the case of random traffic demand matrix	33
2.12	Average load on each node	35
2.13	Classified load on nodes without traffic change: the integrated routing method . . .	36
2.14	Network throughput	36

3.1	Example of network consisting of three layers: optical, packet, and overlay	41
3.2	Interaction between layered traffic engineering and overlay routing	44
3.3	European Optical Network topology	45
3.4	Maximum link utilization	46
3.5	Fluctuation of maximum link utilization ($\alpha = 0.2$, total traffic: 10)	48
3.6	Traffic volume on each link ($\alpha = 0.2$, total traffic: 10)	49
3.7	Fluctuation of traffic demand ($\alpha = 0.2$, total traffic: 10)	50
3.8	Fluctuation of maximum link utilization (Utilization hysteresis, $\alpha = 0.2$, total traffic: 10)	53
3.9	Fluctuation of maximum link utilization (Demand hysteresis, $\alpha = 0.2$, total traffic: 10)	54
3.10	Number of changed lightpaths (Utilization hysteresis, $\alpha = 0.2$, total traffic: 10)	55
3.11	Number of changed lightpaths (Demand hysteresis, $\alpha = 0.2$, total traffic: 10)	56
3.12	Fluctuation of maximum link utilization (Utilization hysteresis, $\alpha = 0.3$, total traffic: 10)	57
3.13	Fluctuation of maximum link utilization (Demand hysteresis, $\alpha = 0.3$, total traffic: 10)	58
3.14	Fluctuation of maximum link utilization (Two-state utilization hysteresis, $\alpha = 0.3$, total traffic: 10, $k = 3.0$)	60
3.15	Fluctuation of maximum link utilization (Two-state utilization hysteresis, $\alpha = 0.3$, total traffic: 10, $k = 5.0$)	61
3.16	Number of lightpaths ($\alpha = 0.3$, total traffic: 10, $k = 5.0$)	62
3.17	Fluctuation of maximum link utilization (Two-state utilization hysteresis, filtering, $\alpha = 0.3$, total traffic: 10, $k = 5.0$)	64
3.18	Fluctuation of maximum link utilization (Two-state utilization hysteresis, filtering, $\alpha = 0.2$, total traffic: 10, $k = 3.0$)	65
3.19	Fluctuation of maximum link utilization (Two-state utilization hysteresis, filtering, $\alpha = 0.2$, total traffic: 10, $k = 5.0$)	66
4.1	Gene regulatory and metabolic reaction networks	69
4.2	Interpretation of attractor selection into layered traffic engineering	73

4.3	Control loop for layered traffic engineering based on attractor selection	74
4.4	Sigmoid function	76
4.5	Mapping $y_{p_{ij}}$ to $\theta_{p_{ij}}$	77
4.6	A sample curve of activity	80
4.7	European Optical Network topology	82
4.8	Maximum link utilization	83
4.9	Control values	84
4.10	Activity	85
4.11	Ratio of number of changed lightpaths to total number of lightpaths	85
4.12	Adaptability of layered traffic engineering methods against changes in traffic demand	87
4.13	Recovery ratio of first VNT reconfiguration over variance in traffic demand	89
4.14	Recovery ratio over number of VNT reconfigurations with variance in traffic de- mand of 1.5	90
4.15	Robustness against changes in traffic demand and link failures	90

Chapter 1

Introduction

1.1 Background

The volume of Internet traffic has been increasing rapidly due to the growth of the population of Internet users, the popularization of high-speed access networks like Fiber To The Home (FTTH), and the emergence of various applications and services, such as peer-to-peer (P2P) networks, voice over IP, video on demand, and grid computing [1–3]. The capacity of Internet is being exhausted, and therefore, backbone networks have to enhance their capacity to accommodate the increasing Internet traffic. *Wavelength division multiplexing* (WDM) technology, which carries multiple optical signals on a single fiber as shown in Figure 1.1, is expected to accommodate the bulk of traffic over the current and future Internet [4–6].

To transport Internet traffic, which is mainly processed in an electronic format, over an optical network, electronic signals have to be converted to optical signals. Transmitters of optical signals convert electronic data streams into the optical format and send them on fibers while receivers convert optical signal into the electronic format and pass them to electronic routers or switches. In the case that traffic is transmitted along multi-hop paths, optical-electronic (O-E) and electronic-optical (E-O) conversions are required at every intermediate node, and therefore, the high-speed links provided by the optical transmission technology cannot be fully utilized. To reduce O-E and E-O conversions at intermediate nodes and prevent those nodes from being bottlenecks, optical cross connects (OXC) are installed to each node. An OXC is an optical device that switches optical signals without any O-E/E-O conversions. This capability of switching optical signals within the

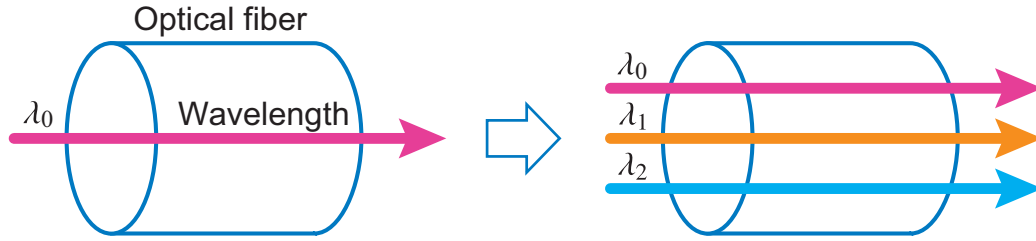


Figure 1.1: Wavelength division multiplexing technology

optical domain is called *wavelength-routing* and optical networks that consist of optical fibers and OXCs are called *wavelength-routed networks* [4–6]. We illustrate an example of a wavelength-routing capable node in Figure 1.2. At the optical de-multiplexer, multiplexed optical signals from input fibers are de-multiplexed into two wavelengths, λ_0 and λ_1 . All the input signals are passed into the OXC and the OXC redirects those optical signals. The optical signal λ_0 from the input fiber 0 is passed to the electronic router via the optical receiver. The other signals are redirected without any O-E/E-O conversions. Those signals are again multiplexed into one signal at the optical multiplexer and transmitted on the output fibers. By reducing O-E/E-O conversions, wavelength-routed networks provide efficient transportation of traffic over optical networks.

In such wavelength-routed networks, a set of optical transport channels, which are called *lightpaths*, are established between nodes via OXCs. Since there is no electric processing of traffic at intermediate nodes that lightpaths pass through, two edge nodes of a lightpath seem to be directly connected from the upper layer’s view. Therefore, by establishing lightpaths in a wavelength-routed network, a set of those lightpaths forms a logical topology on top of the physical topology, which consists of optical fibers and OXCs [7–9]. We call this logical topology as *virtual network topology* (VNT) in this thesis. The upper layer uses a VNT as its network infrastructure and transports its traffic on the VNT. Figure 1.3 illustrates a wavelength-routed network that consists of five OXCs and four optical fibers. Each OXC is connected with an electronic router R_i ($1 \leq i \leq 5$). The arrows in the figure are lightpaths of wavelengths of λ_1 and λ_2 . The lightpaths of λ_1 are single hop while the lightpaths of λ_2 pass a few hops. In this situation, the electronic routers’ layer is expressed as in Figure 1.4. Node pairs that are not adjacent in the physical topology, (R_1, R_3) and (R_4, R_5) , have direct connections whose entities are lightpaths of λ_2 .

In order to fully utilize the capacity provided by optical networks, it is an important issue to develop approaches to traffic engineering. Without traffic engineering, several links will be

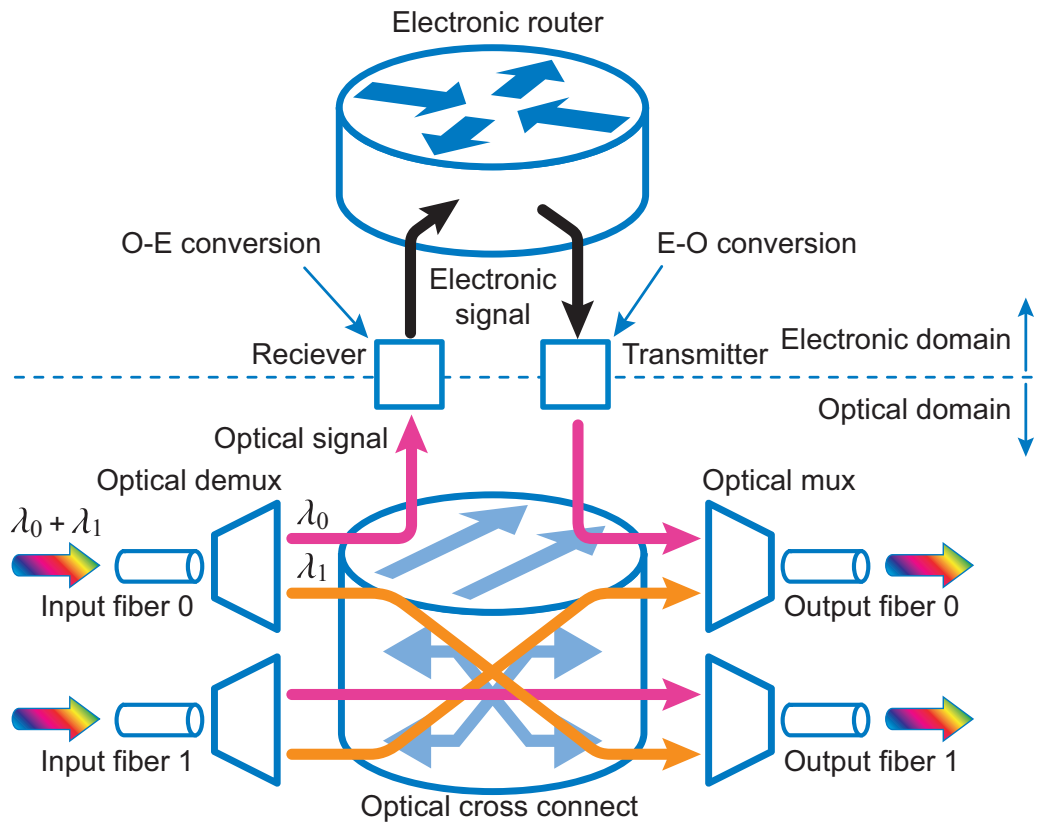


Figure 1.2: An architecture of a wavelength-routing capable node

heavily congested while others will be underutilized. The main objective of traffic engineering in wavelength-routed networks is to realize effective transportation of traffic over optical networks and efficient utilization of resources in optical networks. This objective can be achieved by appropriately deciding where to establish lightpaths, i.e., designing a proper VNT, according to characteristics of the upper layer's traffic with considering the efficient utilization of resources in optical networks [7–9]. Since traffic engineering in wavelength-routed optical networks has to consider characteristics of both optical and upper layers, we refer to traffic engineering in wavelength-routed optical networks as *layered traffic engineering* in this thesis. The following section describes the issues to be solved for achieving useful layered traffic engineering in wavelength-routed optical networks.

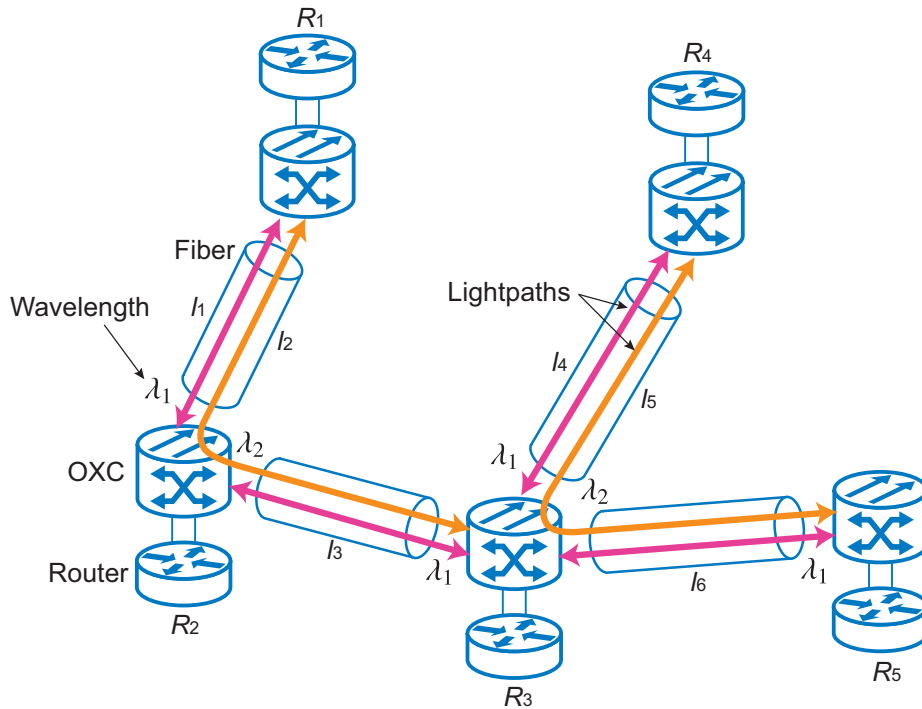


Figure 1.3: Wavelength-routed network (physical topology)

1.2 Issues for Layered Traffic Engineering in Wavelength-Routed Optical Networks

With the growth of Internet, layered traffic engineering in wavelength-routed optical networks has been faced to a lot of issues. In this section, we show the issues to be solved for realizing useful layered traffic engineering in wavelength-routed optical networks. First, we focus on effectiveness in transporting IP traffic, which is the majority of Internet traffic, on wavelength-routed networks. However, recently, various application layer services emerge and they cause difficulties in effective accommodation of traffic on wavelength-routed networks. Thus, we need to tackle their harmful behavior to layered traffic engineering. Furthermore, those applications bring out not only the difficulties in transporting traffic but also large fluctuations in network environments. Hence, we discuss the other important issue, adaptability to changes in environments, to be addressed for realizing a feasible wavelength-routed optical network as the current and future Internet backbone networks.

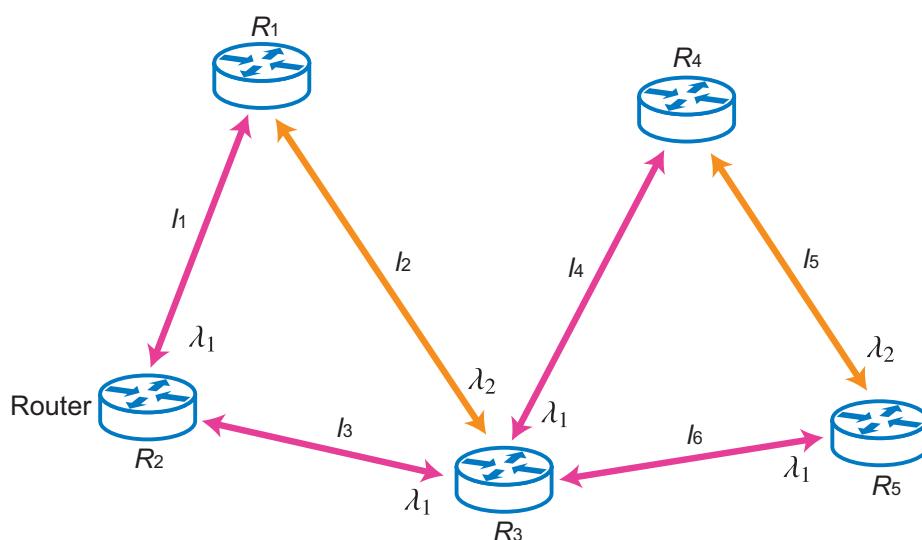


Figure 1.4: Wavelength-routed network (logical topology)

1.2.1 Effectiveness in IP Traffic Transportation

It is an essential objective for traffic engineering to accommodate traffic effectively. In layered traffic engineering, it is necessary to construct appropriate VNTs in consideration of characteristics of both upper layer's traffic and a WDM transmission technology. Since the majority of Internet traffic is IP, much research has been devoted to methods of carrying IP traffic on wavelength-routed networks (we call such networks IP over wavelength-routed networks hereafter) [10–21]. To accommodate IP traffic effectively on wavelength-routed networks, layered traffic engineering needs to configure a VNT based on statistics of IP traffic, e.g., traffic demand matrices. Given the traffic demand, an optimal VNT can be obtained by solving a mixed integer linear programming (MILP). Some heuristic design methods can also configure nearly optimal topologies [8,9].

To configure VNTs according to statistics of IP traffic, a method is needed to obtain current network information such as link utilization. There are three different inter-networking models for IP over wavelength-routed networks; peer, augmented, and overlay models [13]. One of the most important differences between these models is the type of information shared between the IP network and the wavelength-routed network. In the peer model, the network topology and all other information. That is, both layers share routing information and link state, and a unified routing mechanism controls the whole network, i.e., both IP and wavelength-routed networks. In contrast

with the peer model, in the overlay model, no network information is shared between the IP and wavelength-routed networks. The wavelength-routed network and IP network each have their own control planes, that is, the routing protocols, topology information, and signaling protocols in the IP network are independent of those in the wavelength-routed network. The augmented model is a hybrid of the peer and overlay models. Some agreed-upon information such as reachability is shared between the two networks, but the two networks are managed independently as in the overlay model.

The peer model excels at efficient route control, since all network information is available. However, collecting this information requires the advertisement of the information of both the IP and optical layers. This solution leads to an excessive update overhead, and therefore lacks scalability. In contrast, only the information of each layer needs to be advertised in the overlay model. This model thus scales well compared to the peer model, but has difficulty in routing traffic efficiently since available information on the network status is limited. Moreover, in the overlay model, lightpaths provided by wavelength-routed networks may not be fully utilized by IP networks even if layered traffic engineering constructs VNTs on the basis of statistics of IP traffic. This is because the IP network and the wavelength-routed network each has its own routing mechanism. Routes for forwarding IP traffic is decided by the IP routing mechanism, and thus the IP network does not always utilize lightpaths established in the wavelength-routed network. This results in the inefficient utilization of resources in the wavelength-routed networks. Hence, layered traffic engineering must consider the behavior of the IP routing mechanism in addition to the statistics of IP traffic to achieve effective transportation of IP traffic on wavelength-routed networks.

However, it is insufficient for achieving effective wavelength-routed networks only to accommodate IP traffic effectively. This is because a variety of emerging application layer technologies recently appears, and thus various traffic as well as legacy IP traffic, such as web and e-mail, flows on Internet. In the next section, we discuss those applications and their ill behavior to layered traffic engineering.

1.2.2 Stability against Emerging Application Layer Technologies

A variety of emerging application layer technologies recently appears, and thus various traffic in addition to legacy IP traffic flows on Internet. In especial, overlay networks, such as P2P networks and content distribution networks (CDNs), have recently received much attention as a way to achieve

new functionality and enhance network performance over existing network infrastructures. One of the key technologies in overlay networks lies in overlay routing [22, 23]. The fundamental idea of overlay routing is to construct a logical network above the IP network and to allow routing to be controlled on that logical topology. In the literature, a virtual network topology provided by a set of lightpaths is sometimes called “logical topology”. In this thesis, we use the term “logical topology” in the context of an overlay’s logical topology, and we use the term “VNT” for virtual network topology provided by lightpaths. Each overlay node measures the status, such as throughput and delay, of the underlying network and determines the appropriate route to destination nodes on the overlay network to improve performance and resilience. The resilient overlay network (RON) architecture was proposed in [22]. The RON provides fast detection and recovery from network failures and performance degradation using the existing Internet infrastructure as the underlay network. Another architecture is Detour [23]. It is revealed in [23] that a large percentage of flows can locate better alternative routes by relaying among overlay nodes, which improves the performance of those flows.

As the amount of traffic generated by overlay networks increases, the dynamics of overlay routing have significant impact on traffic engineering [24–26]. One typical type of impact is the selfish behavior of overlay routing, as discussed in [25]. Since overlay nodes independently select their route in a selfish manner to optimize their own performance, system-wide performance may not be optimized [27]. In [25], the authors revealed that interaction between overlay routing and packet layer traffic engineering causes degradation in the performance of packet layer traffic engineering. They argue that the main reason for this degradation is a conflict between two different routing objectives performed at each layer. The impact of selfish routing in intra-domain networks was also investigated in [28]. According to [28], selfish routing can achieve almost optimal performance if an underlay network performs static routing. However, if packet layer traffic engineering is used, the performance of the packet layer traffic engineering is degraded due to the interaction between overlay routing and packet layer traffic engineering. Furthermore, interaction of multiple overlay routing mechanisms also causes fluctuations in network state in the same way as the interaction between traffic engineering and overlay routing [29–31]. The authors revealed in [29] that coexisting multiple overlay networks result in fluctuations in both route select and network load. They also argued that these fluctuations occur across a wide range of parameter settings of the overlay networks, and thus the ill effects of the fluctuations should not be ignored. These papers show that the

performance of packet layer traffic engineering is degraded in terms of maximum link utilization, network cost, and average latency. Since many layered traffic engineering approaches configure VNTs on the basis of traffic demand, fluctuations in traffic demand induced by overlay routing are much more severe for layered traffic engineering.

Therefore, it is an important issue to realize a layered traffic engineering approach that can effectively accommodate traffic due to emerging application layer technologies such as overlay networks in addition to existing IP traffic. Among those applications, the selfish behavior of overlay routing is one of the most problematic issues for traffic engineering as it has been revealed in many papers [25,26]. In this thesis, we focus on overlay routing as one of those applications and propose a layered traffic engineering approach to accommodate traffic due to overlay routing stably.

However, the interaction between traffic engineering and overlay routing brings out not only difficulties in the effective accommodation of traffic on wavelength-routed networks but also the large fluctuations in the network environments. The following section describes another issues to be solved, i.e., adaptability against changes in environments, for achieving a feasible wavelength-routed network for current and future Internet backbone networks.

1.2.3 Adaptability against Environmental Changes

New application layer services such as P2P networks have emerged and these applications cause large fluctuations in network environments. As described above, for instance, the hugely fluctuating traffic demand caused by interactions between overlay networks and existing traffic engineering mechanisms has been revealed [25]. Therefore, it is important to achieve a layered traffic engineering approach that is adaptive to changes in network environments.

The approaches to efficiently accommodating changing traffic demand on VNTs can basically be classified into offline and on-line approaches. In offline approaches, VNTs are statically constructed to efficiently accommodate one or multiple traffic demand matrices [10, 12, 32]. These approaches mainly assume that these traffic demand matrices will be available before the VNT is constructed or assume that changes in the traffic demand matrices can be predicted. However, it is obvious that offline approaches cannot efficiently handle unexpected changes in traffic demand since VNTs are configured for a certain set of traffic demand matrices.

In contrast with offline approaches, on-line approaches dynamically reconfigure VNTs based on their detection of degraded performance or periodic measurements of the network status without a

priori knowledge of future traffic demand [33–38]. Therefore, on-line approaches adapt to changes in traffic demand. We develop an on-line approach to achieve an adaptive layered traffic engineering method. In [33], a VNT reconfiguration method that uses given traffic demand matrices and configures an optimal VNT for the new traffic demand matrix was proposed. For the smooth transition of VNTs, this method designs a new VNT by solving linear programming with constraints on the number of changing lightpaths between the old and the new VNTs. In [34,35], the authors proposed an optimization-based and heuristic VNT reconfiguration method based on periodic measurements of the load on lightpaths. This method adapts to changes in traffic demand by adding one new lightpath when congestion occurs on the VNT or deleting one underutilized lightpath on the assumption that traffic demand is changing gradually over long timescales.

Existing on-line layered traffic engineering methods assume that traffic demand is changing gradually and periodically as observed in [39]. However, if the above-mentioned interaction between layered traffic engineering and overlay networks occurs, traffic demand fluctuates greatly and unpredictably as has been pointed out [25]. More importantly, environmental changes include not only changes in traffic demand but also various changes such as link failures. Therefore, an important objective is to develop a layered traffic engineering method that is robust against various environmental changes.

1.3 Outline of Thesis

In this thesis, we propose following three approaches for layered traffic engineering to solve above-mentioned issues and achieve effective and adaptive wavelength-routed networks.

Integrated Routing for Effective Transport of IP Traffic over Wavelength-Routed Optical Networks [40–43]

In Chapter 2, we address the inefficiency of network utilization caused by the independent routing mechanisms of IP and wavelength-routed networks and realize the effective transportation of IP traffic over wavelength-routed networks. To achieve this objective, we integrate IP routing and wavelength routing for IP over wavelength-routed networks and propose a routing method that always forwards IP packets along lightpaths configured by the wavelength routing process. For this purpose, we introduce the concept of *virtual-links*, which are configured between IP routers. A

virtual-link is a logical link that is not configured as a lightpath, but can be activated as a lightpath by requesting the required wavelength resources. In the IP network, our method first calculates routes on a topology including these virtual-links. If a virtual-link is selected as part of a route for the IP packets, a lightpath corresponding to the virtual-link will be established. In this manner, we can calculate routes on the IP network and lightpaths simultaneously. The cost function for virtual-links is chosen to minimize the load on the nodes. The results of computer simulations show that our proposed method is effective in terms of both average end-to-end delay and throughput.

Hysteresis Based Layered Traffic Engineering for Stable Accommodation of Overlay Routing Services [44–46]

The selfish behavior of overlay routing causes the interaction between layered traffic engineering and overlay routing as described above. In Chapter 3, we address the problem of this interaction between layered traffic engineering and overlay routing. We first show that overlay routing highly degrades the performance of layered traffic engineering. Then we focus on the instability of layered traffic engineering caused by the interaction between overlay routing and layered traffic engineering. Simulation results show that the instability appears in link utilization, traffic demand, and VNTs due to layered traffic engineering.

To overcome the instability due to the interaction between layered traffic engineering and overlay routing and achieve a stable layered traffic engineering approach against overlay routing services, we propose three extensions for layered traffic engineering. First, to improve the stability of layered traffic engineering, we introduce *hysteresis*, which absorbs traffic demand fluctuations. We show that simple hysteresis applications can improve stability, but cannot always improve performance. We extend the hysteresis application, *two-state utilization hysteresis*, and show that this extension can improve both the stability and performance of layered traffic engineering. However, this extension requires a lot of time for the layered traffic engineering to become stable. Thus, we achieve faster convergence by using a *filtering* method. Through simulations, we show that the proposed approaches reduce the fluctuation caused by the interaction between layered traffic engineering and overlay routing and achieve stable and effective accommodation of traffic due to overlay routing on layered traffic engineering.

Adaptive Layered Traffic Engineering against Changes in Environments [47–50]

In chapter 4, we propose a layered traffic engineering approach that is adaptive against various changes in environments. The objective of this approach is to achieve the adaptability to various changes in environments, not to optimize the efficiency in terms of achievable performance such as decreasing the maximum link utilization. To achieve this objective, we adopt a non-rule-based approach and not rule-based approaches that are used by existing heuristic layered traffic engineering methods. A rule-based approach is defined as one that assumes a certain set of scenarios for environmental changes and prepares countermeasures to those changes as rules, i.e., algorithms for VNT reconfigurations. For these assumed changes in environments, these approaches may guarantee optimal performance or adaptability but they cannot guarantee if unexpected changes will occur. In contrast with rule-based approaches, non-rule-based approaches do not use predefined algorithms for adapting to changes in environments. Instead of predefined algorithms, non-rule-based approaches mainly use stochastic behavior for adapting to changes in environments. Therefore, they do not guarantee optimal performance but do have capabilities for adapting to unexpected environmental changes. Unlike most other rule-based layered traffic engineering methods, we aim at a layered traffic engineering method that will be robust against various changes in environments by using a non rule-based approach. This thesis focuses on mechanisms found in biological systems, which are adaptive against changes in their surrounding environments, as one of the non-rule-based approaches.

It is a well-known fact that mechanisms found in biological systems are robust and can handle changes in the environment [51]. Therefore, many methods that have been inspired by certain behaviors found in nature have been proposed in information science. In this thesis, we focus on *attractor selection*, which models behaviors where living organisms adapt to unknown changes in their surrounding environments and recover their conditions. In [52], the authors show an attractor selection model for *Escherichia coli* (*E. coli*) cells to adapt to changes in the availability of a nutrient. As another model of an attractor selection, the mechanism for adaptability of a cell, which consists of a gene regulatory network and a metabolic network, is introduced in [53]. One successful proposal for adaptive network control based on attractor selection was presented in [54]. They proposed a path selection mechanism, which was robust against changes in the delay of paths, based on the attractor selection model introduced in [52]. The fundamental concept underlying attractor selection is that the system is driven by stochastic and deterministic behaviors, and these

are controlled by simple feedback of current system conditions. This characteristic is one of the most important differences between attractor selection and other rule-based heuristic or optimization approaches. While existing rule-based approaches cannot handle unexpected changes in the environment, attractor selection has the capability of adapting to unknown changes since the system is driven by stochastic behavior and simple feedback of current system conditions. Therefore, we adopt attractor selection as the key mechanism in our layered traffic engineering method to attain adaptability against various changes in environments.

In Chapter 4, we propose an adaptive layered traffic engineering method based on the attractor selection described in [53]. We focus on the similarity of the layered architecture between this attractor selection model and the IP over wavelength-routed network. The reason we adopt attractor selection to achieve an adaptive layered traffic engineering method instead of a rule-based approach is because our attention is on adaptability. Unlike most other heuristic layered traffic engineering methods [8], we prefer a method that will be robust in the presence of fluctuations in environmental conditions, which may not achieve optimal performance.

Furthermore, both the *E. coli* cell and the gene-metabolic network adapt to changes in their surrounding environments without any molecular machinery for signal transduction from the environment to the gene-regulation apparatus. These biological systems adaptively respond to environmental changes with only simple feedback of system conditions. Our approach uses this feature to react against changes in the environment as quickly as possible. Unlike most existing layered traffic engineering methods that construct VNTs according to traffic demand matrices [8, 34], our method only uses the load on links as the network status. The quantity of information on the load on links is less than that obtained from traffic demand matrices, but information about the load on links is retrieved directly using SNMP. Therefore, we can achieve fast reaction and adaptation against changes in traffic demand by only using the load on links.

Both the IP over wavelength-routed network and attractor selection in the gene regulatory and metabolic reaction networks have layered structures. However, there are various differences that are mainly derived from the constraints of the physical network such as the number of transmitters and receivers. We need to interpret the attractor selection model for the layered traffic engineering method appropriately to develop an adaptive method based on attractor selection. By appropriately incorporating the essential idea of the attractor selection model, we achieve adaptability of layered traffic engineering. Through simulations, we show that our proposed method adapts changes in

traffic demand and link failures with achieving at least the same level of the efficiency as the existing heuristic approaches.

Finally, Chapter 5 concludes this thesis.

Chapter 2

Integrated Routing for Effective Transport of IP Traffic over Wavelength-Routed Optical Networks

One approach to accommodating IP traffic on a wavelength-routed network is to construct a virtual network topology, establishing a set of lightpaths between nodes. The lightpaths carry IP traffic but do not require any electronic packet processing at intermediate nodes, thereby reducing the load on those nodes. However, when the IP and wavelength-routed networks have independent routing functions, the lightpaths in the wavelength-routed network may not be fully utilized by the IP network. Therefore, it is necessary to integrate the two routing mechanisms to utilize resources efficiently. In this chapter, we propose an integrated routing mechanism for IP over wavelength-routed networks. The key idea is to first prepare a set of *virtual-links* representing the lightpaths that can be established by the wavelength-routed network, then calculate the minimum cost route on an IP network including those links. Our simulation results show that when traffic patterns do not change, the throughput of our method is almost the same as that of a VNT optimally designed for a given traffic demand. When traffic patterns change, the throughput of our method is about 50% higher than that of the VNT.

2.1 Routing in IP over Wavelength-Routed Optical Networks

As mentioned above, it is important to develop a traffic engineering approach that can fully utilize the bandwidth provided by WDM networks. Traffic engineering objectives can be achieved by developing efficient routing methods. In this section, we describe routing methods for the overlay and peer models of IP over WDM networks.

2.1.1 Overlay Model

In the overlay model, a VNT is constructed as follows. First, lightpaths are established between nodes of the WDM network. Conventional IP routing protocols, such as Open Shortest Path First (OSPF) and Intermediate System to Intermediate System (IS-IS), then work on the VNT of the WDM network. In this model, the routing protocols are not modified to account for the properties of the WDM network. The IP routing mechanism and WDM routing mechanism are designed independently, so the IP mechanism does not necessarily select the links provided by the WDM network. One typical example of such a problem is the minimum delay routing of IP networks, illustrated in Figure 2.1. In this example, we assume that each optical fiber has two wavelengths, and that the propagation delay of each fiber is 1 time unit. The delay incurred by an IP router, including processing delay and queuing delay, is also 1 time unit but that of an OXC is 0. In this figure, six lightpaths are configured in the WDM network (l_1 to l_6), so the VNT has six links. l_5 , the long hop lightpath, has been configured using wavelength λ_2 between nodes N_2 and N_4 . l_5 must take the longer path because wavelength λ_2 has already been used by l_2 on the optical fiber connecting nodes N_2 and N_3 . There are thus two possible routes from node N_2 to N_4 : R_1 and R_2 . R_1 is the one-hop route $N_2 \rightarrow N_4$ using l_5 , and R_2 is the two-hop route $N_2 \rightarrow N_3 \rightarrow N_4$ using l_2 and l_3 . The end-to-end delay of R_1 is 4, while that of R_2 is 3. Thus, if the IP routing mechanism uses end-to-end delay as its metric, R_1 will never be used as the route from N_2 to N_4 . This leads to inefficient utilization of the wavelength resources. We therefore need an integrated routing mechanism, whose main goal is to utilize resources efficiently. Some integrated routing methods have already been proposed, mainly assuming the peer model; that is, they use information from both networks such as bandwidth availability (IP) and wavelength availability (WDM). In the following section, we summarize some related works on the problem of integrated routing.

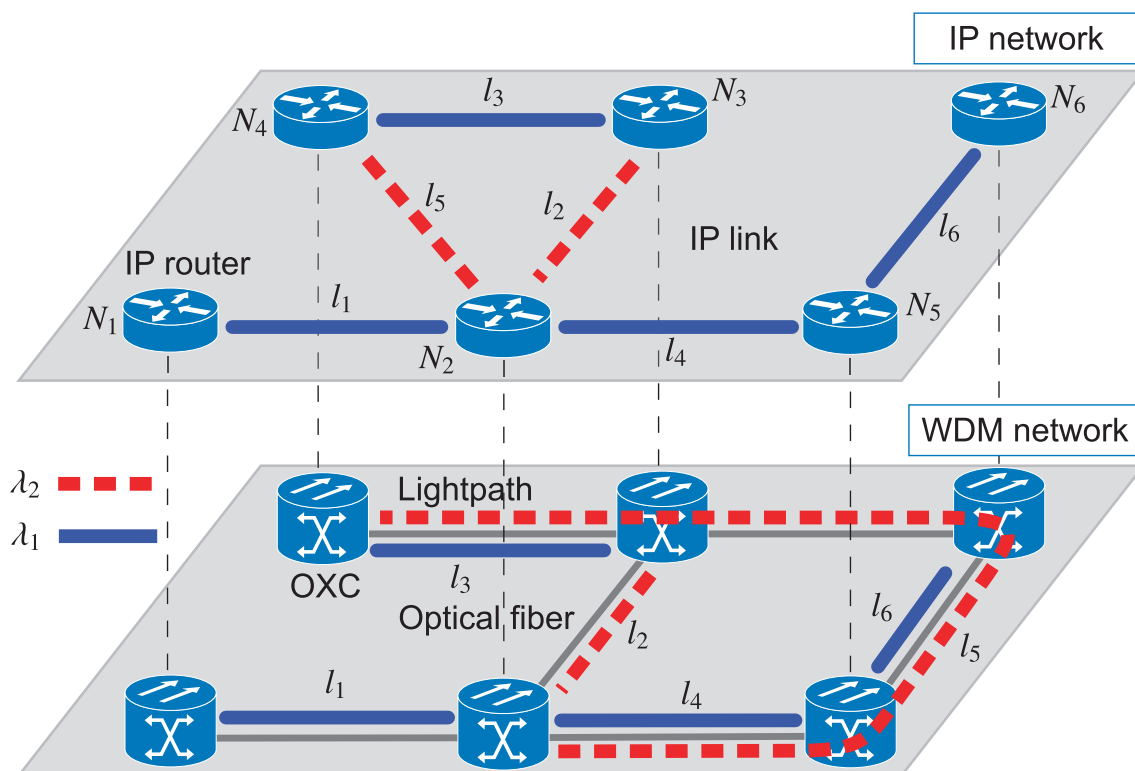


Figure 2.1: An example showing that IP routing does not always select the links provided by the WDM network

2.1.2 Peer Model

Integrated routing methods for the peer model are proposed in references [16, 19]. These papers investigate IP/MPLS over WDM networks, where the routes of IP packets can be explicitly determined by the MPLS algorithm as LSPs. In reference [19], MIRA (Minimum Interference Routing Algorithm) is proposed as an integrated routing algorithm for LSPs and lightpaths. The IP/MPLS over WDM network has a unified routing entity that collects all the topology information and link state information from both IP/MPLS and WDM networks. For incrementally arriving traffic flows where the required bandwidth is explicitly specified, MIRA calculates the routes of traffic flow. MIRA also keeps track of the residual bandwidth that can be used by future LSP requests, and tries to maximize this resource. When there is no appropriate route, LSP requests are blocked. In reference [14], another integrated routing method is developed which takes into account inaccuracy in the link state information. This method incorporates the level of uncertainty in link states and

hop counts into its link cost metric for LSPs. Reference [16] proposes an integrated routing method for the peer model based on the Generalized MPLS (GMPLS) framework [55]. In this work, cost values are assigned to links with the goal of reusing existing lightpaths for new LSP setting requests as much as possible.

All these works assume that IP traffic is mapped onto a series of bandwidth guaranteed LSP requests. Their main objective is to minimize the blocking probability of LSP setting requests. Few works have focused on the performance metrics of IP traffic, e.g., end-to-end delay or throughput. The works just described have all assumed a peer model network, which as mentioned above lacks scalability. Furthermore, very few works have studied integrated routing in an overlay model network. This thesis therefore proposes a new integrated routing method within the overlay model of IP over WDM networks, aimed at maximizing the traffic volume that can be accommodated. In the next section, we describe this new routing method.

2.2 Integrated Routing for Layered Traffic Engineering

In this section, we introduce our network model and the concept of a *virtual-link*, which is central to our integrated routing method. We then elaborate on our routing algorithm and discuss possible cost metrics.

2.2.1 Network model

We consider a network consisting of optical fiber links with W independent wavelengths and nodes that consist of IP routers with WDM interfaces, and OXCs. Figure 2.2 illustrates the node architecture used in this these. The upper part of this figure shows an IP router, and the lower part shows an OXC. The IP router is connected to the OXC via a WDM interface, which converts optical signals to electronic signals and vice versa. The control plane in the WDM layer manages the topology database and wavelength availability information. The IP router has a route manager with three main blocks: the routing controller, the topology database, and OSPF. The route manager calculates routes using an integrated algorithm based on the VNT specified in the topology database. This topology database includes only information from the IP layer such as links, router status, and network connectivity, since we assume that the internetworking architecture follows the overlay model. The OSPF-TE block advertises and collects IP link state information. Note that since we

assume the overlay model, our method does not require any extension of existing IP routing protocols. The route manager in the IP layer sends setup or teardown lightpath requests to the WDM layer control plane according to the results of its route calculation. The WDM layer control plane carries out these requests and returns the results to the IP route manager.

In our network architecture, a static lightpath is set up between all adjacent nodes using one wavelength resource, to ensure end-to-end reachability. We refer to these lightpaths as *persistent lightpaths*. The other wavelength resources are used for non-persistent lightpaths, which are set up dynamically according to changes in traffic.

2.2.2 Virtual-Links

To integrate IP routing and wavelength routing, we propose a concept of *virtual-links*. A virtual-link is a logical link used by our routing algorithm. That is, they are configured on a VNT database, and the IP routing mechanism selects routes for IP traffic from that topology. An example of a network with virtual-links is shown in Figure 2.3. In this figure, persistent lightpaths are configured between all adjacent nodes, and one non-persistent lightpath is configured from router R_1 to router R_6 . Three virtual-links (from router R_1 to routers R_2 , R_4 , and R_5) are illustrated as dashed arrows in the figure. Each link and virtual-link has an associated cost value, which is used by the IP routing mechanism. Routes are therefore calculated from a VNT that includes virtual-links as well as existing lightpaths. Note that in our proposal, the cost of the virtual-links has a great impact on network performance. We discuss our choice of cost function for the virtual-links in Sec. 2.2.5.

2.2.3 Topology Database

The OSPF component of the IP router advertises the link state information, and each IP router collects all the link state information. The IP routers then configure following the VNT, which includes all virtual-links and their cost.

- Step 1: Set virtual-links from the source node to all destination nodes for which there is no lightpath configured.
- Step 2: Assign cost values to each virtual-link using the cost function described in Sec. 2.2.5.
- Step 3: Update the link cost values of existing non-persistent lightpaths. The same cost function described in Sec. 2.2.5 is used.

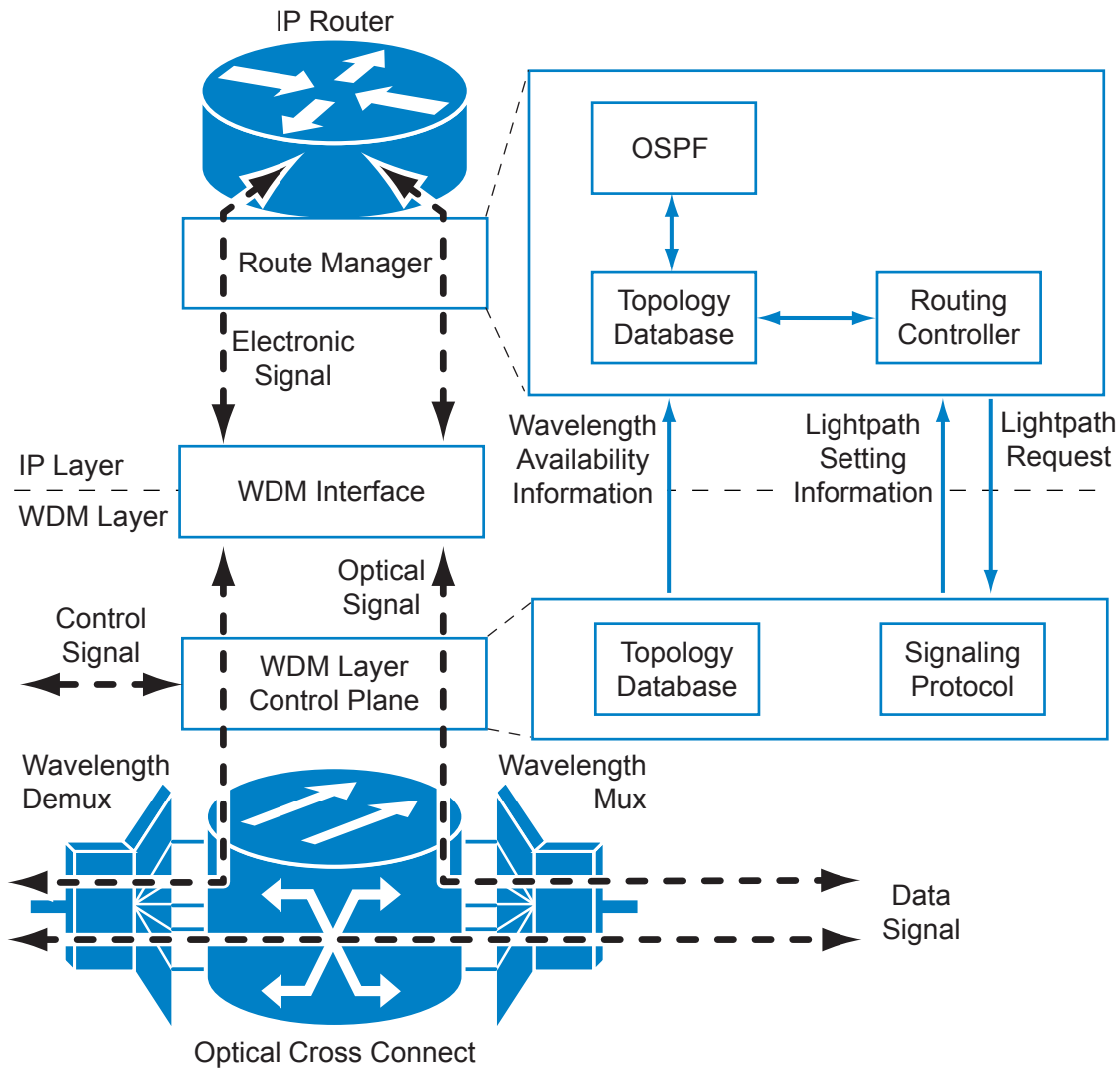


Figure 2.2: Node architecture

Step 4: Set the link cost values of persistent lightpaths to 1.

We can set the cost values of all persistent lightpaths to 1 without loss of generality, as long as the cost of virtual-links is scaled accordingly.

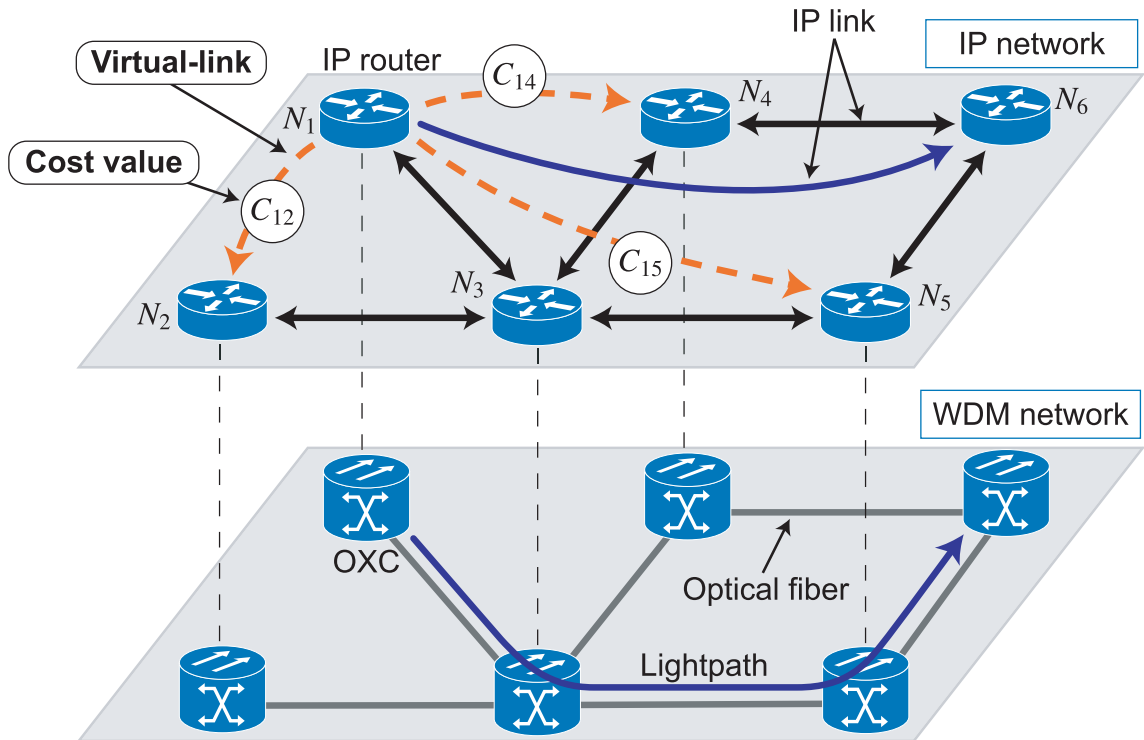


Figure 2.3: A network example with virtual-links

2.2.4 Route Selection

The routes of IP packets are calculated using the topology database obtained by the above procedure, and if any virtual-links are selected as the part of IP routes then the corresponding lightpath is dynamically configured on the WDM network. Each node in the network performs following steps.

- Step 1: Calculate the routes with minimum cost on the VNT, including virtual-links and existing lightpaths, via the IP routing algorithm.
- Step 2: If the resulting routes contain one or more virtual-links, send requests to the WDM network to set up the corresponding lightpaths. If some of those requests are blocked due to the lack of wavelength resources, existing lightpaths are used for those routes.
- Step 3: Send teardown requests for all existing lightpaths that are not used in the IP routes just calculated. Here, an unused lightpath means that a link that is not included in the minimum cost routes just calculated, and whose source node is the node performing these steps.

Routing in the IP and WDM layers is integrated by searching for minimum cost routes in a VNT including virtual-links. Using this method, IP traffic will be forwarded on virtual-links, i.e., lightpaths, since lightpaths are selected by the IP routing.

2.2.5 Cost Assignment to Virtual-Links

The fundamental question in this approach is how to select a cost function for the virtual-links. Our main objective in choosing this cost function is to maximize the network throughput. Reducing the load on the IP routers is therefore an important criterion. Load on IP routers is the total amount of traffic to be processed at the IP router. Activating virtual-links as lightpaths may increase the load on some nodes, however, because more traffic will pass through the destination nodes of lightpaths. We show a simple example of this scenario in Figure 2.4. In Figure 2.4(a) two flows, f_1 and f_2 , are forwarded along the routes $N_1 \rightarrow N_3 \rightarrow N_5$ and $N_2 \rightarrow N_4 \rightarrow N_6 \rightarrow N_5$ respectively. Figure 2.4(b) illustrates the network after a lightpath has been configured from node N_2 to N_3 . Since the lightpath has just been set, the route of flow f_2 changes to $N_2 \rightarrow N_3 \rightarrow N_5$. In this case, f_2 traffic that used to pass through nodes N_4 and N_6 now passes through node N_3 . Consequently, the load on N_3 increases. We therefore use the load on the destination node of a virtual-link as the main parameter of our cost function, to avoid concentrating traffic on frequently used nodes. Note that the IP router status can be obtained using Simple Network Management Protocol (SNMP).

The cost function C_{ij} of a virtual-link between nodes i and j is thus given by

$$C_{ij} = v_j^2 + \beta, \quad (2.1)$$

where v_j is the load on node j , and β is a constant offset. As noted above, our main purpose is to reduce the load on the IP routers. By using a cost function that is quadratic in v_j , we expect to strongly discourage any increase in the node load factor. By setting β to 0.5, we prevent the IP routing method from selecting routes with too many hops. Setting the offset value to 0.5 also forces the IP routing mechanism to select persistent lightpaths whenever possible, since the cost of a persistent lightpath is always 1 and the sum of the cost of two virtual-links is more than 1.

The number of lightpaths N_{ij} connecting node i to node j is decided by $N_{ij} = \lceil b_{ij} \rceil$, where b_{ij} is the incoming traffic volume at node j from node i . This assumes that the traffic volume going to node j can be measured at node i . A minimum of N_{ij} lightpaths will be configured so that the

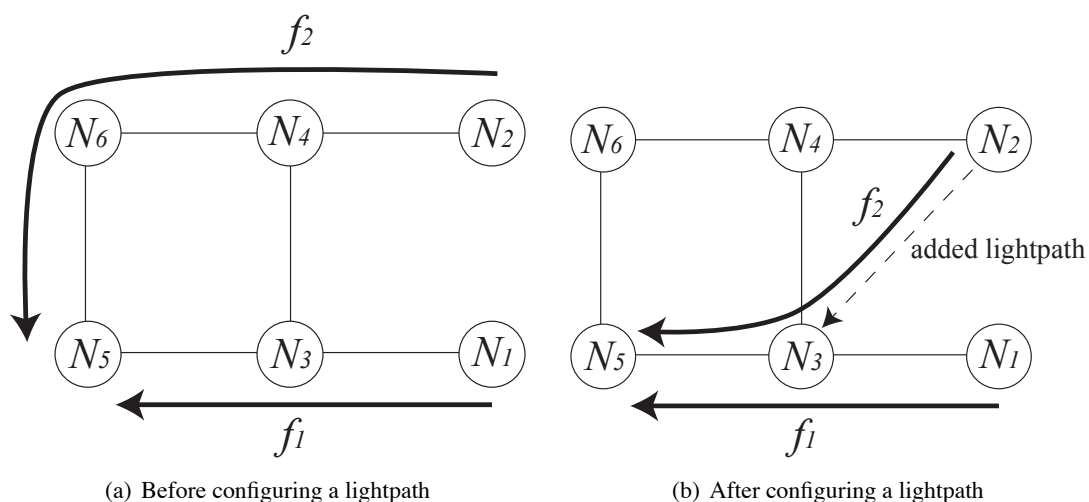


Figure 2.4: Congestion resulting from activating a virtual-link

current traffic volume can be satisfied.

2.3 Flow-Level Simulation of Packets in Wavelength-Routed Networks

In this section, we describe a simulation of network traffic based on the fluid flow model (a flow-level simulation). Conventionally, traffic flow is modeled with a discrete event simulation that processes every packet (a packet-level simulation). A flow-level method is necessary, however, if simulations of large-scale networks are to finish in a reasonable amount of time. First, we detail the reasons that a flow-level simulation is needed, and then we describe the fluid flow approximation used by the simulation. Finally, we compare the results of a flow-level simulation to those of a packet-level simulation, in order to validate the method.

2.3.1 Difficulties in Packet-Level Simulations

Computer simulations are commonly used to analyze and evaluate the performance of communication networks. Discrete event network simulators (such as OPNET [56] or NS-2 [57]) simulate the movement of individual packets through the network. Although this method provides accurate insight into the network state and performance, a great many events must be processed to properly simulate the network. With the growth of the Internet, the scale of networks has become even larger.

Moreover, new network technologies such as WDM provide high bandwidth links, significantly increasing the traffic volume that networks can accommodate. The simulation of modern networks consumes an enormous amount of time and resources.

Many recent papers have described simulation methods based on the fluid flow model [58,59]. These works mainly develop simulations for TCP-based networks; that is, they focus on transient states of TCP flow. In this thesis, however, we only focus on the state of IP traffic over the WDM network. We therefore simplify the model of the simulation method, and just apply the fluid flow model, which requires fewer packets to be processed during simulations, and evaluate our integrated routing mechanism.

2.3.2 Flow-Level Simulation Method

Fluid Flow Model

First, we describe the fluid flow approximation. In simulation methods based on the fluid flow model, data traffic is modeled not as a sequence of packets but as a continuous fluid. Network simulators based on the fluid flow approximation abstract the model further, focusing only on *changes* in the arrival rates of traffic flow. This can lead to a significant decrease in computation time, although any information regarding the motion of individual packets is lost.

Application of Fluid Flow Model to Network Simulations

We define the following terms to explain the flow-level simulation.

t_n : n -th timestep, when the arrival or departure of flows can occur.

$L(t_n)$: Number of packets in a node at time t_n .

$a(t_n)$: Packet arrival rate at a node at time t_n .

a_i : Packet arrival rate in flow i .

μ : Service rate of the node.

$W(t_n)$: Delay in the node at time t_n .

The packet arrival rate of each flow is drawn from a Poisson distribution with constant average rate a_i .

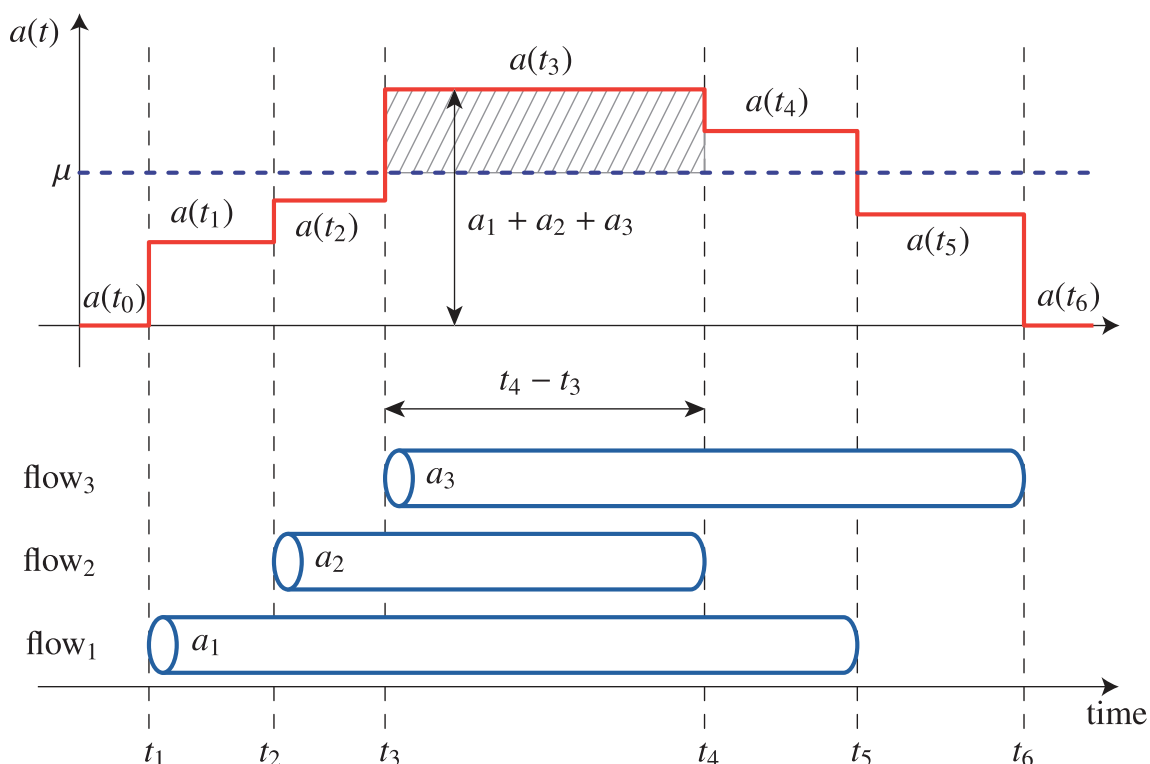


Figure 2.5: Calculation of the number of packets at a node

Figure 2.5 illustrates the algorithm for calculating the packet arrival rate at a node. The figure illustrates three flows ($\text{flow}_1, \text{flow}_2, \text{flow}_3$) that arrive at the node at consecutive timesteps t_1, t_2 , and t_3 . The flows, which are not all the same length, depart at times t_6, t_4 , and t_5 , respectively. Each flow i has the parameter a_i , which is the arrival rate of packets in the flow i . In other words, the time spacing between individual packets in flow i is $1/a_i$. The packet arrival rate for a given node a (denoted $a(t_n)$) is the sum of the packet arrival rates a_i for each flow, so $a(t_n)$ changes with the arrival/departure of flows as shown in the upper part of Figure 2.5.

The increase in packet number at the node from time t_{n-1} to time t_n can be represented by $\{a(t_{n-1}) - \mu\} \times (t_n - t_{n-1})$. The factor $a(t_{n-1}) \times (t_n - t_{n-1})$ is the total number of packets arriving at the node between t_{n-1} and t_n , and the factor $\mu \times (t_n - t_{n-1})$ is the number of packets departing from the node in the same interval. Note that if $\{a(t_{n-1}) - \mu\} \times (t_n - t_{n-1}) < 0$, the number of packets in the node decreases. Since the number of packets at time t_{n-1} is denoted $L(t_{n-1})$, the total number of

packets in the node at time t_n can be expressed as

$$L(t_n) = \{a(t_{n-1}) - \mu\} \times (t_n - t_{n-1}) + L(t_{n-1}).$$

Since $L(t_n)$ must be a non-negative number, we further set $L(t_n) = 0$ if the calculation results in $L(t_n) < 0$. The delay experienced at a node can be calculated as $W(t_n) = L(t_n)/a(t_n)$, applying Little's theorem [60].

In the flow-level simulation, only the head and tail packets of each flow are processed to update parameters $a(t_n)$, $L(t_n)$, and $W(t_n)$. In a packet-level simulation, every packet in the flow has to be processed; $a(t_n)$, $L(t_n)$, and $W(t_n)$ are updated whenever a packet arrives at the node.

2.3.3 Verification of Flow-Level Simulation Method

To validate the fluid flow approximation, we compare the results of a flow-level simulation with those of a packet-level simulation.

We compare the two simulation methods under identical conditions, i.e., the NSFNET topology with 14 nodes and 21 edges. The number of wavelengths for each link is eight, and wavelength converters are not used in this simulation. The bandwidth of each wavelength is assumed to be 10 Gbps. The processing capacity of the IP router is set to 1 Gbps to perform the packet-level simulation within a reasonable amount of time. The flow lengths are drawn from an exponential distribution with a mean value of 12 MByte, i.e., the packet size is 1500 bytes and the average length of a flow is 1000 packets. The flows connecting each node pair ij arrive according to a Poisson process with average rate $\gamma \times d_{ij}$, where $D = \{d_{ij}\}$ is the traffic demand matrix and γ is a scale factor. We use the traffic demand matrix given in [8]. Moreover, we use the same sequence of random numbers for both simulations.

Figure 2.6 shows the average end-to-end delay as a function of the total amount of traffic, which is controlled by means of the scale factor γ . We observe that the average end-to-end delay obtained by the flow-level simulation agrees well with that obtained by the packet-level simulation. Although a difference appears at high loads (greater than 3.5 Gbps), the saturation point is almost the same. Networks are generally operated at loads much lower than the saturation point, so we can ignore the difference between these two methods. Evaluating the queue behavior at a node also confirms the validity of the flow-level simulation method. Due to space limitations, we omit the results of

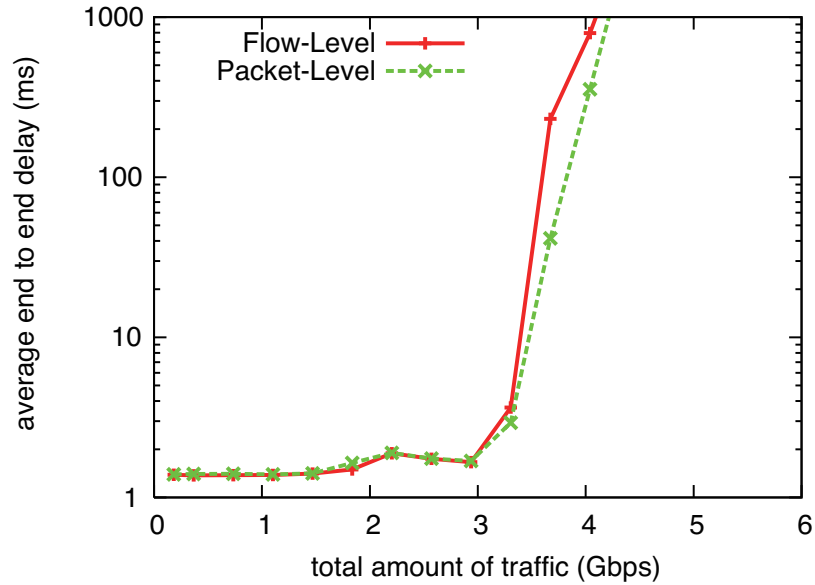


Figure 2.6: The average end-to-end delay of flow-level and packet-level simulations

this test.

The flow-level method greatly reduces the simulation time because only two packets per flow are processed. In this validation, we chose a small average number of packets (1000) per flow, so that the packet-level simulation could run in a reasonable time. The packet-level network simulator must therefore process 500 times more packets than the flow-level simulator. The actual simulation time of the flow-level simulation for one choice of parameters was a few seconds, while that of the packet-level simulation was more than ten minutes (the exact times depend on the implementation). Moreover, the memory requirement of the flow-level simulation is much less than that of the packet-level simulation. Computer simulations based on the fluid flow model are therefore a very effective method for evaluating the performance of high-bandwidth networks.

2.4 Performance Evaluation

In this section, we evaluate the performance of the proposed algorithm through flow-level computer simulations.

2.4.1 Simulation Conditions

The simulation model used here is almost the same as that described in Section 2.3.3. We change the router capacity to 100 Gbps, the link capacity to 40 Gbps. As the number of wavelengths multiplexed on a single fiber increases, the processing capacity of electronic routers will become the bottleneck of a network. We therefore evaluate our method and conventional methods under these parameter settings, that is, the bottleneck of the network is processing capacity of electronic routers. We set the average flow length to 75 Mbytes; the packet size is 1500 bytes, and the average length of a flow is 50000 packets. In addition to the NSFNET topology, we also show results for the European Optical Network (EON), which has 19 nodes and 39 bidirectional links. For the NSFNET topology, we use a random traffic demand matrix, generated according to an exponential distribution, in addition to the matrix described in [8]. For the EON topology, we use only a randomly generated traffic matrix.

For the purpose of comparison, we use three VNTs. First two VNTs are designed by the algorithms SHLDA (Shortest-Hop Logical topology Design Algorithm) [17] and MLDA (Minimum delay Logical topology Design Algorithm) [8]. These algorithms generate VNTs based on a given traffic demand matrix in order to achieve their namesake performance objectives. Since both MLDA and SHLDA have a prior knowledge about the traffic demand matrices, they generate nearly optimal topologies. For the third VNT, we use a full mesh topology, which is generated by configuring lightpaths between all node pairs by assuming that there are unlimited number of wavelengths on a fiber. All IP traffic in the full mesh topology is directly forwarded from source nodes to destination nodes. Since IP routers do not need to process the traffic for other node pairs, full mesh topologies are optimal and give upper bounds of networks. We compare the results of our method to these near-optimal topologies in order to demonstrate the efficiency of our method. In our simulation experiments, we use minimum hop routing for IP packets on the VNTs generated by MLDA and SHLDA. For the full mesh topology, we configure the sufficient number of lightpaths for accommodating IP traffic between nodes.

We evaluate the performance of our integrated routing method with three metrics: the average end-to-end delay in Section 2.4.2, the load on the nodes in Section 2.4.3, and the network throughput in Section 2.4.4.

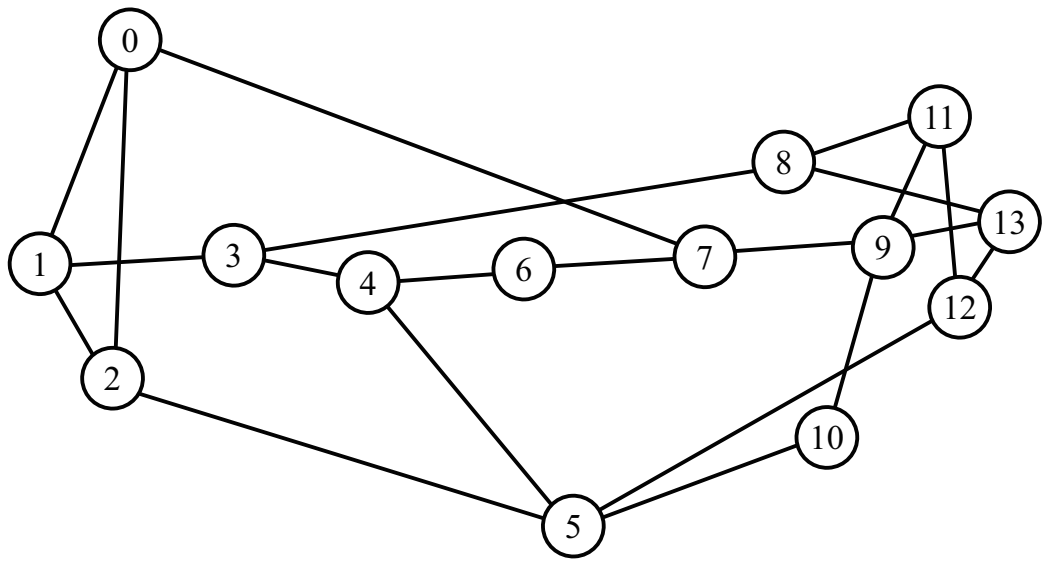


Figure 2.7: NSFNET topology

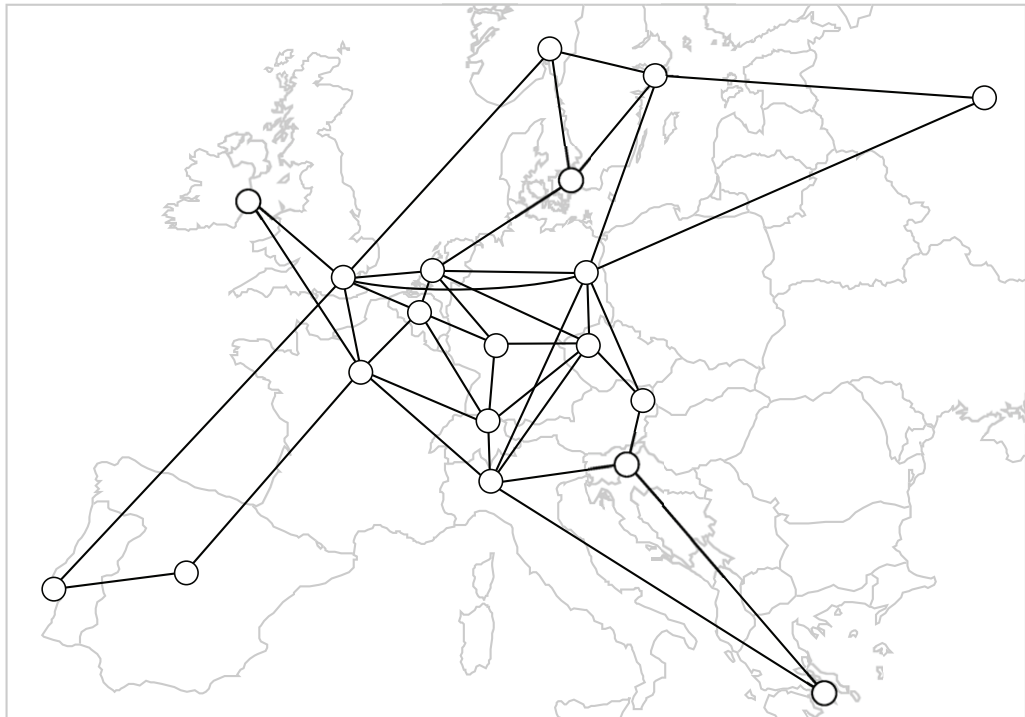


Figure 2.8: European Optical Network topology

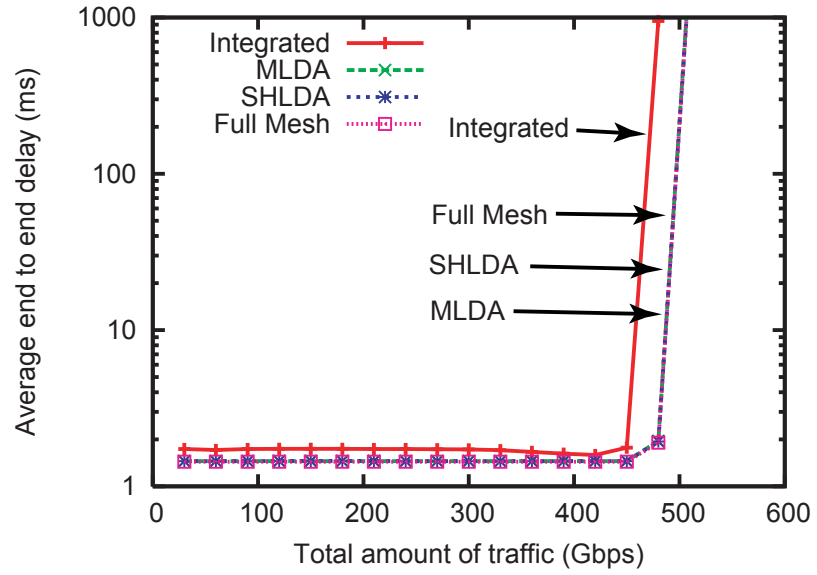
2.4.2 Average End-to-End Delay

Figures 2.9(a) and 2.9(b) show the average end-to-end delay on NSFNET. The horizontal axis shows the total traffic volume in the network. The result in Figure 2.9(a) is based on the traffic matrix in [8]. The average end-to-end delay achieved by our routing method is slightly worse than that achieved by the topologies generated by MLDA, SHLDA, and the full mesh topology. Our method shows nearly optimal end-to-end delay performance without the information of traffic demand matrix. In Figure 2.9(b), we show results from the three methods in a scenario where the traffic matrix is randomly regenerated four times in one simulation but the sum of the matrix (i.e., x -axis value in the figure) is held constant. Note that, for obtaining result of the full mesh topology, we configure the sufficient number of lightpaths between nodes for each of the regenerated traffic matrices. Thus, the results show the upper bound of the performance. As expected, changing traffic patterns degrade the performance of the SHLDA and MLDA methods drastically. Our algorithm, however, shows little increase in the average end-to-end delay in this situation. Moreover, our method does not require any prior knowledge of traffic statistics whereas SHLDA and MLDA create VNTs according to previously measured statistics. This feature is a great advantage, since it takes a long time to measure traffic statistics accurately and IP traffic does not always follow the pattern described. Thus, statically generated VNTs may not always perform optimally, as shown in Figure 2.9(b).

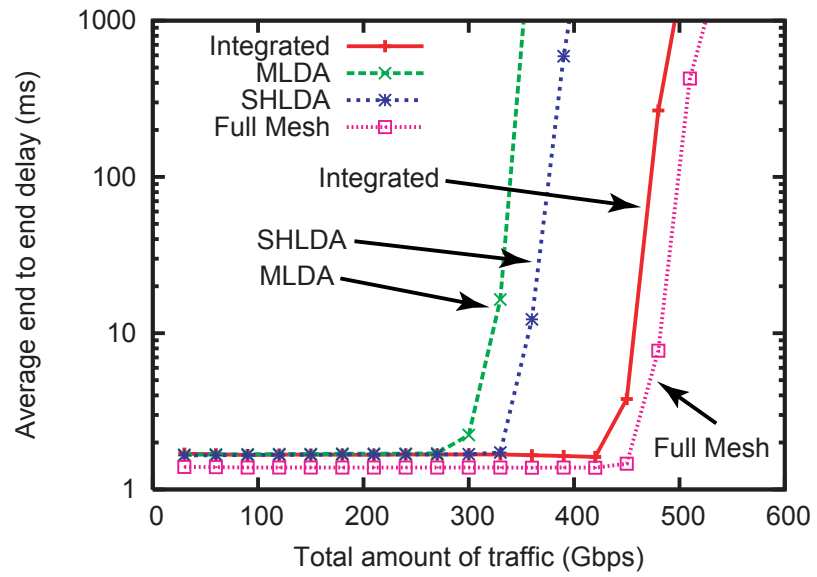
We next evaluate our proposed method on the NSFNET topology using a random traffic matrix. Figures 2.10(a) and 2.10(b) show the average end-to-end delay on the NSFNET topology as a function of the total traffic. In this figure, we observe that our routing method outperforms conventional VNT design methods. Moreover, the average end-to-end delay in our method is constant regardless of traffic change, while the delay using SHLDA or MLDA depends strongly on the traffic demand matrices. Figures 2.11(a) and 2.11(b) depict the results of our routing mechanism on the EON topology. These figures show tendencies similar to those observed on the NSFNET topology.

2.4.3 Load on Nodes

To see the efficiency of our method more clearly, we show the average load on each node in Fig. 2.12. The load on a node is the traffic volume processed in that node divided by the processing capacity of the node. In this simulation, we use the NSFNET topology and the traffic demand matrix given in Ref. [8]. In obtaining this figure, we set the total traffic demand to the point where the

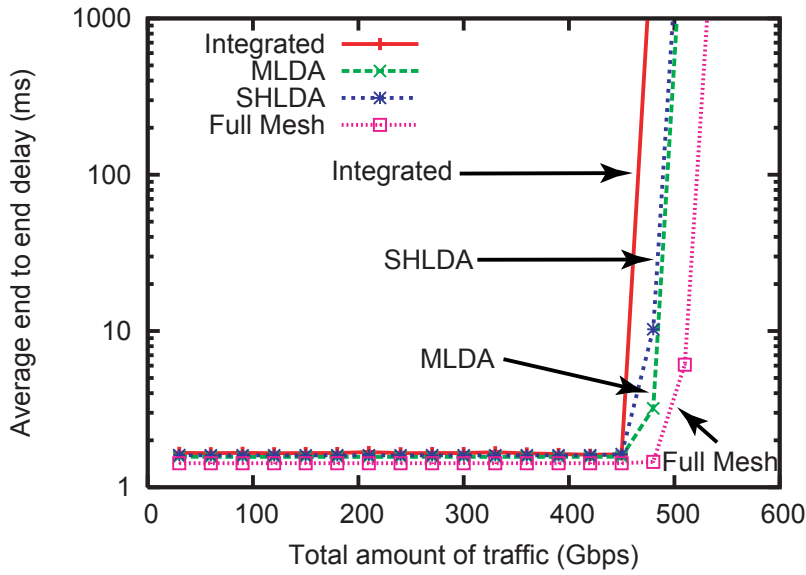


(a) Without traffic change

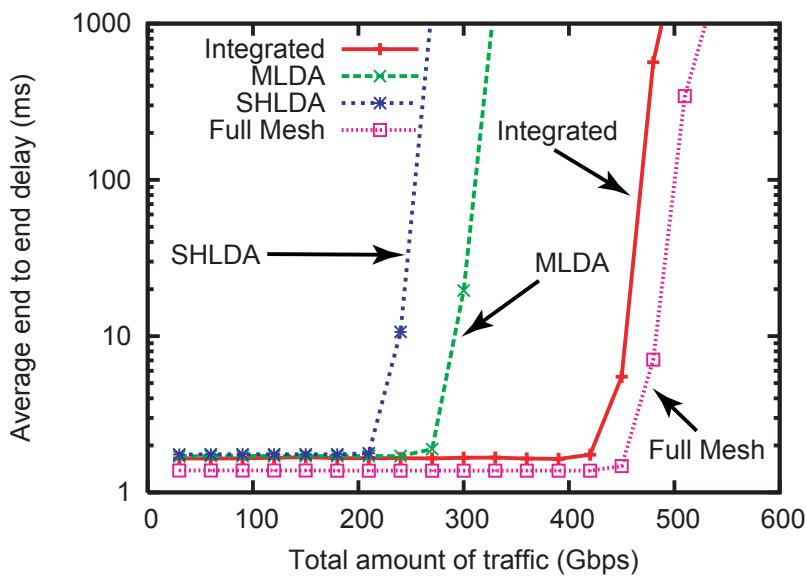


(b) With traffic change

Figure 2.9: Average end-to-end delay: NSFNET topology, the case of realistic traffic demand matrix



(a) Without traffic change



(b) With traffic change

Figure 2.10: Average end-to-end delay: NSFNET topology, the case of random traffic demand matrix

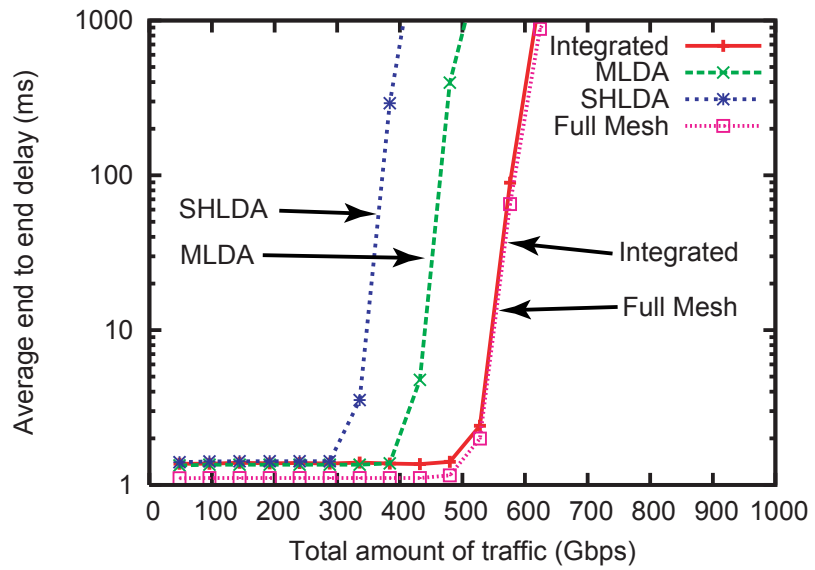
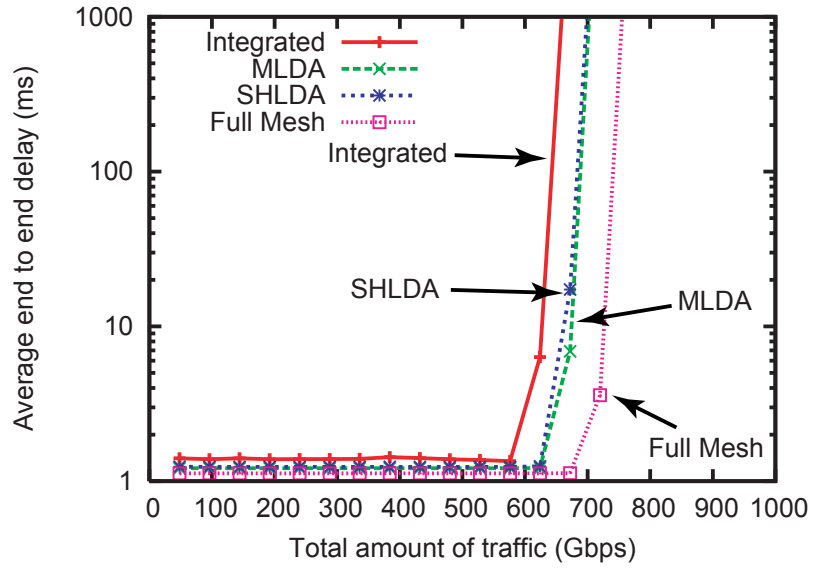
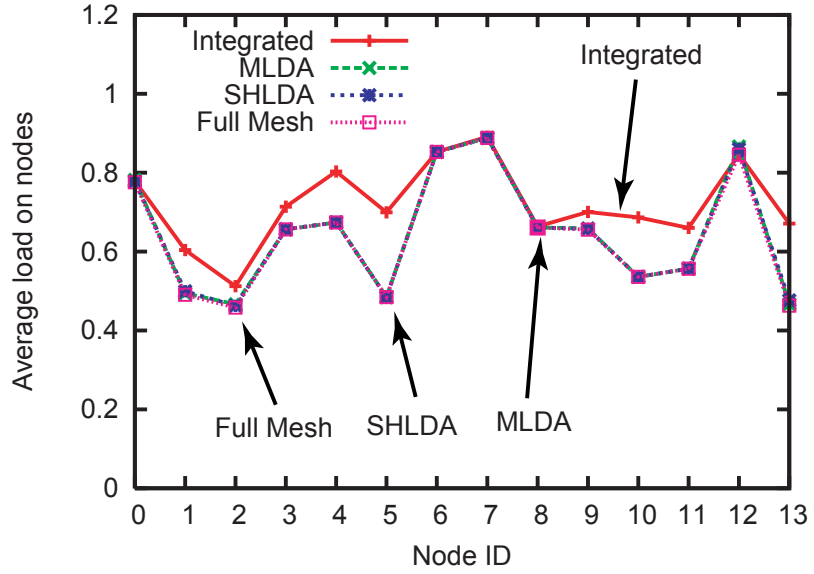


Figure 2.11: Average end-to-end delay: EON topology, the case of random traffic demand matrix

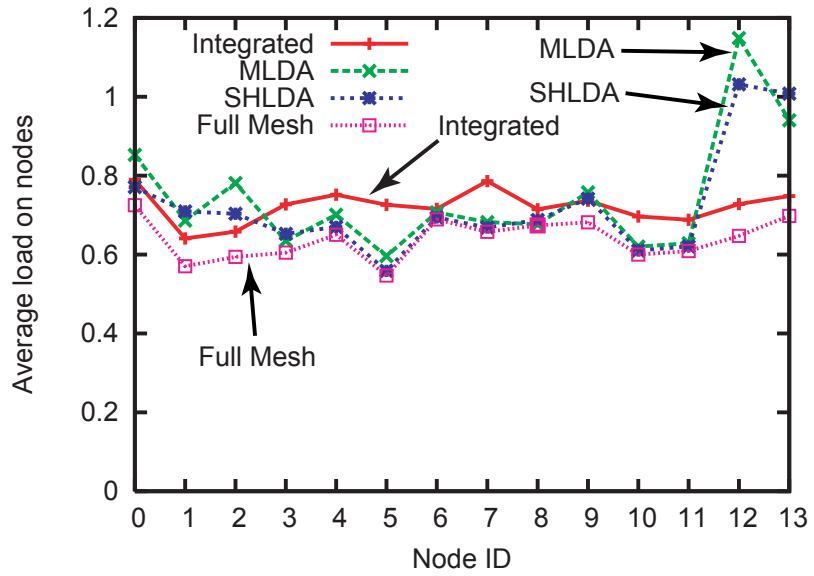
average end-to-end delay just begins to increase, as seen in Fig. 2.9(a) and Fig. 2.9(b). We set the total traffic volume in the network to 450 Gbps for all methods, for both the static and dynamic traffic patterns. Figure 2.12(b) shows that our algorithm balances the load at an average value around 0.7 when slight congestion occurs in the network. In the SHLDA and MLDA methods, on the other hand, most of the nodes remain under-utilized even though node 12 is saturated. Fig. 2.12(a), however, shows that some nodes are highly loaded in all methods. To investigate the reasons for this, we classify the traffic volume into three types; ingress traffic, egress traffic, and transit traffic. Ingress traffic is traffic that arrives at the node from outside the network, and egress traffic is traffic that leaves the network at the node. Transit traffic is traffic that is being forwarded from the ingress line card to the egress line card. Figure 2.13 shows the load on each node caused by each kind of traffic. In obtaining this result, we evaluate our method on the NSFNET topology without traffic change. It is revealed that most of the volume is either ingress or egress traffic, which must be processed at the nodes. Since the ingress and egress traffic depend on the traffic demand matrix, hereafter we focus on the behavior of the transit traffic. Note that the amount of transit traffic processed at nodes with high ingress and egress traffic (nodes 6, 7, and 12) is nearly 0. In general, the transit traffic in loaded nodes is much less than that in nodes with little load. This means that our method detours IP traffic through the less active nodes, and achieves the central goal of load balancing. SHLDA and MLDA balance the load on nodes using the information of the traffic demand matrix. Our method, on the other hand, does not require any information of traffic demand matrix, and balances the load on nodes using the information of nodal load. In the full mesh VNT, IP routers does not need to process transit traffic, and therefore, the load on nodes is the lowest among all methods. Our method, however, shows almost the same performance as the full mesh VNT by balancing the load.

2.4.4 Network Throughput

We next measure the network throughput achieved by cross-layer traffic engineering. We define network throughput as the maximum traffic volume that the network can accommodate while keeping the average end-to-end delay under 10 ms. This simulation also uses the NSFNET topology. Fig. 2.14 shows the throughput using the traffic demand matrix given in Ref. [8]. The throughput of our method is slightly lower than that of MLDA, SHLDA, and full mesh topology when traffic does not change. Changing traffic patterns, however, degrade the throughput of MLDA/SHLDA



(a) Load on nodes without traffic change: NSFNET topology, total traffic volume is 450 Gbps for all method



(b) Load on nodes with traffic change: NSFNET topology, total traffic volume is 450 Gbps for all method

Figure 2.12: Average load on each node

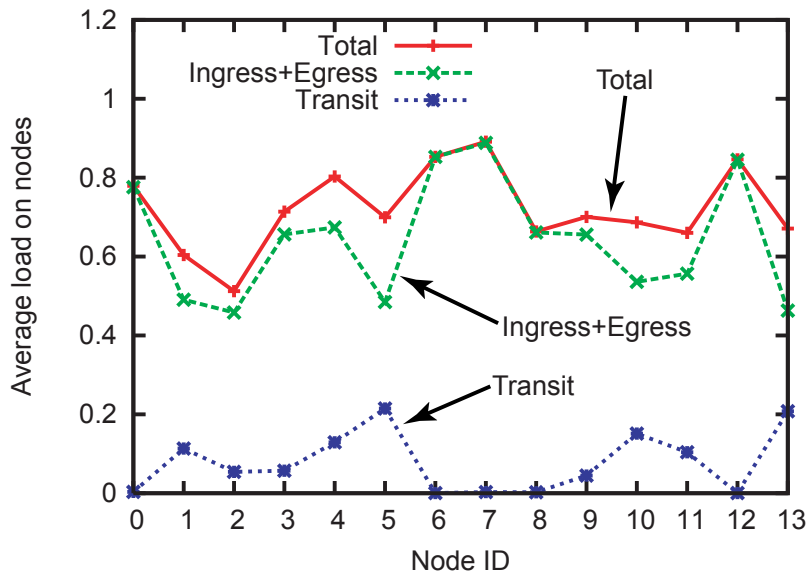


Figure 2.13: Classified load on nodes without traffic change: the integrated routing method

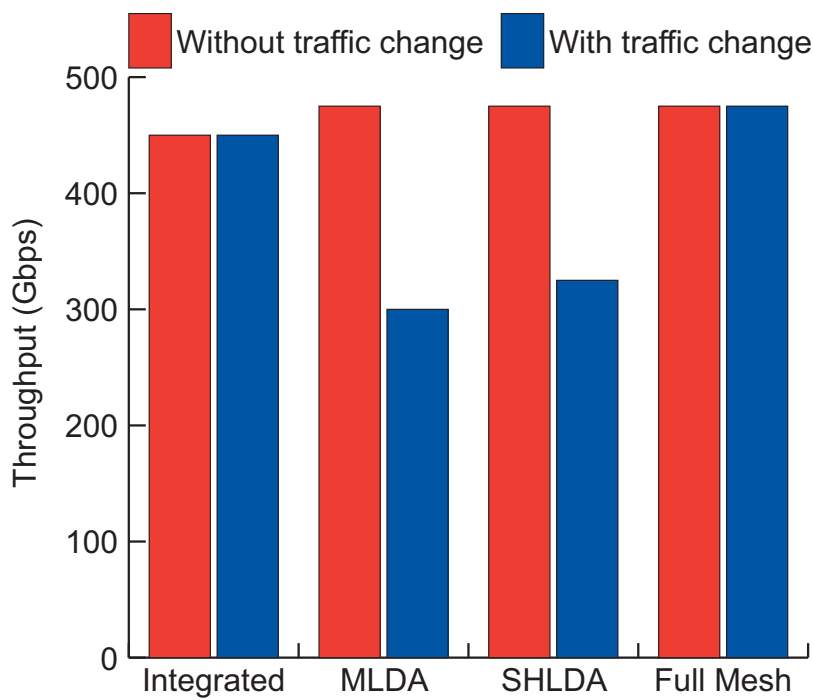


Figure 2.14: Network throughput

dramatically. Under these conditions, the VNT generated by SHLDA can accommodate only 68% of the static traffic throughput. The VNT generated by MLDA can accommodate 63% of the static traffic throughput. Changing traffic patterns does not greatly affect the throughput of our method.

2.5 Summary

In this chapter, we propose a new integrated routing algorithm that uses virtual-links in selecting routes for IP packets, and demonstrate the necessity of dynamic lightpath configuration in IP over WDM networks. The main objectives of our algorithm are to reduce the load on IP routers and maximize the traffic volume that can be accommodated by the network. Simulation results show that our method balances the load on IP routers where static VNT design methods cannot. Under changing traffic patterns, the throughput of our method was 38–50% higher than that of two static VNT design methods. To reduce the costs of computer simulation, we developed a method using the fluid flow model. The flow-level simulations were validated by comparing them to conventional packet-level simulations. The flow-level and packet-level simulations achieved similar results with respect to average end-to-end delay and number of packets per node. The flow-level simulation ran about 500 times faster than the packet-level simulation and reduced the required memory, so it is a good technique for modeling large scale and high-bandwidth networks.

Chapter 3

Hysteresis Based Layered Traffic Engineering for Stable Accommodation of Overlay Routing Services

Overlay networks achieve new functionality and enhance network performance by enabling control of routing at the application layer. However, this approach results in degradations of underlying networks due to the selfish behavior of overlay networks. In this chapter, we discuss the stability of layered traffic engineering under overlay networks that perform dynamic routing updates. We find that the dynamics of routing on overlay networks cause a high fluctuation in the traffic demand matrix, which leads to significant instability of layered traffic engineering. To overcome this instability, we introduce three extensions, *hysteresis*, *two-state utilization hysteresis*, and *filtering*, to layered traffic engineering. Simulation results show that the hysteresis mechanism improves network stability, but cannot always improve network performance. We therefore extend the hysteresis mechanism and improve both network stability and performance. However, this extension requires a lot of time for the VNT to converge to a stable state. To achieve fast convergence, we use a filtering method for layered traffic engineering. Through simulations, we prove that our methods achieve stability against overlay routing without loss of adaptability for changes in traffic demand.

3.1 Interaction between Layered Traffic Engineering and Overlay Routing

In this section, we investigate the influence of overlay routing on dynamically configured VNT. Through simulation experiments, we show that the presence of overlay routing services increases the maximum link utilization of the VNT. We also show that the coexistence of overlay routing and layered traffic engineering leads to VNT instability.

3.1.1 Network Model

In our view, a network consists of three layers: an optical layer, a packet layer, and an overlay layer, as shown in Figure 3.1. On the optical layer, the WDM network consists of OXCs and optical fibers. The layered traffic engineering configures lightpaths between IP routers via OXCs on the WDM network and, these lightpaths and the IP routers form a VNT. On the packet layer, packets are forwarded along the routes that are determined by IP routing on this VNT. On the overlay layer, overlay nodes built on the packet layer form an overlay network. In this network, two types of traffic are carried over the VNT: traffic from overlay networks and traffic from non-overlay networks, which are illustrated as solid and dashed arrows in Figure 3.1, respectively. We refer to “*overlay traffic*” as the traffic in the overlay network and to “*non-overlay traffic*” as the traffic in the non-overlay network. We also use the term “*underlay traffic*” for all traffic on the VNT, which contains both overlay and non-overlay traffic.

Figure 3.1 shows an example of a network. In this figure, the VNT that has six IP routers and nine links is configured on the WDM network that has six OXCs and six fibers. On the VNT, three overlay nodes, 1, 5, and 6, which are built on IP routers 1, 5, and 6, respectively, form an overlay network, and these nodes are interconnected with overlay links. Solid arrows show overlay traffic from overlay nodes 1 to 6, and dashed arrows show non-overlay traffic from IP routers 1 to 6. Routes for overlay traffic on an overlay network are determined by overlay routing. The overlay traffic in this figure is forwarded from overlay nodes 1 to 6 by relaying through overlay node 5. First, the overlay traffic is sent to overlay node 5. Overlay links are IP tunnels over the VNT in the sense that the traffic on the overlay links is forwarded on the VNT and their routes are determined by IP routing. Thus, the traffic on the overlay link between overlay nodes 1 and 5 is forwarded along the route determined by IP routing, that is, from IP routers 1 to 5 through router 2 on the VNT. The

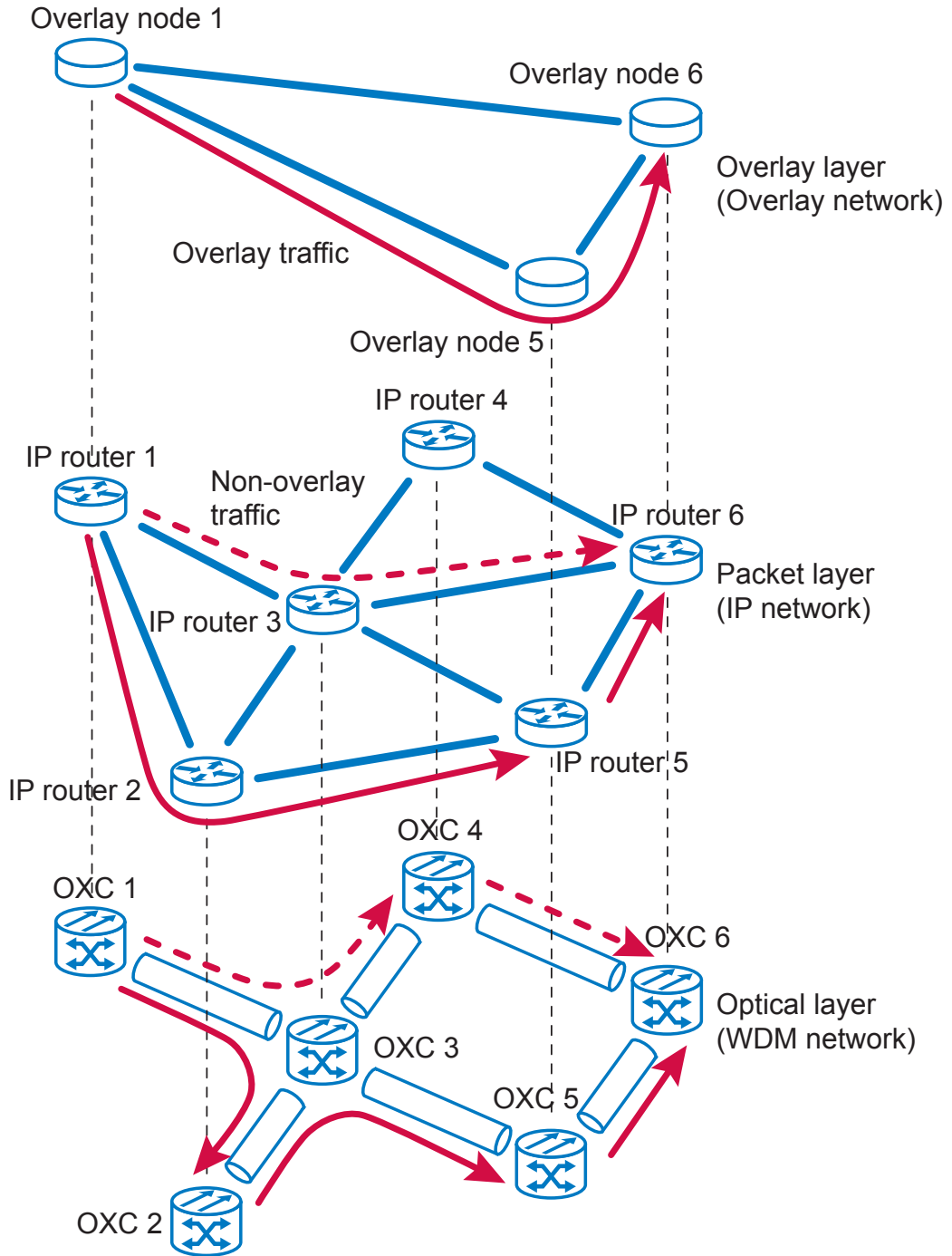


Figure 3.1: Example of network consisting of three layers: optical, packet, and overlay

overlay traffic is then forwarded from overlay nodes 5 to 6 in the same way. The non-overlay traffic is forwarded from IP routers 1 to 6 through router 3, which is also controlled by IP routing. The underlay traffic is transported on the WDM network in a similar way as that of the overlay traffic in the sense that lightpaths are transport tunnels over the WDM network and their routes are decided by layered traffic engineering. Thus, the underlay traffic from IP routers 1 to 3 is transported from OXCs 1 to 3 via OXC 2. In this chapter, we discuss an interaction between the overlay routing and layered traffic engineering through the IP layer. Before we introduce this interaction, we describe overlay routing and layered traffic engineering more precisely.

3.1.2 Overlay Routing

Several routing policies for overlay networks, such as overlay selfish routing and overlay optimal routing, have been proposed and evaluated in many papers [28, 30, 31]. We use overlay selfish routing, in which each overlay node selects the route that has the largest available bandwidth. This selection is done in a selfish manner aiming at maximizing the throughput experienced by the overlay nodes. The available bandwidth a_l on link l is calculated as $a_l = c_l - x_l$, where c_l is the capacity of link l , and that along route r is represented by $a(r) = \min_{l \in r}(a_l)$. The overlay network selects the route r that satisfies $a(r) = \max_{i \in R} a(i)$, where R denotes the set of all possible routes.

Several papers have proposed means for improving the performance of the overlay network by relaxing the selfishness or greediness of overlay routing [30, 31]. Moreover, selfish routing of which metric of the route selection is the available bandwidth is one of the greediest overlay routing services, as reported in [30]. In this chapter, since our objective is to obtain a robust layered traffic engineering method against selfish and greedy overlay networks, we use the overlay network that selects the route with the most available bandwidth and do not assume that it uses the previously mentioned cooperative approaches.

3.1.3 Layered Traffic Engineering

The VNT is configured on the basis of its performance objective by the layered traffic engineering method. Several performance objectives for selecting VNTs have been investigated in [4, 6, 7]. These investigations have aimed at minimizing the average weighted number of hops, minimizing the maximum link utilization, minimizing the average delay, and maximizing single hop traffic. Many layered traffic engineering algorithms for achieving those performance objectives have been

investigated [8, 11, 17, 61]. Since the link utilization directly affects the available bandwidth, which the overlay network seeks to optimize, we use algorithms for minimizing the maximum link utilization to investigate the interaction between overlay routing and layered traffic engineering. For minimizing the maximum link utilization, we investigated the MLDA (Minimum delay Logical topology Design Algorithm) [8] and the e-MLDA (extended MLDA) [11]. The MLDA aims to minimize average delay as its performance objective by solving the RWA problem, but the main objective for configuring VNTs is to minimize the maximum link utilization. The e-MLDA is proposed as an extension of the MLDA to ensure accommodation of the traffic demand. The e-MLDA also tries to decrease the maximum link utilization in the network by taking into account the minimum hop IP routing. All these algorithms configure VNTs on the basis of traffic demand to optimize their performance objectives. Note that layered traffic engineering cannot distinguish between the traffic demand caused by the overlay and non-overlay traffic. The layered traffic engineering uses only combined traffic demand, that is, the traffic demand caused by the underlay traffic. Hereafter, we refer to the traffic demand caused by overlay traffic, non-overlay traffic, and underlay traffic as “overlay traffic demand”, “non-overlay traffic demand”, and “underlay traffic demand”, respectively.

3.1.4 Model for Interaction between Layered Traffic Engineering and Overlay Routing

A model for evaluating an interaction between overlay routing and packet layer TE was introduced in [25]. Their model consists of an overlay layer and a packet layer. In this chapter, we introduce an optical layer to that model and evaluate the interaction between overlay routing and layered traffic engineering through the packet layer. Figure 3.2 shows our model. When the overlay network switches routes, the overlay traffic demand changes. In response to this traffic change, layered traffic engineering reconfigures its VNT. This reconfiguration updates the available bandwidth. The overlay network again switches to a new route that is superior to the previous one to improve the throughput of the overlay traffic. In our simulation experiments, each layer performs the above-mentioned actions and updates their status alternately. More specifically, overlay routing makes its decisions at odd rounds, and layered traffic engineering reconfigures its topology at even rounds. We use an OSPF routing protocol for the routing in the packet layer. Since the main purpose of our current research is to investigate the interaction between overlay routing and layered traffic

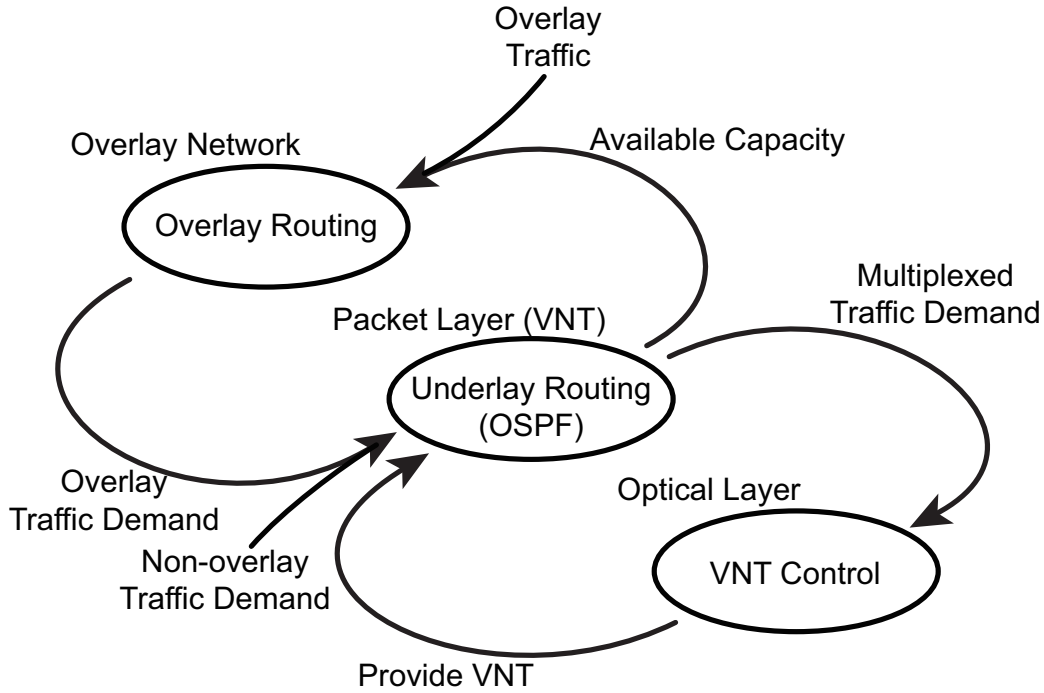


Figure 3.2: Interaction between layered traffic engineering and overlay routing

engineering, shortest hop paths are used for forwarding traffic on the packet layer.

3.1.5 Simulation Conditions

We evaluated the interaction described above with the maximum link utilization, which is the total amount of traffic on a link divided by its capacity, since the main objective of the MLDA and e-MLDA is to minimize the maximum link utilization. We noted that links are overloaded if the utilization exceeds 1, and in this case, no bandwidth is available at these links. We set the capacity of a lightpath to 1, that is, the link capacity was equivalent to the number of lightpaths, and all traffic used in our evaluation was normalized by the capacity of a lightpath.

In our simulation, the overlay network constructs a fully-connected topology in the same way as the environments described in [22, 28]. We also placed overlay nodes on all IP routers. Each overlay node independently searched for the route with the largest available bandwidth in a selfish manner. We assigned a proportion of the underlay traffic demand, D , as overlay traffic demand, D_o , and the rest as non-overlay traffic demand, D_n , that is, the traffic demand of the overlay traffic was

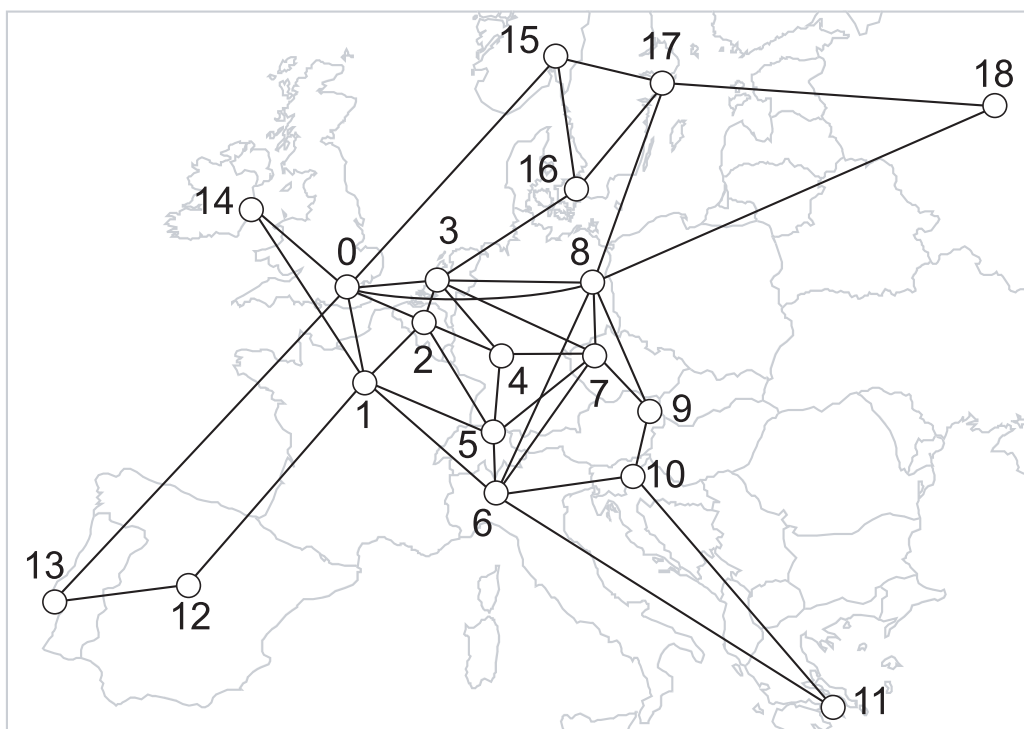


Figure 3.3: European Optical Network topology

$D_o = \alpha \cdot D$, and that of the non-overlay traffic was $D_n = (1 - \alpha) \cdot D$.

We used the European Optical Network (EON) topology with 19 nodes and 39 bidirectional links (Figure 3.3) for the physical topology. To simplify the interaction model, we did not take into account the wavelength continuity constraint in these experiments, that is, we assumed that all nodes have full wavelength converters on all input and output ports and each node has 8 ports for each direction (i.e., 8 input ports and 8 output ports). We used a randomly-generated traffic demand in the following evaluations.

3.1.6 Degradation of Underlay Network Performance

The main objective of this section is to discuss the influence that overlay routing has on layered traffic engineering. For the purposes of comparison, we used fiber topologies, on which lightpaths are statically configured on a single fiber, i.e., the VNT is equivalent to the physical topology, and the configured topology is fixed.

We show the maximum link utilization in Figure 3.4. In this figure, the horizontal axis shows

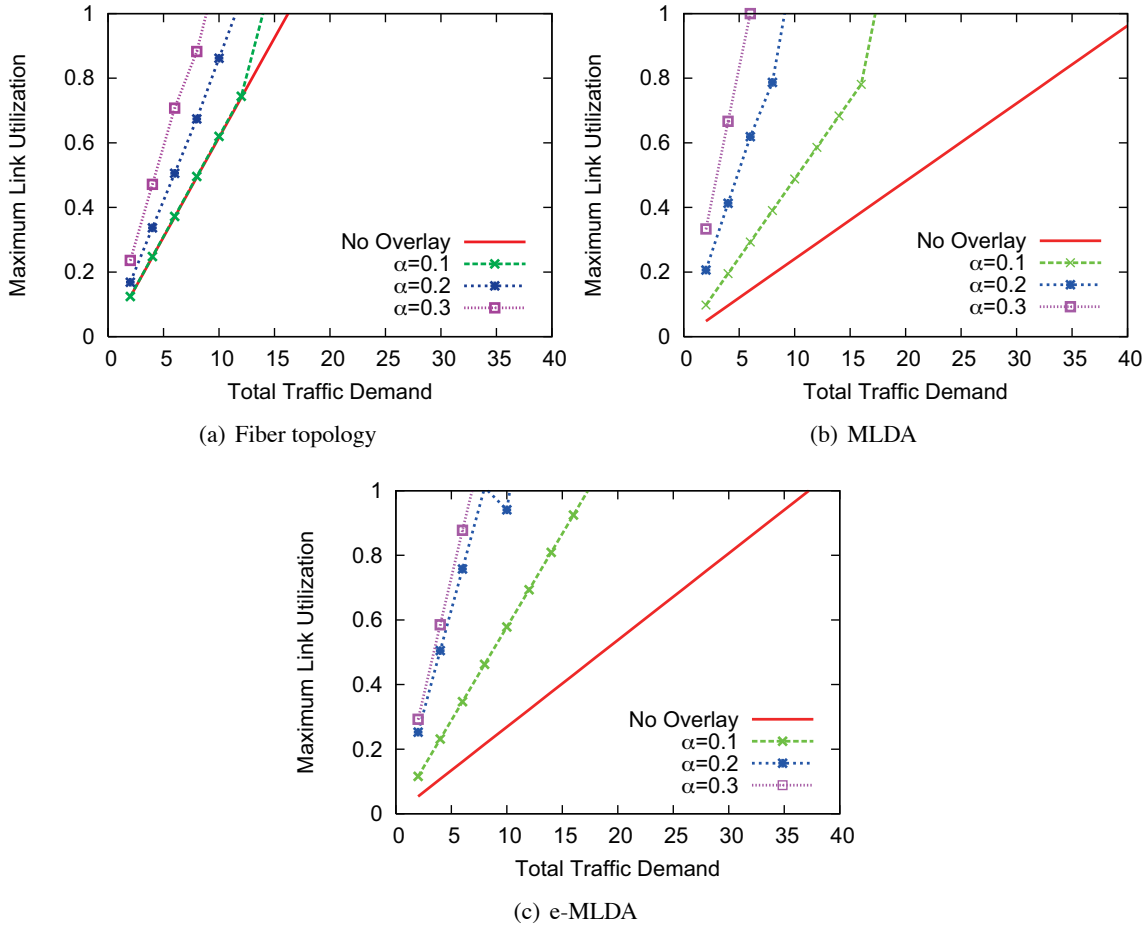


Figure 3.4: Maximum link utilization

the total amount of traffic demand, and the vertical axis shows the maximum link utilization. We observed that the maximum link utilization increases as the proportion of the overlay traffic increases in the case of all the layered traffic engineering algorithms. With a small amount of overlay traffic ($\alpha = 0.1$), the maximum link utilization of the MLDA and e-MLDA with overlay traffic is twice as large as the result without overlay traffic, and a slight degradation is observed in the case of the fiber topology. Although the utilization of the fiber topology gets larger as α increases, the utilization of the MLDA and e-MLDA increases much more severely compared with the result of the fiber topology. This degradation is caused by two factors. One is due to the interaction between overlay nodes, and the other is due to the interaction between overlay routing and layered traffic engineering. We refer to the interaction between overlay routing and layered traffic engineering as

the “*vertical interaction*” and the interaction between overlay nodes as the “*horizontal interaction*”. Note that only the horizontal interaction appears in the fiber topology since no VNT reconfiguration occurs. In the case of the MLDA and e-MLDA, both the vertical interaction and horizontal interaction degrade the maximum link utilization since a VNT is reconfigured in response to the dynamics of overlay routing. By comparing the results of the MLDA or e-MLDA with the results of the fiber topology, we can see that the vertical interaction has more effect than the horizontal interaction on the degradation of the maximum link utilization.

3.1.7 Instability of Underlay Network State

In the previous section, we showed that the vertical interaction between overlay routing and layered traffic engineering degraded the maximum link utilization. In this section, we show that the coexistence of both overlay routing and layered traffic engineering leads to layered traffic engineering instability.

Figure 3.5 shows that the maximum link utilization depends on the rounds at which layered traffic engineering or overlay routing takes their actions. As we described above, for the all layered traffic engineering methods, the maximum link utilization increases if the amount of the overlay traffic is larger than 0.1. Therefore, we set α to 0.2, as shown in this figure, and looked for causes of the degradation mentioned above. When a VNT is dynamically controlled, (i.e., the MLDA or e-MLDA is applied), the fluctuation of the maximum link utilization is larger and the cycle of the fluctuation is irregular. That is, the network becomes unstable due to the vertical interaction.

Figure 3.6 shows the fluctuation of the traffic volume on each link. The error bars show the maximum and minimum values of the traffic volume in the evaluation, and a point in the bar indicates the average value during the simulation. The horizontal axis represents the link index that is specified uniquely by the source-destination pair. For the all VNTs, the traffic volume of almost all links fluctuates. This result indicates that the horizontal interaction fluctuates the traffic volume on each link. However, the vertical influence is significant in the traffic demands for source-destination pairs on the VNT. Figure 3.7 shows the maximum, minimum, and average traffic demand for each node pair. We also observed that the traffic demand fluctuates drastically when the VNT is dynamically controlled via the MLDA or e-MLDA. If overlay routing and layered traffic engineering coexist on the same network, the network state becomes unstable and its performance is drastically degraded. The main reason for this instability is that the layered traffic engineering algorithms generate VNTs

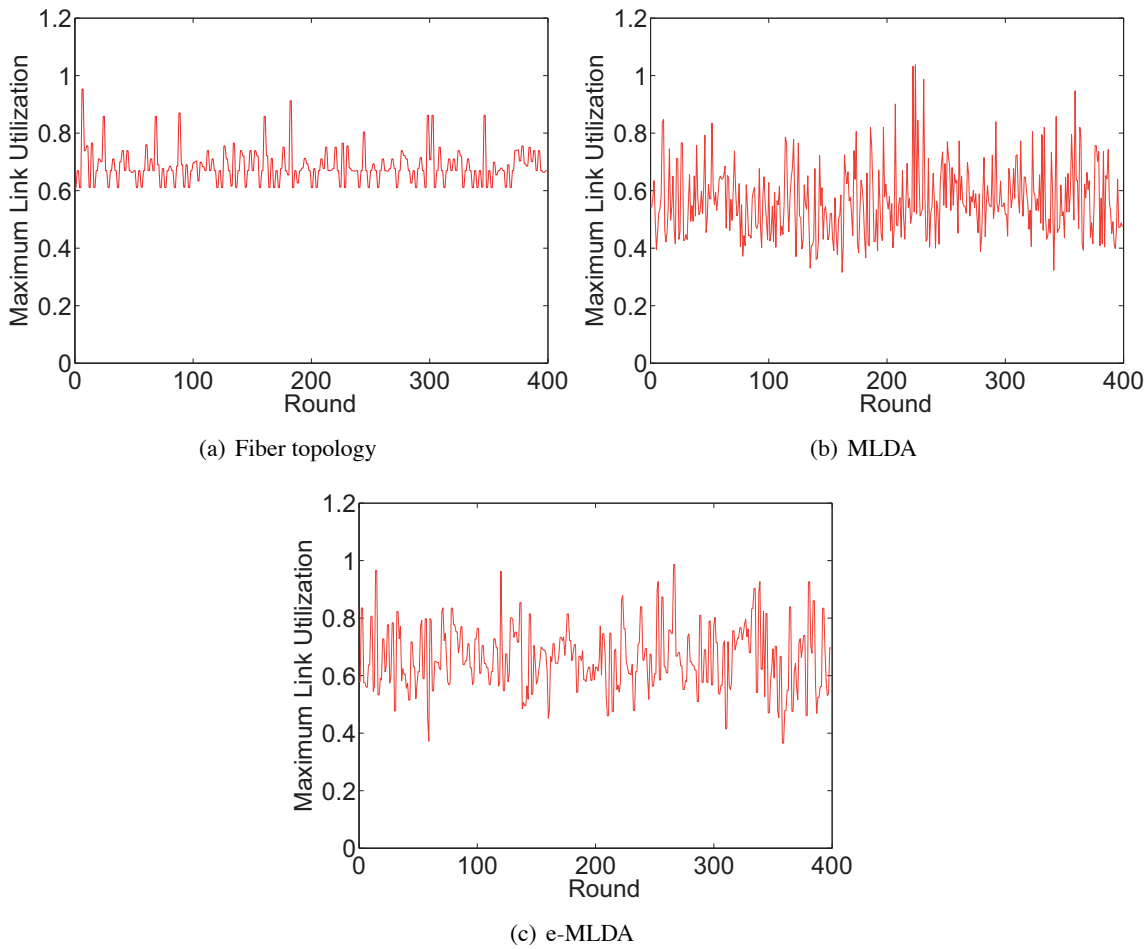
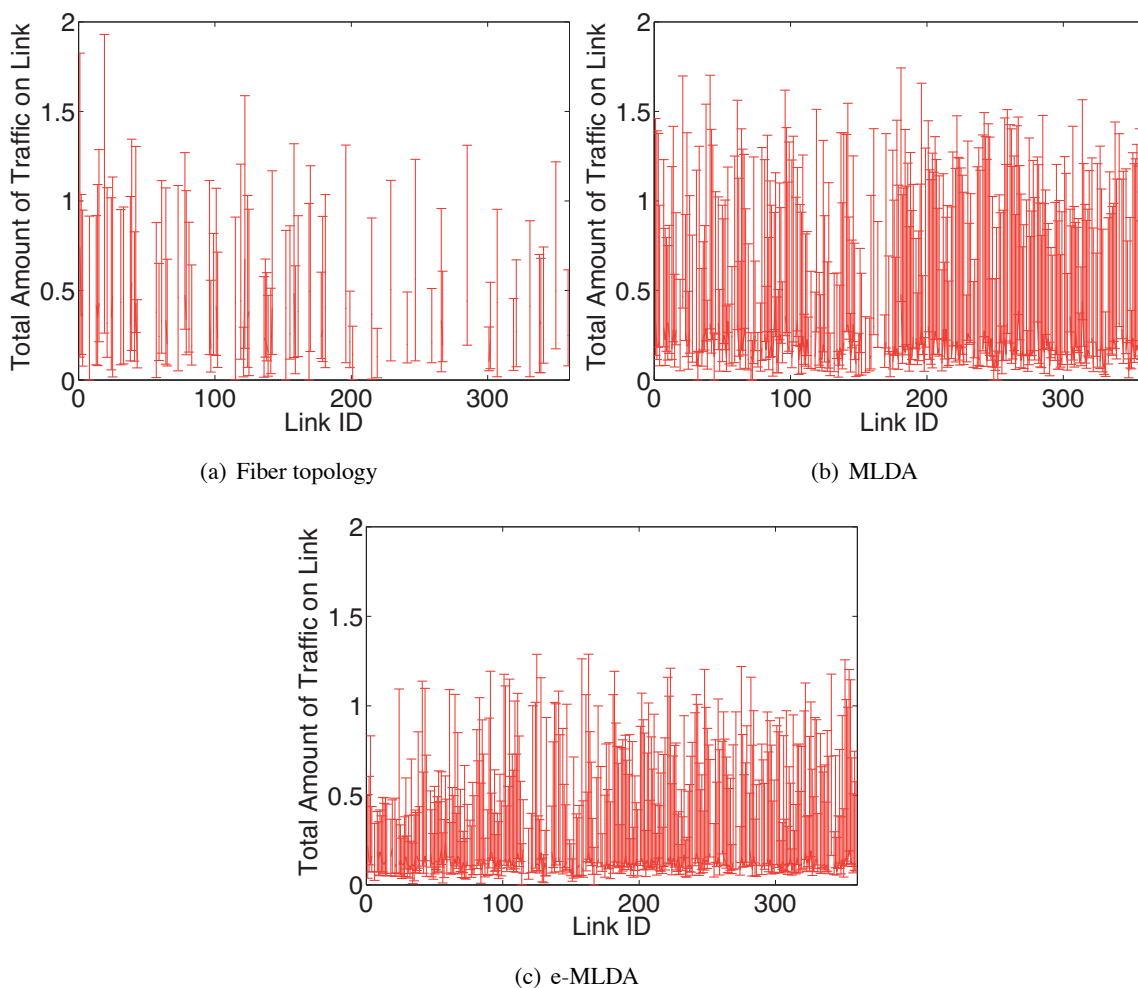


Figure 3.5: Fluctuation of maximum link utilization ($\alpha = 0.2$, total traffic: 10)

on the basis of the current traffic demand. As shown in Figure 3.7, if there is selfish overlay routing in the network, the traffic demand drastically changes. Since the traffic demand is the most important input parameter for designing VNTs, traffic demand fluctuation leads to a significant layered traffic engineering instability.

Figure 3.6: Traffic volume on each link ($\alpha = 0.2$, total traffic: 10)

3.2 Improving Stability of Network State

3.2.1 Hysteresis

In this section, we apply *hysteresis* to layered traffic engineering in order to overcome the problem of vertical interaction. Hysteresis is the property of systems that do not immediately react to forces applied to them. This property is often used to avoid routing fluctuation [22, 30, 62].

As discussed in the previous section, the traffic demand heavily fluctuates in the case that overlay routing and layered traffic engineering coexist. Because the traffic demand is the input parameter of the layered traffic engineering algorithms, applying hysteresis to the traffic demand in order to

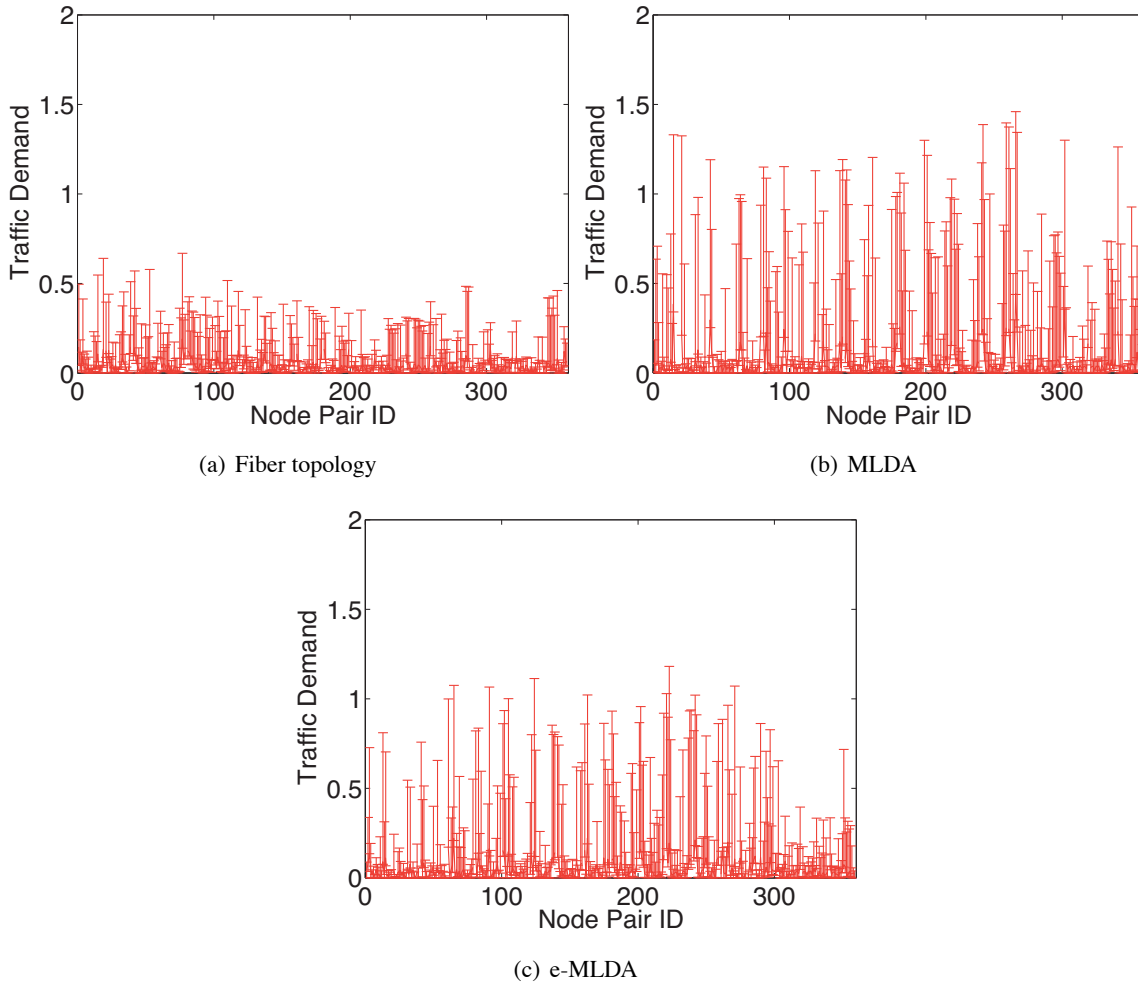


Figure 3.7: Fluctuation of traffic demand ($\alpha = 0.2$, total traffic: 10)

suppress the influence imposed by overlay routing is one possible application. We refer to this application as “*demand hysteresis*”. Another application is *utilization hysteresis*, in which the hysteresis property is used for the maximum link utilization. In the case of utilization hysteresis, the current VNT is kept if the improvement in the link utilization of the new VNT is less than a particular hysteresis threshold. We expect this leads to a decrease in the number of VNT reconfigurations. We describe each application in more detail in the following sections.

Demand Hysteresis

Demand hysteresis works as follows. Let $D(t) = \{d_p(t)\}$ denote the traffic demand for node pair p at the round t and $D(t-2)$ denote the previously observed traffic demand at round $t-2$. Note that the overlay network updates its routes at round $t-1$. We first temporarily calculate a VNT $C^h(t)$ using the current traffic demand $D(t)$. The VNT $C^h(t)$ is represented by a set of $c_p^h(t)$, where $c_p^h(t)$ is the capacity between node pair p at round t . We then compare the traffic demand $d_p(t)$ with $d_p(t-2)$ for each node pair. If the current traffic demand $d_p(t)$ decreases below the ratio of H_l or increases above the ratio of H_u , we use $c_p^h(t)$ as the new capacity for node pair p . Otherwise, $c_p(t-2)$ is kept. More precisely, $c_p(t)$, where $C(t) = \{c_p(t)\}$ is the VNT that is actually used as the IP layer topology, is updated by the following equations.

$$c_p(t) = \begin{cases} c_p^h(t) & \text{if } d_p(t) > (1 + H_u) \cdot d_p(t-2) \\ c_p^h(t) & \text{if } d_p(t) < (1 - H_l) \cdot d_p(t-2) \\ c_p(t-2) & \text{otherwise} \end{cases}$$

Demand hysteresis is aimed at stabilizing layered traffic engineering by absorbing the fluctuation of the traffic demand and reduces unnecessary topology changes. That is, layered traffic engineering, to which demand hysteresis is applied, reacts slowly against the heavy fluctuation of the traffic demand.

Utilization Hysteresis

Utilization hysteresis works as follows. Similar to demand hysteresis, we first temporarily calculate the VNT, $C^h(t)$, using the current traffic demand $D(t)$. We then calculate the expected link utilization $U^h(t)$ using $D(t)$ and $C^h(t)$. We next compare the maximum link utilization $\max(U^h(t))$ with $\max(U(t-1))$, where $U(t-1)$ is the link utilization after the overlay network updates its route. If the improvement in the maximum link utilization is larger than the ratio of H , we use $C^h(t)$ as the new VNT. Utilization hysteresis is formulated as follows.

$$C(t) = \begin{cases} C^h(t) & \text{if } \max(U^h(t)) < (1 - H) \cdot \max(U(t-1)) \\ C(t-2) & \text{otherwise} \end{cases}.$$

Utilization hysteresis stabilizes layered traffic engineering by keeping the current VNT if there is little benefit of changing to the new VNT.

3.2.2 Performance Evaluation

We evaluated demand hysteresis and utilization hysteresis via computer simulations. We used the same simulation model as presented in Section 3.1, but in this section, the MLDA is selected as the layered traffic engineering algorithm. In obtaining the following figures, the hysteresis mechanisms are not applied during the first 20 rounds to disregard the transient phase. Figures 3.8 and 3.9 show the fluctuation of the maximum link utilization when utilization hysteresis and demand hysteresis are applied. The vertical axis shows the maximum link utilization, and the horizontal axis shows the rounds. Looking at these figures, we observe that the maximum utilization with utilization hysteresis is stable compared to that without hysteresis. However, in contrast to utilization hysteresis, the maximum utilization still fluctuates for demand hysteresis. The main purpose of demand hysteresis is to decrease the number of changed lightpaths by absorbing the fluctuation of the traffic demand caused by overlay routing. However, decreasing the number of changed lightpaths cannot lead to an improvement in the stability of the maximum link utilization. To explain this more clearly, we evaluated two hysteresis applications, and we compared the number of changed lightpaths to investigate the efficiency of demand hysteresis. The results of our evaluation are shown in Figures 3.10 and 3.11. We define the number of changed lightpaths at round t as $\sum |c_e(t) - c_e(t-2)|$. The number of changed lightpaths is decreased by more than 50% in the case that demand hysteresis is applied. However, demand hysteresis cannot make the number of changed lightpaths zero since traffic demand still fluctuates due to the selfish behavior of overlay routing. In the case of utilization hysteresis, the number of changed lightpaths is always zero if layered traffic engineering maintains the current VNT. These results show that the changes in the VNT lead to the fluctuation of the maximum link utilization, even if those changes are small.

More detailed observations of these figures show that the performance does not strongly depend on the decision of the hysteresis threshold H in the case that utilization hysteresis is applied. If a large hysteresis threshold H is used, the layered traffic engineering does not immediately react against the changes in the network environments. This means that a large H leads to a worse performance since the VNT configured for the previously observed traffic demand is kept. However, the results shown in Figure 3.8 are different from expected results. We changed the ratio of overlay

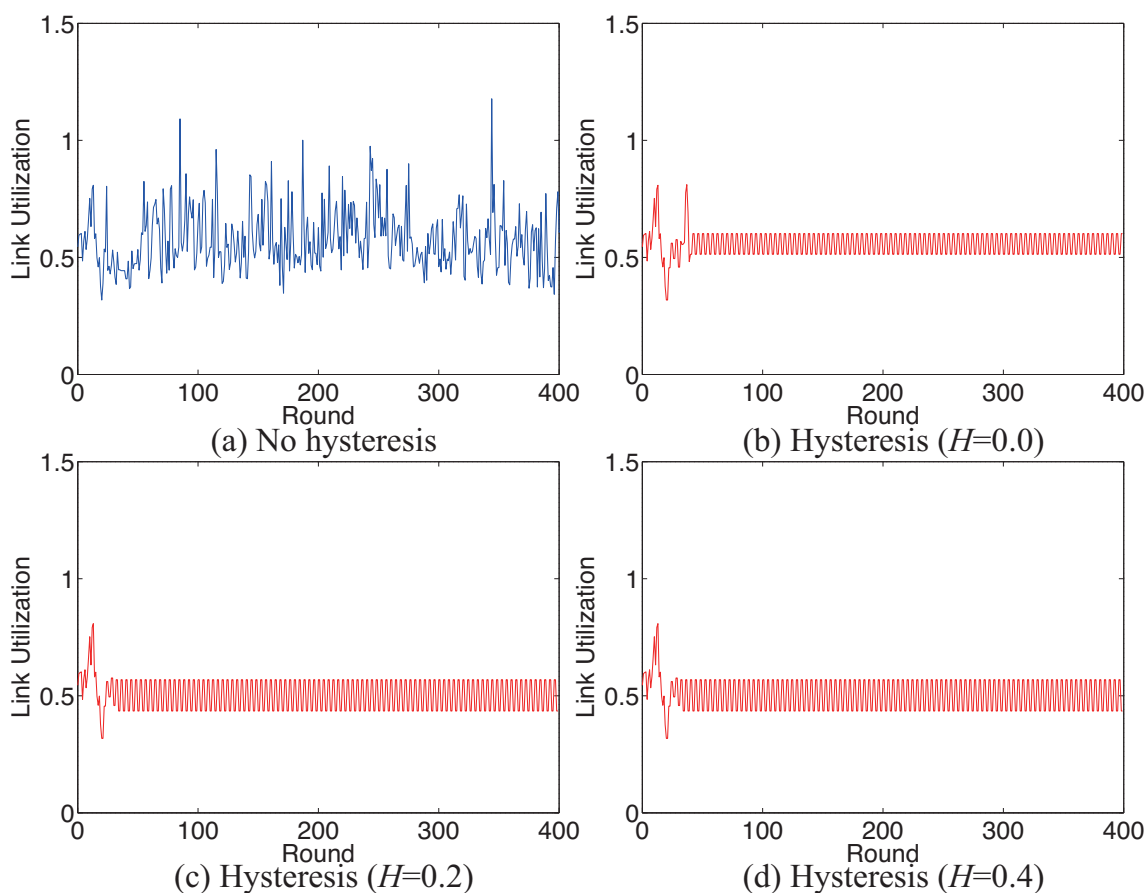


Figure 3.8: Fluctuation of maximum link utilization (Utilization hysteresis, $\alpha = 0.2$, total traffic: 10)

traffic α from 0.2 to 0.3 in Figures. 3.12 and 3.13. In Figure 3.12, the maximum link utilization of $H = 0.0$ is the lowest, while the utilization of $H = 0.0$ in Figure 3.8 is the highest. Moreover, the average maximum link utilization with hysteresis is worse than that without hysteresis. These results show that the network performance does not strongly depend on the hysteresis threshold H itself. The layered traffic engineering method with demand hysteresis ($\alpha = 0.3$), the results of which are shown in Figure 3.13, does not lead to a stable state. Since demand hysteresis is not effective compared with utilization hysteresis, in the next section, we will focus on utilization hysteresis and extend it to avoid slipping into undesirable stable states.

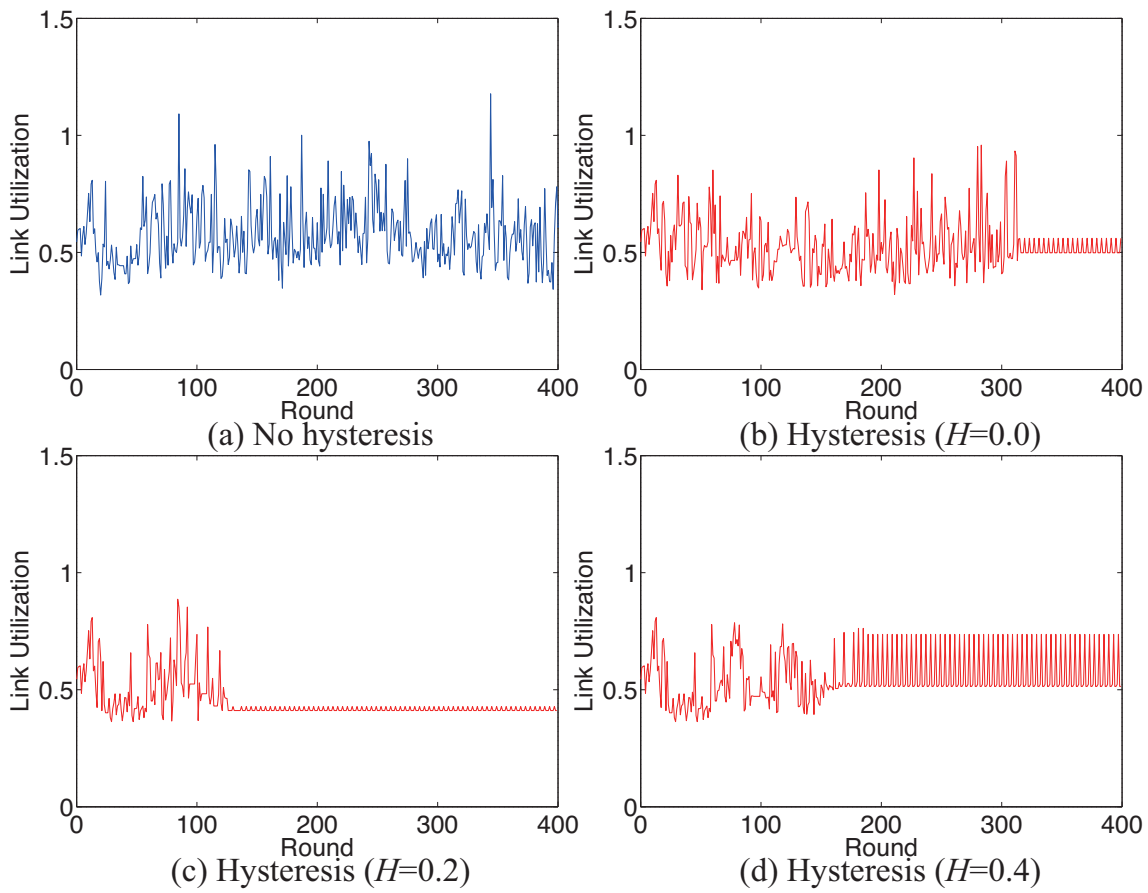


Figure 3.9: Fluctuation of maximum link utilization (Demand hysteresis, $\alpha = 0.2$, total traffic: 10)

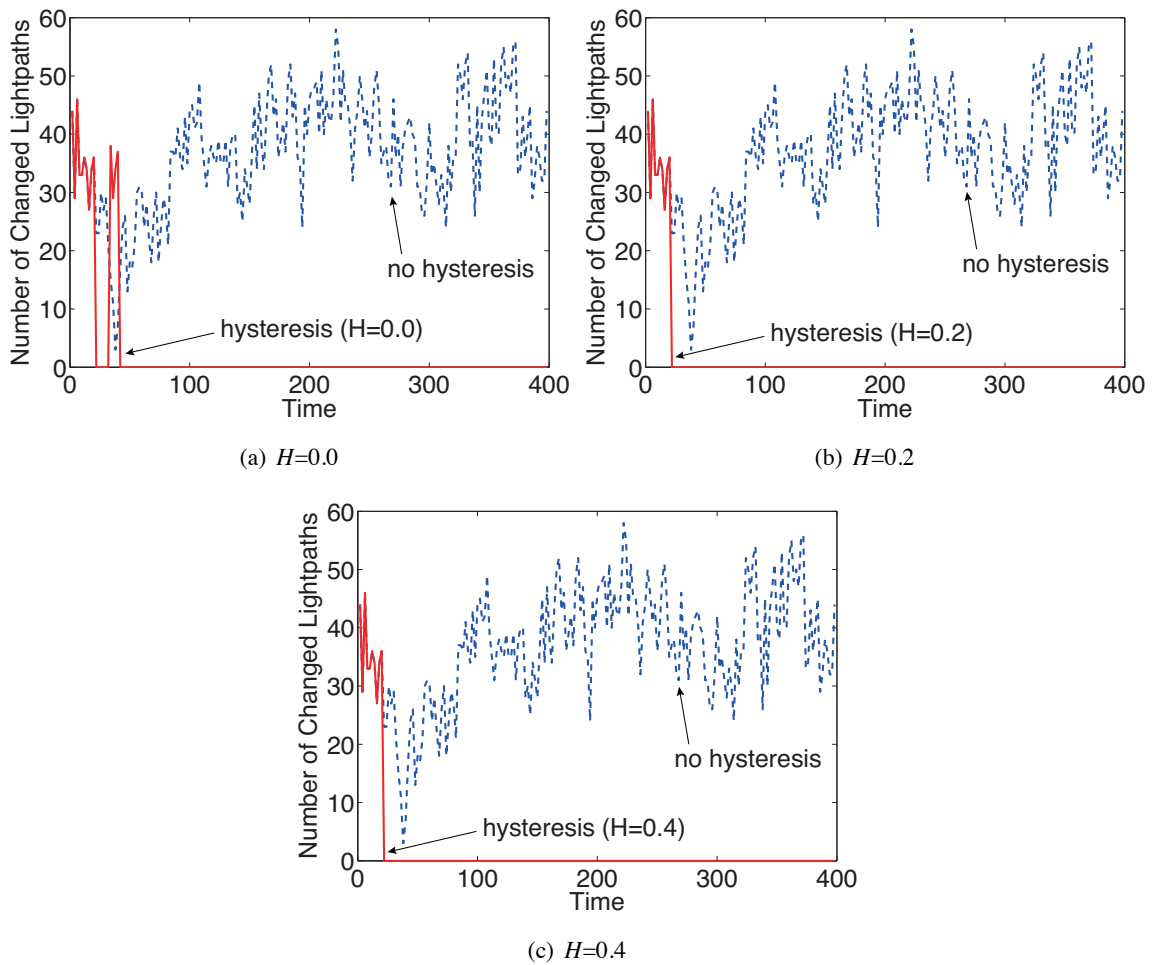


Figure 3.10: Number of changed lightpaths (Utilization hysteresis, $\alpha = 0.2$, total traffic: 10)

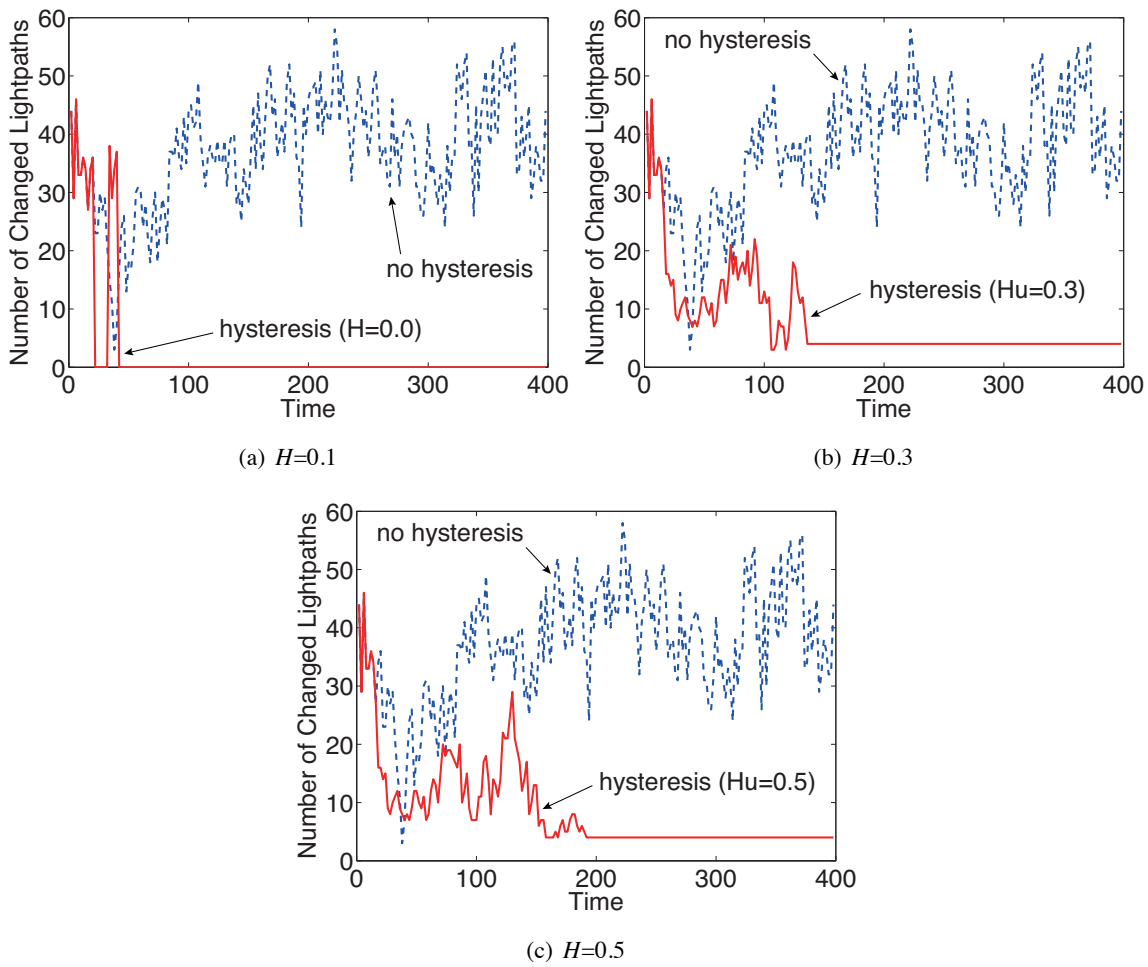


Figure 3.11: Number of changed lightpaths (Demand hysteresis, $\alpha = 0.2$, total traffic: 10)

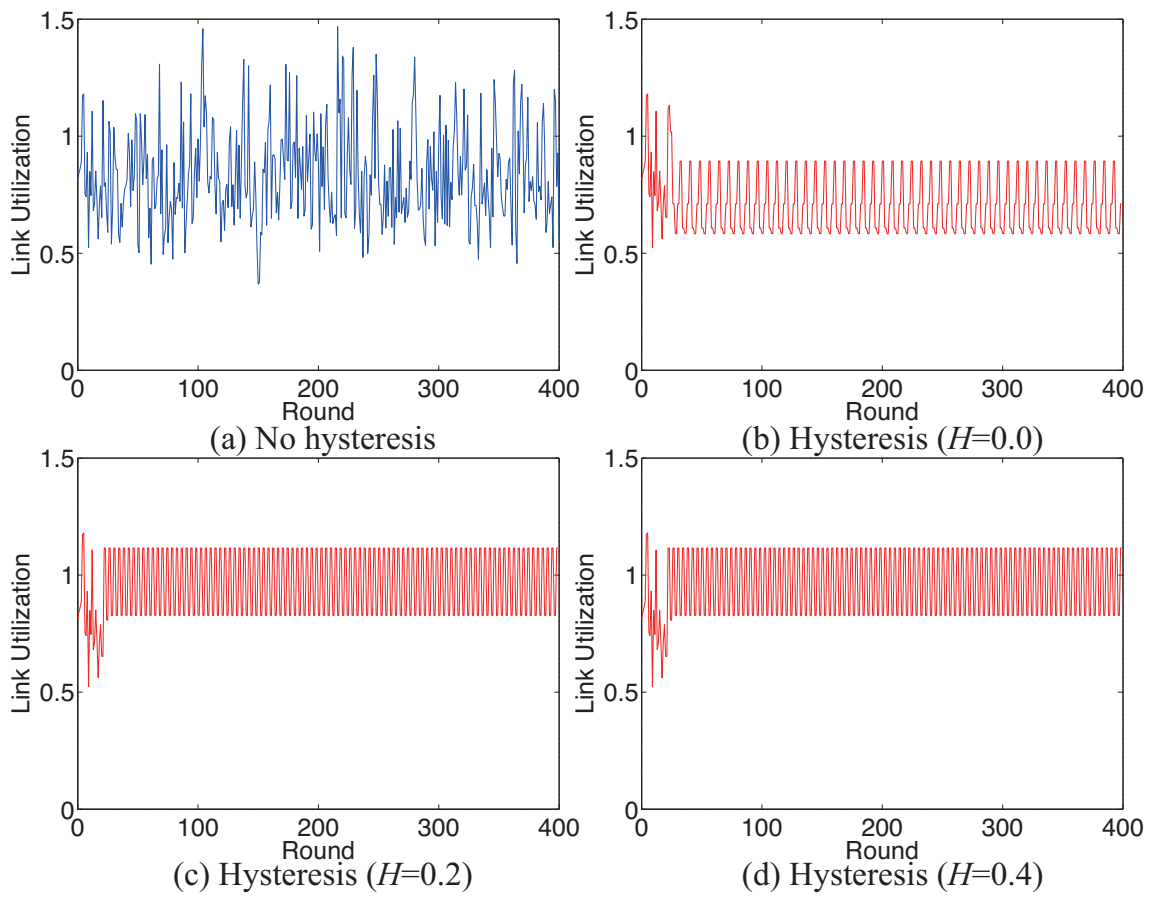


Figure 3.12: Fluctuation of maximum link utilization (Utilization hysteresis, $\alpha = 0.3$, total traffic: 10)

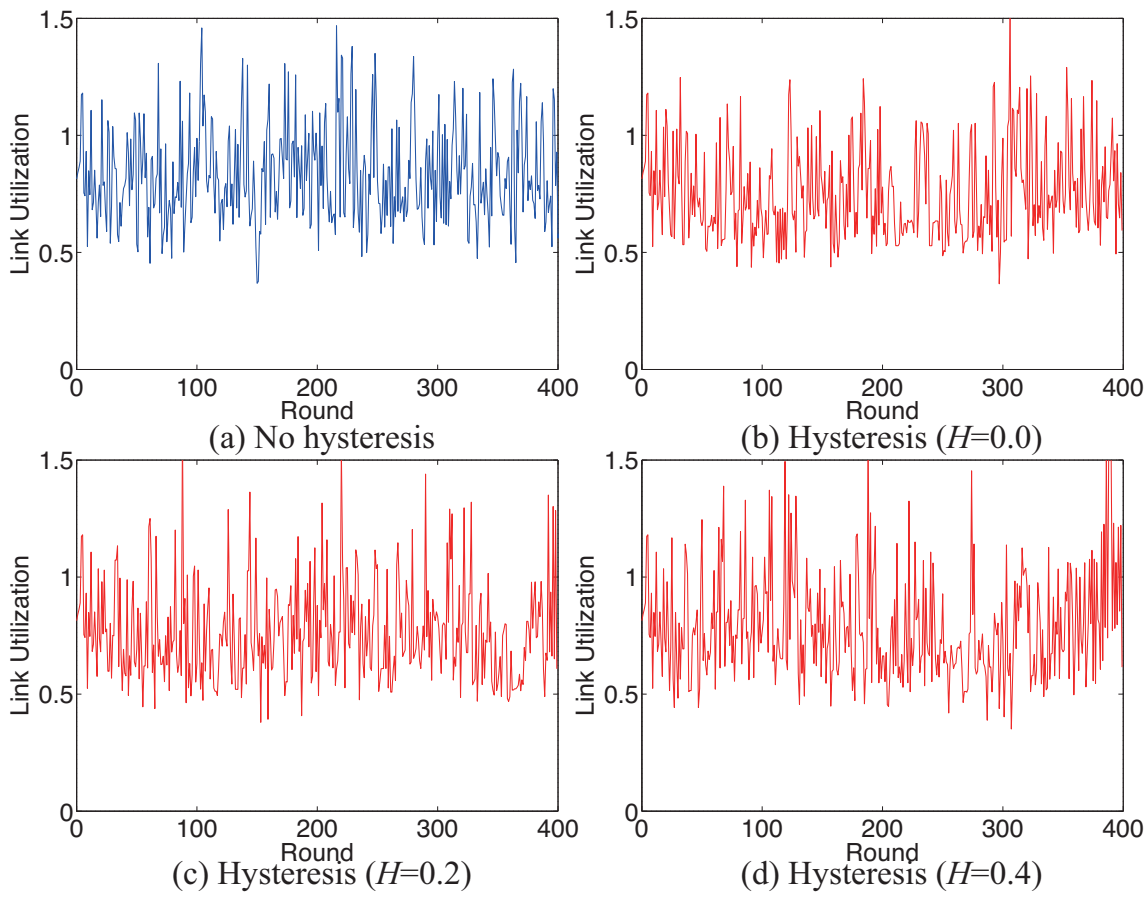


Figure 3.13: Fluctuation of maximum link utilization (Demand hysteresis, $\alpha = 0.3$, total traffic: 10)

3.3 Improving Network Performance

Applying utilization hysteresis to layered traffic engineering can improve the stability of the network, but cannot always improve the performance, as discussed in the previous section. In this section, we extend utilization hysteresis to improve both the stability and performance.

3.3.1 Two-State Utilization Hysteresis

As we discussed in Section 3.2, utilization hysteresis can improve the network stability, but cannot always converge to a state that has lower maximum link utilization. Route flapping occurs, and the routes of the overlay network oscillate between approximately two routes, which results in high link utilization and relatively low link utilization if the VNT is fixed. Hence, the method with utilization hysteresis causes the layered traffic engineering to slip into a stable state when the hysteresis decides to continue using the current VNT for two consecutive rounds of layered traffic engineering. Therefore, we extended utilization hysteresis, called “*two-state utilization hysteresis*”, to prevent layered traffic engineering from slipping into a stable state when the maximum link utilization is high. To do this, we introduced another threshold θ that determines whether utilization hysteresis is applied or not. If the current maximum link utilization u is higher than θ , utilization hysteresis is not applied to layered traffic engineering so that it does not slip into an undesirable state, where u is high. Otherwise, utilization hysteresis, described in Section 3.2, is performed. We define the threshold $\theta = u_l + (u_u - u_l)/k$, where u_l and u_u are the minimum and maximum value of the maximum link utilization obtained up to this point, respectively, and k is a control parameter for adjusting θ . The utilizations u_l and u_u are updated every time layered traffic engineering is performed. When u is higher than θ , layered traffic engineering regards the maximum link utilization of the current VNT as high. In this case, utilization hysteresis is not applied to layered traffic engineering, and the VNT is immediately reconfigured so that it does not slip into a stable state that has high maximum link utilization. Then layered traffic engineering again searches for another stable state where the maximum link utilization is sufficiently low.

3.3.2 Performance Evaluation

We evaluated two-state utilization hysteresis under the same simulation model as the one described in the previous section. The simulation parameters were set to the same as those in Figure 3.12.

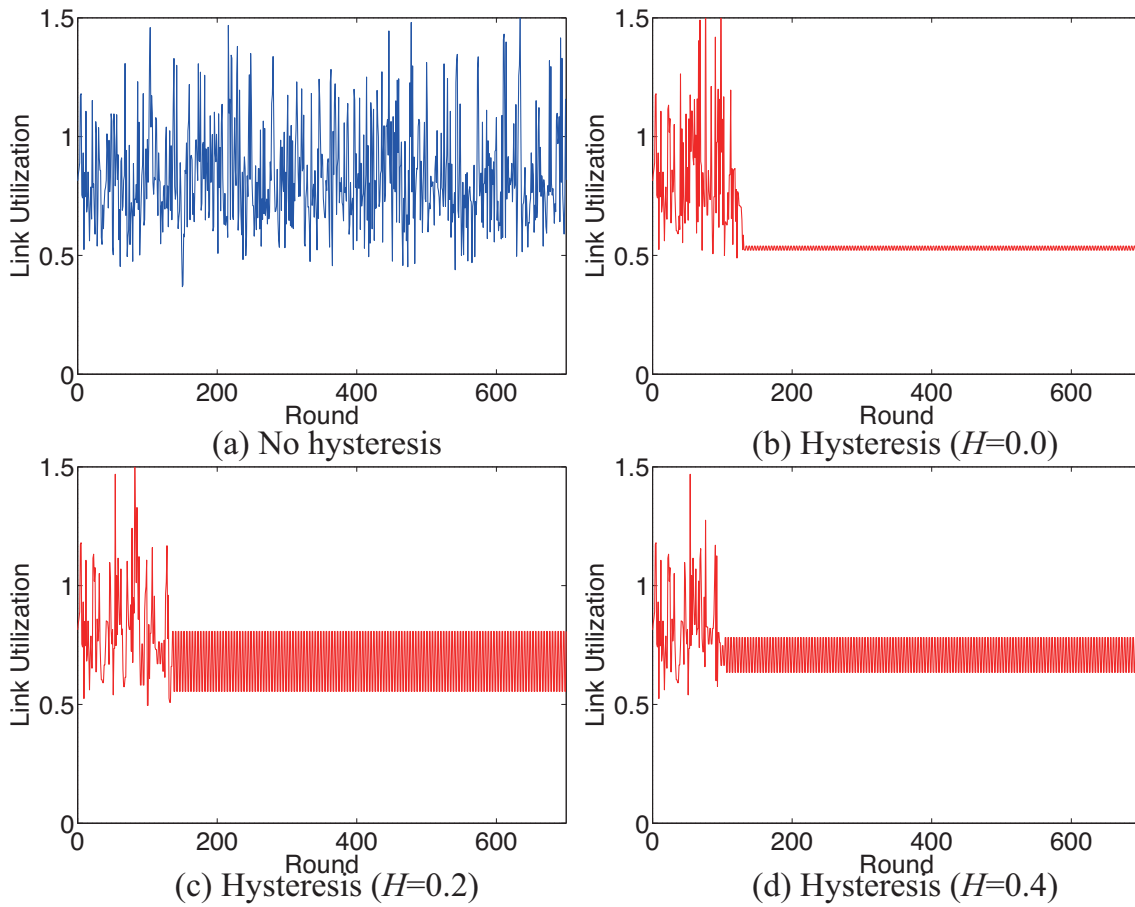


Figure 3.14: Fluctuation of maximum link utilization (Two-state utilization hysteresis, $\alpha = 0.3$, total traffic: 10, $k = 3.0$)

Figures 3.14 and 3.15 respectively show the fluctuation of the maximum link utilization in the case that k is 3.0 and 5.0. These figures clearly show that layered traffic engineering becomes stable and the maximum link utilization is lower than that shown in Figure 3.12. However, these figures also show that the convergence time, which is defined as the period of time before the VNT is stable, becomes longer than that shown in Figure 3.12. This is because a larger value of k places more restriction on the region where utilization hysteresis is applied and thus seeking a stable state that has lower maximum link utilization is difficult. In the next section, we show another extension that shortens the convergence time.

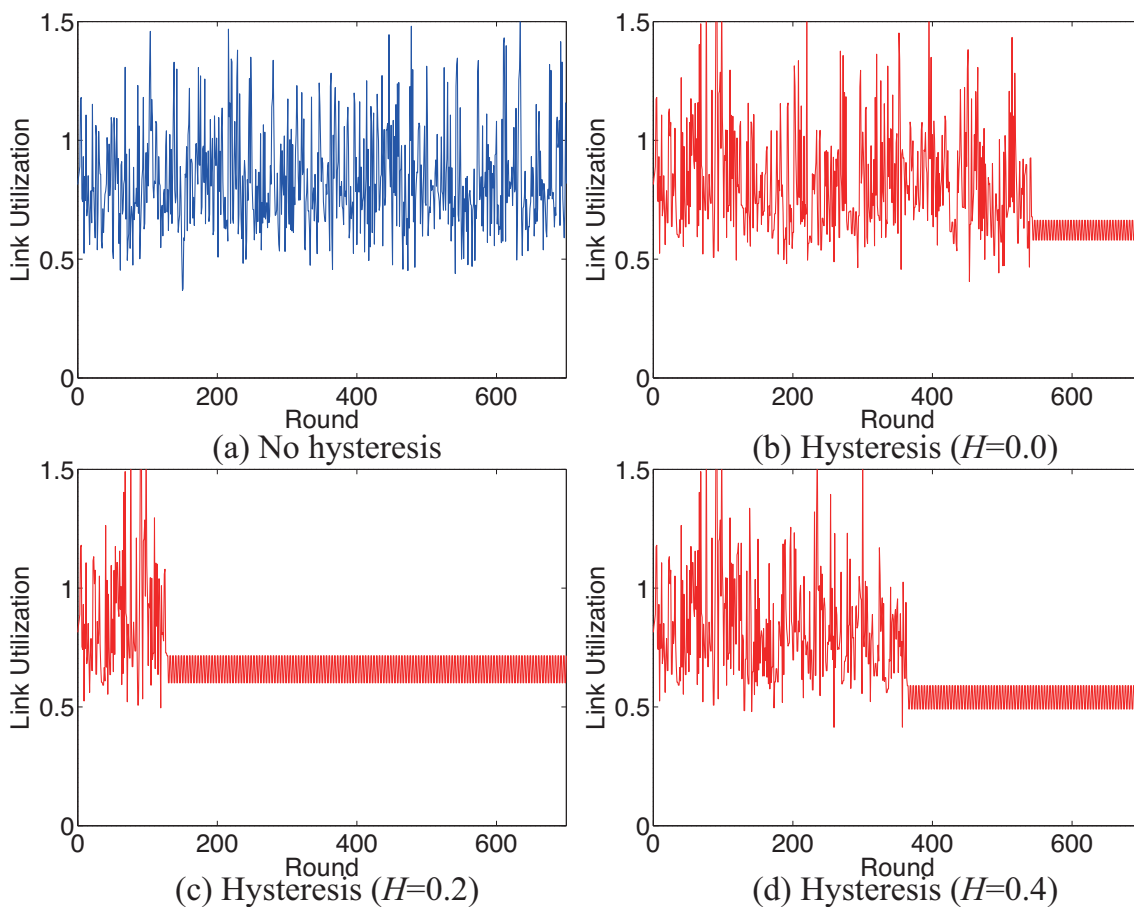


Figure 3.15: Fluctuation of maximum link utilization (Two-state utilization hysteresis, $\alpha = 0.3$, total traffic: 10, $k = 5.0$)

3.4 Enhancing Adaptability to Fluctuations in Traffic Demand

In this section, we introduce a *filtering* method to achieve fast convergence of layered traffic engineering with two-state utilization hysteresis.

3.4.1 Filtering

As mentioned in the previous section, the convergence time is longer if the layered traffic engineering method with two-state utilization hysteresis is used. Since two-state utilization hysteresis restricts the region in which utilization hysteresis is applied, the chances that layered traffic engineering converges to a stable state decrease and therefore the convergence time becomes longer.

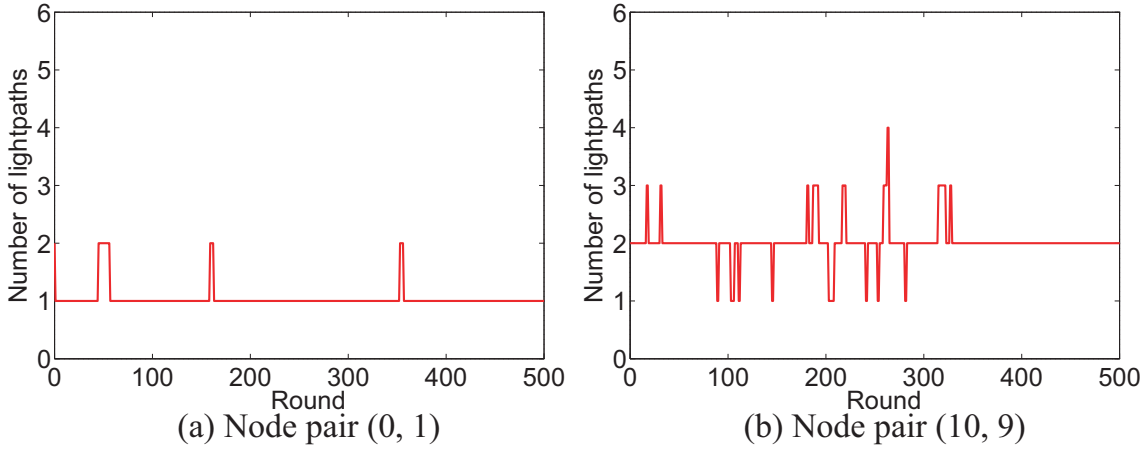


Figure 3.16: Number of lightpaths ($\alpha = 0.3$, total traffic: 10, $k = 5.0$)

When utilization hysteresis is not applied due to the high maximum link utilization, the VNT is re-configured in the same way as the layered traffic engineering method without utilization hysteresis. These changes in the VNTs lead to network instability. To achieve fast convergence, a mechanism to reduce the changes in VNTs is needed.

To investigate changes in VNTs in more detail, we observed the number of lightpaths between node pairs. We selected two node pairs that have a typical tendency, and we show the results of using these node pairs in Figure 3.16. Node ID in this figure is shown in Figure 3.3. The horizontal axis shows the rounds, and the vertical axis shows the number of lightpaths between a node pair. In Figure 3.16(a), one lightpath is configured from node 0 to 1 at most rounds, and the number of lightpaths finally converges to 1; however, only at rounds 60, 160, and 350, are two lightpaths configured. In Figure 3.16(b), two lightpaths are configured at almost all the rounds, and the number of lightpaths finally converges to 2, although the number of lightpaths decreases or increases in a short period. We find these results in more than half of all the node pairs. We refer to these small changes in the number of lightpaths as “spike lightpath changes”. These multiple spike lightpath changes lead to a large change in VNT and the network instability.

To achieve fast convergence of layered traffic engineering, we introduced a filtering method to layered traffic engineering that reduces the spike lightpath changes. The layered traffic engineering method with filtering remembers the number of lightpaths that the layered traffic engineering method has calculated, that is, $C^h(t) = \{c_p^h(t)\}$, described in Section 3.2. Here, the history of the past T rounds of the layered traffic engineering method is maintained, $(C^h(t-2), C^h(t-4), \dots, C^h(t-$

2T)). If n lightpaths were configured between a node pair p at more than $x\%$ of rounds in this history, the number of lightpaths between p is set to n , even if $c_p^h(t)$ is different from n . This is how the filtering method reduces the spike lightpath changes and thus achieves fast convergence. In the following subsection, we show that the filtering method reduces the convergence time of layered traffic engineering.

3.4.2 Performance Evaluation

We evaluated the filtering method under the same simulation environments as those described in the previous section. The simulation parameters were set to the same as those in Figure 3.15. The convergence time in Figure 3.17(b) is 72% shorter than that in Figure 3.15(a). In the case that $H = 0.4$, the convergence time with the filtering method is also 71% rounds shorter than that without the filtering method. The maximum link utilization in the stable state is almost the same since the filtering method only reduces the spike lightpath changes, and the generated VNT is almost the same as the VNT generated by layered traffic engineering without the filtering method. These results show that the filtering method enhances the feasibility of the real network by reducing the convergence time.

We next evaluated adaptability for changes in the traffic demand in the situation when the traffic demand is dynamically changed. To evaluate the adaptability, we randomly generated the traffic demand at the same interval of rounds while keeping the sum of the traffic demand constant. We refer to this interval as the “changing interval”. The other simulation conditions we used are the same as those described in the previous section. Figure 3.18 shows that the maximum link utilization depends on the rounds for $k = 3.0$. In the case that the changing interval is 40, i.e., 20 VNT reconfigurations, layered traffic engineering follows almost all the changes in the traffic demand. However, only at rounds 1440 and 1480 does the layered traffic engineering not converge until the next traffic change occurs. If the changing interval is longer than 40, layered traffic engineering converges, although the maximum link utilization fluctuates for a short period after the traffic change occurs. We next evaluated the adaptability for $k = 5.0$. The results of our evaluation are shown in Figure 3.19. layered traffic engineering cannot follow the changes in the traffic demand in the case that the changing interval is 40. As we mentioned in Section 3.3, the region where hysteresis is applied becomes narrow and therefore the convergence time becomes longer if the large k is used. This also leads to the degradation of the adaptability for the traffic changes. In the case that the

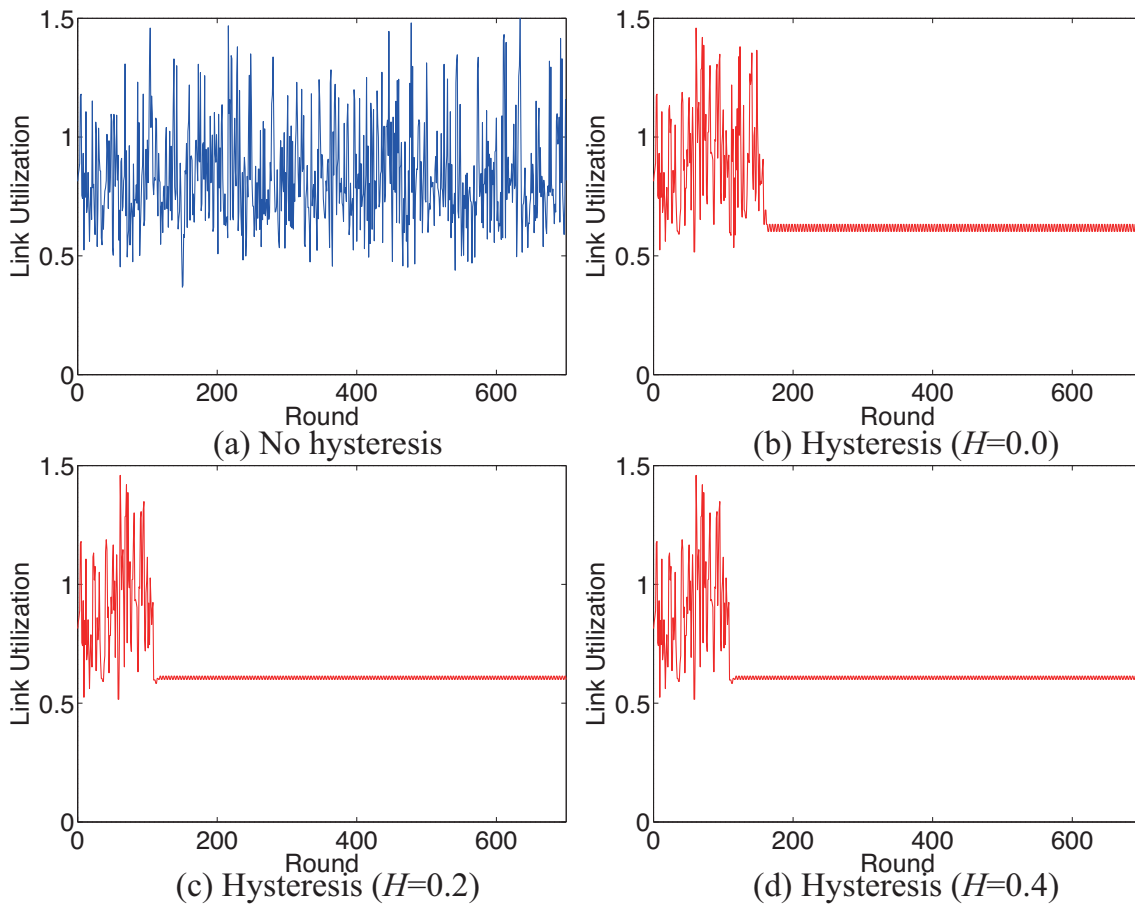


Figure 3.17: Fluctuation of maximum link utilization (Two-state utilization hysteresis, filtering, $\alpha = 0.3$, total traffic: 10, $k = 5.0$)

changing interval is 100, layered traffic engineering follows almost all the changes in the traffic demand except at round 200. Although our methods do not always follow extremely heavy changes in the traffic demand, they follow almost all the changes. The reason for this is that layered traffic engineering with the hysteresis mechanism reconfigures its VNT immediately to adapt to changes in the traffic demand if the performance of the VNT is degraded due to changes in the traffic demand.

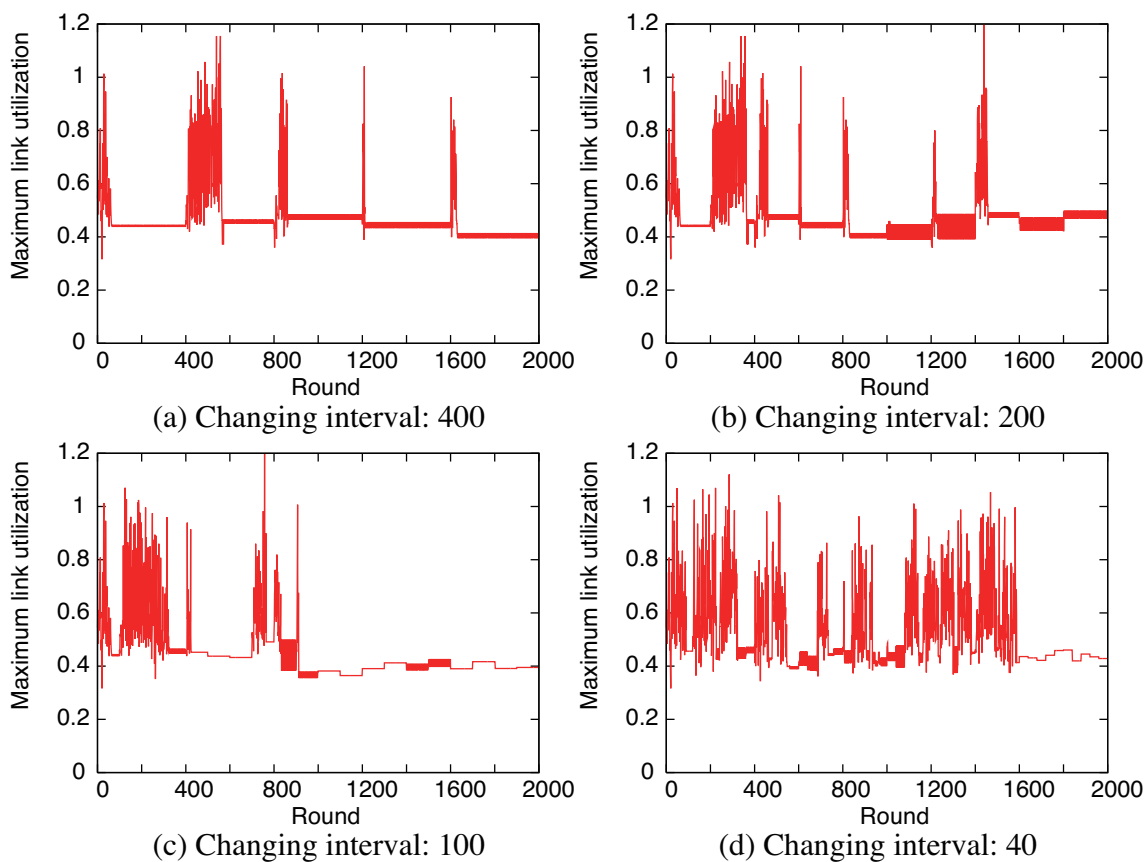


Figure 3.18: Fluctuation of maximum link utilization (Two-state utilization hysteresis, filtering, $\alpha = 0.2$, total traffic: 10, $k = 3.0$)

3.5 Summary

In this chapter, we discussed the selfish behavior of overlay routing on top of a VNT. We revealed that the dynamics of overlay routing cause high fluctuations in traffic demand, which lead to a significant layered traffic engineering instability. To overcome the traffic demand fluctuation and to make layered traffic engineering more stable, we applied demand hysteresis and utilization hysteresis to layered traffic engineering. We found that demand hysteresis improves the stability in terms of the number of changed lightpaths, but does not provide the stable maximum link utilization, especially when the overlay traffic ratio is large. We also found that utilization hysteresis improves the stability, but cannot always improve the maximum link utilization. Because of this, we proposed a two-state utilization hysteresis method that applies utilization hysteresis only when

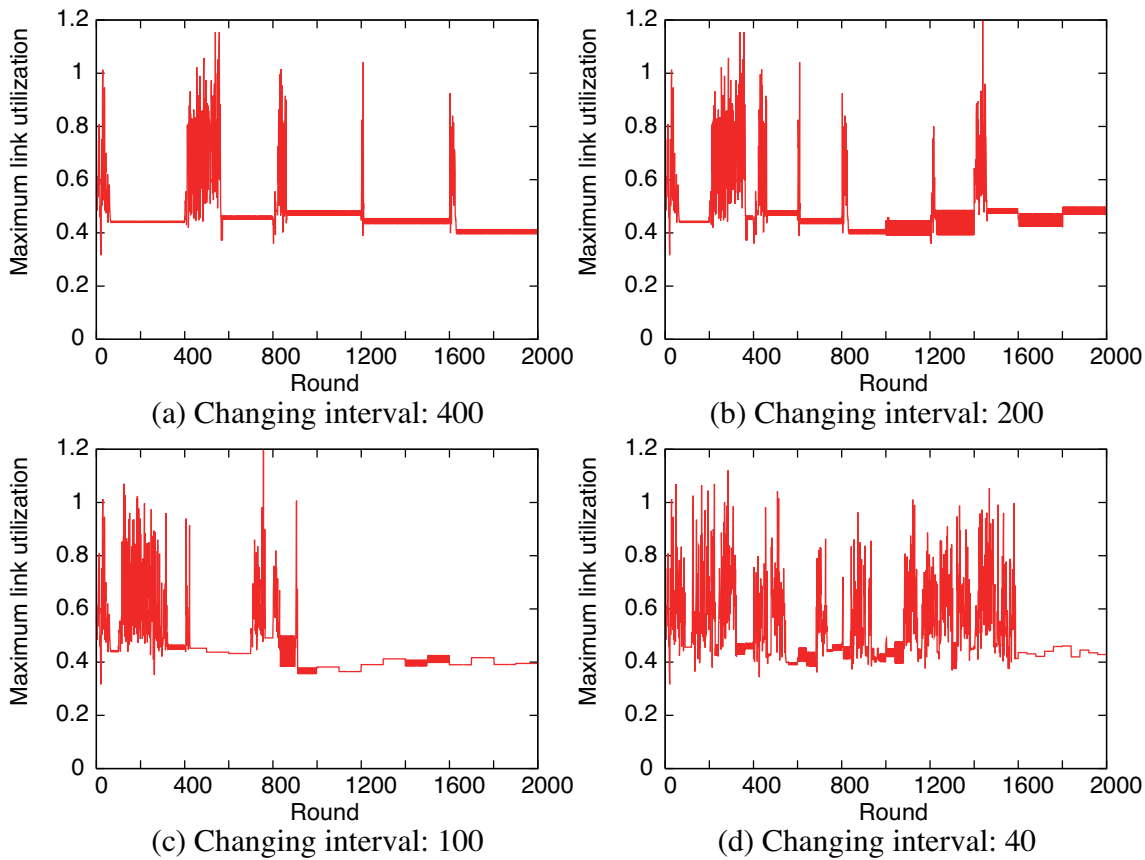


Figure 3.19: Fluctuation of maximum link utilization (Two-state utilization hysteresis, filtering, $\alpha = 0.2$, total traffic: 10, $k = 5.0$)

the maximum link utilization is sufficiently low. Simulation results show that two-state utilization hysteresis improves both the stability and the maximum link utilization. However, the convergence time becomes longer. To achieve faster convergence, we introduced a filtering method to the layered traffic engineering method with two-state utilization hysteresis. Through simulations, we showed that the filtering method reduces the convergence time. Both the hysteresis method and filtering method aim at improving the layered traffic engineering stability by reducing unnecessary changes in the VNT. In general, these types of approaches degrade the adaptability for changes in the traffic demand since the two methods tend to continue using the VNT designed for the old traffic demand. Although the layered traffic engineering method with two-state utilization hysteresis and filtering do not always follow extremely heavy changes in the traffic demand, it follows almost all the changes.

Chapter 4

Adaptive Layered Traffic Engineering against Changes in Environments

The growth of the Internet and emerging application layer technologies cause numerous changes in network environments. Therefore, it becomes important to achieve adaptive methods of controlling networks in addition to optimizing their performance. We propose an adaptive layered traffic engineering method in wavelength-routed WDM networks in this chapter. To achieve adaptability in the layered traffic engineering method, we focus on *attractor selection*, which models behaviors where biological systems adapt to unknown changes in their surrounding environments and recover their conditions. Our layered traffic engineering method uses deterministic and stochastic behaviors and controls these two appropriately by simple feedback of the conditions on an IP network. By using stochastic behavior, our new approach adapts to various changes in environments. Moreover, to define feedback of the conditions on the IP network, our proposed scheme only uses load information on links, which is easily and directly retrieved, and thus achieves quick responses to changes in traffic demand. The simulation results indicate that our layered traffic engineering method based on attractor selection quickly and adaptively responds to various changes in environments, i.e., changes in traffic demand and link failures.

4.1 Attractor Selection

Here, we briefly describe attractor selection, which is the key mechanism in our layered traffic engineering method. The original model for attractor selection was introduced in [53].

4.1.1 Concept of Attractor Selection

The dynamic system that is driven by *attractor selection* uses noise to adapt to environmental changes. In attractor selection, *attractors* are a part of the equilibrium points in the solution space in which the system conditions are preferable. The basic mechanism consists of two behaviors, i.e., deterministic and stochastic behaviors. When the current system conditions are suitable for the environment, i.e., the system state is close to one of the attractors, deterministic behavior drives the system to the attractor. Where the current system conditions are poor, stochastic behavior dominates over deterministic behavior. While stochastic behavior is dominant in controlling the system, the system state fluctuates randomly due to noise and the system searches for a new attractor. When the system conditions have recovered and the system state comes close to an attractor, deterministic behavior again controls the system. These two behaviors are controlled by simple feedback of the conditions of the system. In this way, attractor selection adapts to environmental changes by selecting attractors using stochastic behavior, deterministic behavior, and simple feedback. In the following section, we introduce attractor selection that models the behavior of gene regulatory and metabolic reaction networks in a cell.

4.1.2 Cell Model

Figure 4.1 is a schematic of the cell model used in [53]. It consists of two networks, i.e., the gene regulatory network in the dotted box at the top of Figure 4.1 and the metabolic reaction network in the box at the bottom.

Each gene in the gene regulatory network has an expression level of proteins and deterministic and stochastic behaviors in each gene control the expression level. Deterministic behavior controls the expression level due to the effects of activation and inhibition from the other genes. In Figure 4.1, the effects of activation are indicated by the triangular-headed arrows and those of inhibition are indicated by the circular-headed arrows. In stochastic behavior, inherent noise randomly changes the expression level.

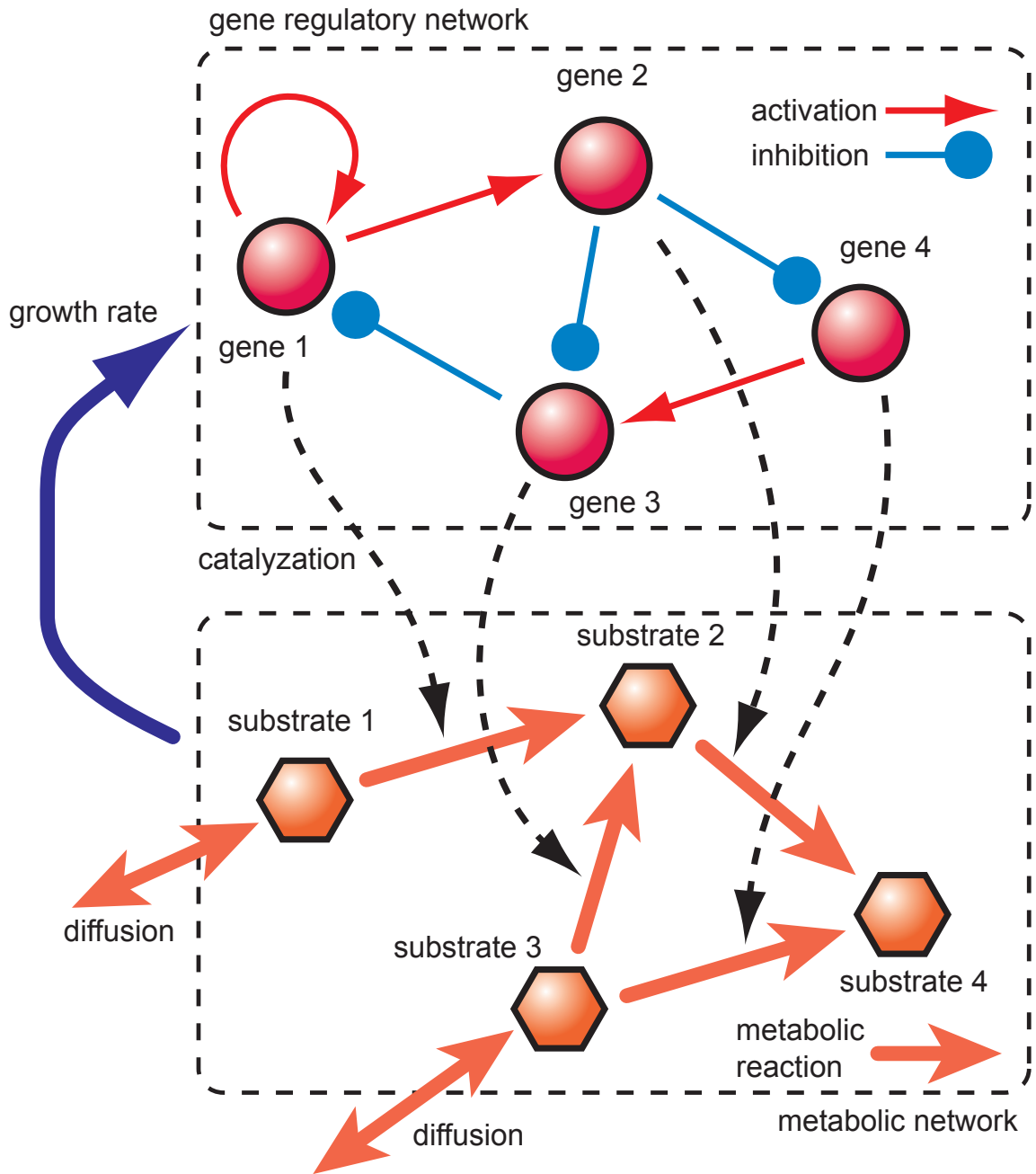


Figure 4.1: Gene regulatory and metabolic reaction networks

In the metabolic reaction network, metabolic reactions consume various substrates and produce new substrates. These metabolic reactions are catalyzed by proteins on corresponding genes. In the figure, metabolic reactions are illustrated as fluxes of substrates and catalyses of proteins are indicated by the dashed arrows. The changes in concentrations of metabolic substrates are given by metabolic reactions and the transportation of substrates from the outside of the cell. Some nutrient substrates are supplied from the environment by diffusion through the cell membrane.

The growth rate is determined by dynamics in the metabolic reactions. Some metabolic substrates are necessary for cellular growth, and thus the growth rate is determined as an increasing function of their concentrations. The gene regulatory network uses the growth rate as feedback of the conditions on the metabolic reaction network and controls deterministic and stochastic behaviors by using the growth rate. If the metabolic reaction network is in poor condition and the growth rate is small, the influence of stochastic behavior dominates deterministic behavior, triggering a search for a new attractor. During this phase, the expression levels are randomly changed by noise, and the gene regulatory network searches for a state that is suitable for the current environment. After the conditions of the metabolic reaction network have been recovered and the growth rate increases, deterministic behavior again drives the gene regulatory network to stable states.

The following section describes the mathematical model of attractor selection in more detail.

4.1.3 Mathematical Model of Attractor Selection

The internal state of a cell is represented by a set of expression levels of proteins on n genes, (x_1, x_2, \dots, x_n) , and concentrations of m metabolic substrates, (y_1, y_2, \dots, y_m) . The dynamics of the expression level of the protein on the gene i , x_i , is described as

$$\frac{dx_i}{dt} = f\left(\sum_{j=1}^n W_{ij}x_j - \theta\right) \cdot v_g - x_i v_g + \eta. \quad (4.1)$$

The first and second terms at the right hand side represent the deterministic behavior of gene i , and the third term represents stochastic behavior. In the first term, the regulation of protein expression levels on gene i by other genes are indicated by regulatory matrix W_{ij} , which takes 1, 0, or -1 , corresponding to activation, no regulatory interaction, and inhibition of the gene i by the gene j . The rate of increase in the expression level is given by the sigmoidal regulation function, $f(z) = 1/(1 + e^{-\mu z})$, where $z = \sum W_{ij}x_j - \theta$ is the total regulatory input with threshold θ for increasing x_i , and μ indicates

the gain parameter of the sigmoid function. The second term represents the rate of decrease in the expression level on gene i . This term means that the expression level decreases depending on the current expression level. The last term at the right hand side in Eq. (4.1), η , represents molecular fluctuations, which is Gaussian white noise. Noise η is independent of production and consumption terms and its amplitude is constant. The change in expression level x_i is determined by deterministic behavior, the first and second terms in Eq. (4.1), and stochastic behavior η . The deterministic and stochastic behaviors are controlled by growth rate v_g , which represents the conditions of the metabolic reaction network.

In the metabolic reaction network, metabolic reactions, which are internal influences, and the transportation of substrates from the outside of the cell, which is an external influence, determine the changes in concentrations of metabolic substrates y_i . The dynamics of y_i are defined as

$$\frac{dy_i}{dt} = \epsilon \cdot \left(\sum_{j=1}^n \sum_{k=1}^m Con(k, j, i) \cdot x_j \cdot y_k - \sum_{j'=1}^n \sum_{k'=1}^m Con(i, j', k') \cdot x_{j'} \cdot y_i \right) + D \cdot (Y_i - y_i), \quad (4.2)$$

where ϵ and D are the coefficients of the metabolic reactions and the diffusion, respectively. The variable Y_i represents the concentration of substrate i in the environment. Metabolic reactions are catalyzed by proteins on corresponding genes. The relations of metabolic reactions and genes are represented by the matrix $Con(i, j, k)$, which takes 1 if there is a metabolic reaction from substrate i to substrate k catalyzed by protein j , and 0 otherwise. The expression level x_j decides the strength of catalysis. A large expression level accelerates the metabolic reaction and a small expression level suppresses it. In other words, the gene regulatory network controls the metabolic reaction network through catalyses.

Some metabolic substrates are necessary for cellular growth. Growth rate v_g is determined as an increasing function of the concentrations of these vital substrates. In [53], for instance, v_g is represented as

$$v_g \propto \min(y_1, y_2, \dots, y_r), \quad (4.3)$$

where (y_1, y_2, \dots, y_r) are the vital substrates. The gene regulatory network uses v_g as the feedback of the conditions on the metabolic reaction network and controls deterministic and stochastic behaviors. If the concentrations of the required substrates decrease due to changes in the concentrations of nutrient substrates outside the cell, v_g also decreases. By decreasing v_g , the effects that the first

and second terms in Eq. (4.1) have on the dynamics of x_i decrease, and the effects of η increase relatively. Thus, x_i fluctuates randomly and the gene regulatory network searches for a new attractor. The fluctuations in x_i lead to changes in the rate of metabolic reactions via the catalyses of proteins. When the concentrations of the required substrates again increase, v_g also increases. Then, the first and second terms in Eq. (4.1) again dominate the dynamics of x_i over stochastic behavior, and the system converges to the state of the attractor. In our method, we mainly use the gene regulatory network and only mentioned concept of the metabolic reaction network. The next section explains the layered traffic engineering method based on this attractor selection model.

4.2 Layered Traffic Engineering Based on Attractor Selection

This section proposes a layered traffic engineering method based on the attractor selection model. We first introduce the network model that we use. Then, we outline our layered traffic engineering method based on attractor selection, and then describe our approach in detail.

4.2.1 Network Model

Our network consists of two layers: an optical and an IP layer as shown in the left of Figure 4.2. On the optical layer, the WDM network consists of OXCs and optical fibers. Layered traffic engineering configures lightpaths between IP routers via OXCs on the WDM network and these lightpaths and IP routers form a VNT. On the IP layer, packets are forwarded along the routes that are determined by IP routing on this VNT. In this chapter, we use the WDM network as a network infrastructure that provides a set of lightpaths.

4.2.2 Overview of Layered Traffic Engineering Based on Attractor Selection

In attractor selection, the gene regulatory network controls the metabolic reaction network, and the growth rate, which is the status of the metabolic reaction network, is recovered when the growth rate is degraded due to changes in the environment. In our layered traffic engineering method, the main objective is to recover the performance of the IP network by appropriately constructing VNTs when performance is degraded due to changes in traffic demand. Therefore, we interpret the gene regulatory network as a WDM network and the metabolic reaction network as an IP network, as shown in Figure 4.2. The layered traffic engineering method drives the IP network in this way by

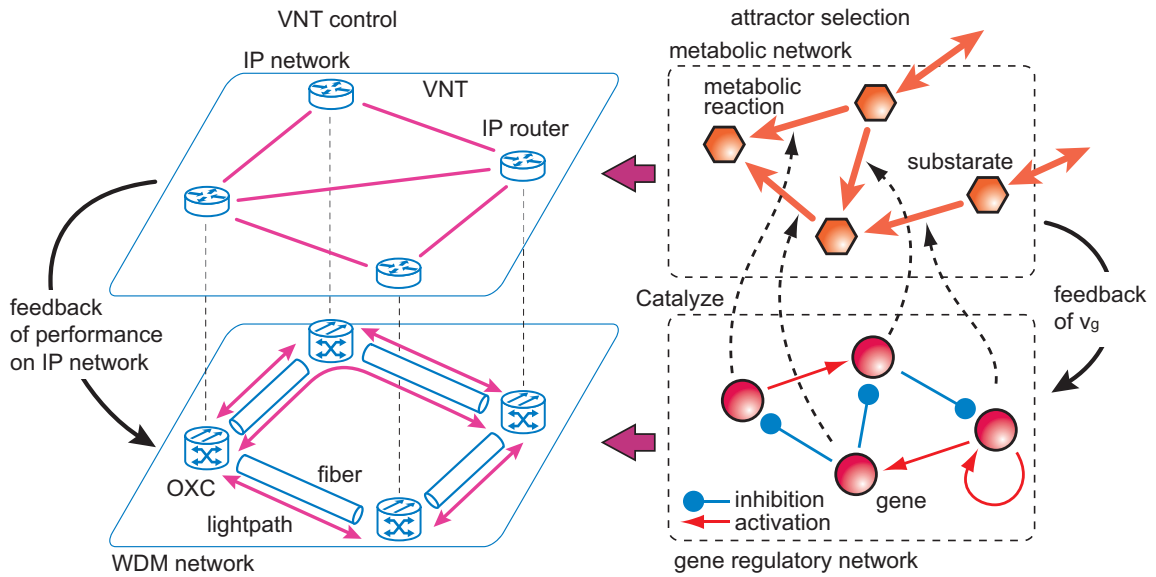


Figure 4.2: Interpretation of attractor selection into layered traffic engineering

constructing VNTs and the performance of the IP network recovers after it has degraded due to changes in traffic demand.

The control loop for our layered traffic engineering method is illustrated in Figure 4.3. Our proposed approach works on the basis of periodic measurements of the link load, which is the volume of traffic on links, and it uses load information on links to know the conditions of the IP network. This information is converted to activity, which is the value to control deterministic and stochastic behaviors. We describe the activity in Section 4.2.5. Our method controls the deterministic and stochastic behaviors in the same way as attractor selection depending on the activity. We describe the deterministic and stochastic behaviors of our layered traffic engineering method in Section 4.2.3. Our method constructs a new VNT according to the system state of attractor selection, and the constructed VNT is applied as the new infrastructure for the IP network. By flowing traffic demand on this new VNT, the load on links in the IP network is changed, and our method again retrieves this information to know the conditions of the IP network.

In addition to the adaptability of attractor selection, we also focus on another feature of biological systems. Biological systems including attractor selection control their state with only limited information since they have limited mechanisms to transmit information. Although the gene regulatory network in attractor selection only uses the growth rate as information to know the conditions

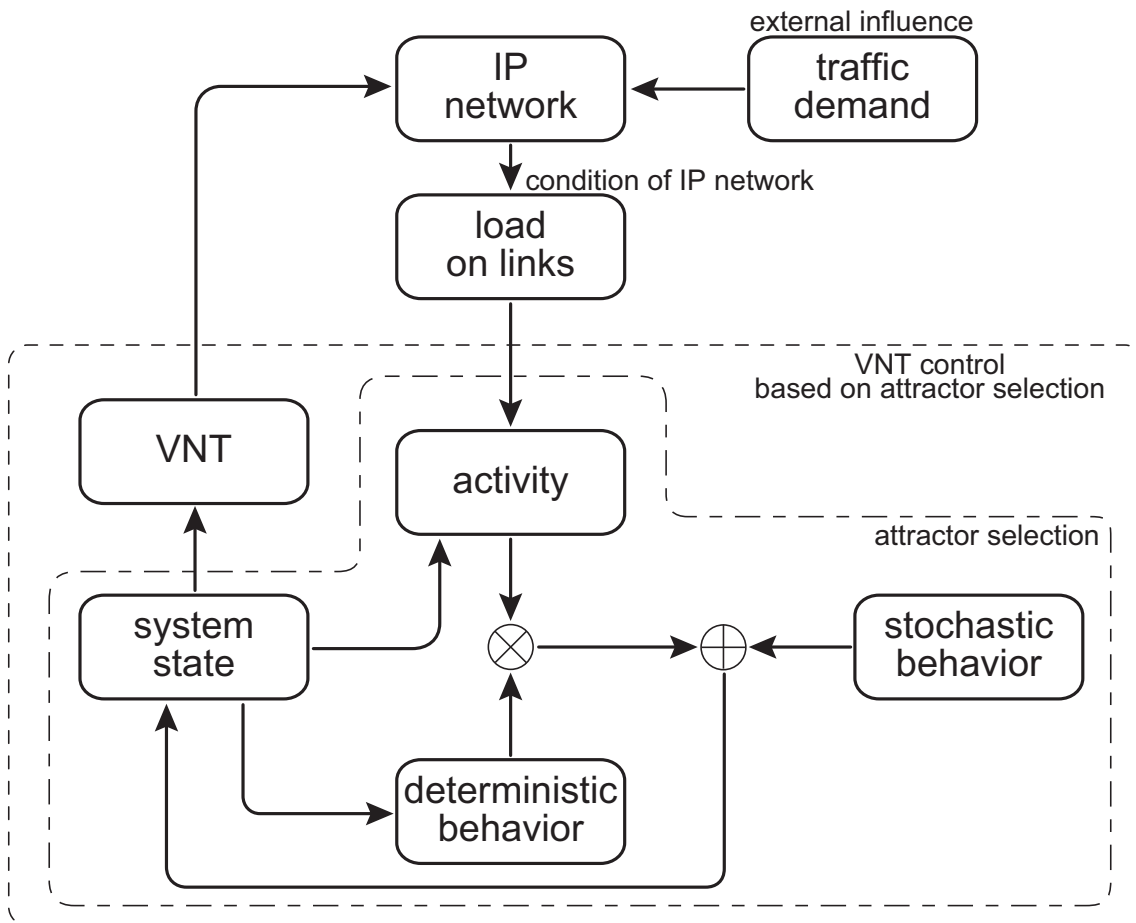


Figure 4.3: Control loop for layered traffic engineering based on attractor selection

of the metabolic reaction network, it is able to adapt to changes in the environment and recover the conditions of the metabolic reaction network by using stochastic behavior. We use this characteristic to achieve quick responses to changes in traffic demand. Unlike many existing heuristic or optimization-based layered traffic engineering methods, which use traffic demand matrices for constructing VNTs, our proposed scheme only collects load information on links to know the conditions of the IP network. It generally requires a long time to measure the network to obtain information on the traffic demand matrix. In contrast, load information on links can easily and directly be retrieved by using SNMP within a short time. Therefore, our approach responds to environmental changes more quickly than existing layered traffic engineering methods.

4.2.3 Dynamics of VNT Control

The following sections describe our layered traffic engineering method in detail. We use i , j , s , and d as indexes of nodes, and p_{ij} as an index of the source-destination pair from node i to j .

We place genes on the source-destination pair where lightpaths can be placed. Expression level of each gene determines the number of lightpaths on those node pairs. Removing genes on the node pairs makes the lightpath not to place on those node pairs. Thus, to incorporate physical constraints imposed by the characteristics of the WDM transmission technology, we should calculate node pairs that satisfy the constraints before performing our proposed method. In this chapter, we do not consider physical constraints of the WDM transmission technology, i.e., we place the genes on every source-destination pair. To avoid confusion, we refer to genes placed on the WDM network as *control units* and the expression levels of the control units as *control values*. In the gene regulatory and metabolic reaction networks, the expression levels on genes control the strength of corresponding metabolic reactions, which are represented as flows between substrates. In our method, the control values determine the number of lightpaths, and those lightpaths form a VNT. Therefore, we control flows on IP network through control values in the same way as the gene regulatory and metabolic reaction networks.

The dynamics of $x_{p_{ij}}$ is defined by the following differential equation,

$$\frac{dx_{p_{ij}}}{dt} = v_g \cdot f \left(\sum_{p_{sd}} W(p_{ij}, p_{sd}) \cdot x_{p_{sd}} - \theta_{p_{ij}} \right) - v_g \cdot x_{p_{ij}} + \eta, \quad (4.4)$$

where η represents white Gaussian noise, $f(z) = 1/(1 + \exp(-z))$ is the sigmoidal regulation function, and v_g is the value that indicates the condition of the IP network. We use the same formula as in Eq. (4.1) to determine the control values. According to the observation in [53], we use white Gaussian noise with a mean of 0 and a variance of 0.1 for η .

Our main objective in this chapter is to achieve the adaptability to changes in traffic demand, not to optimize performance such as minimizing the maximum link utilization. However, we never omit the achievable performance of our proposed method. To achieve at least the same level of the performance as existing heuristic approaches, we control the number of lightpaths by adjusting a parameter $\theta_{p_{ij}}$ in Eq. (4.4) dynamically according to link load. The number of lightpaths between node pair p_{ij} is determined according to value $x_{p_{ij}}$. We assign more lightpaths to a node pair

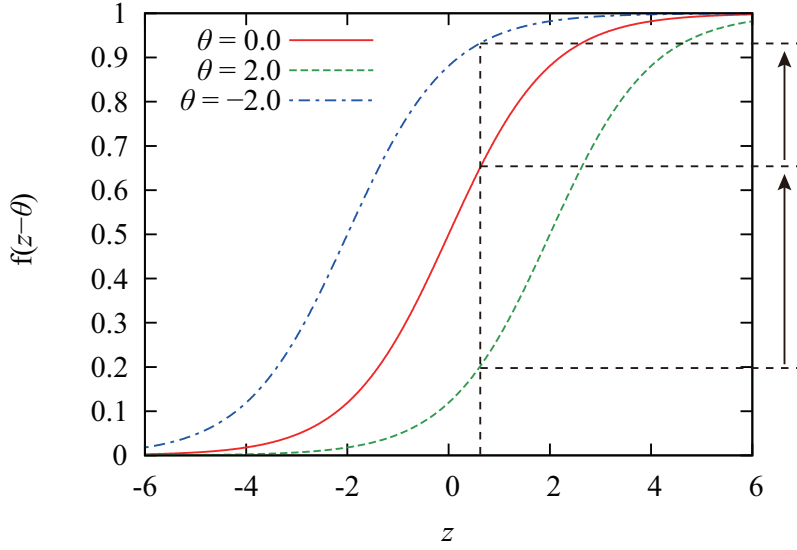
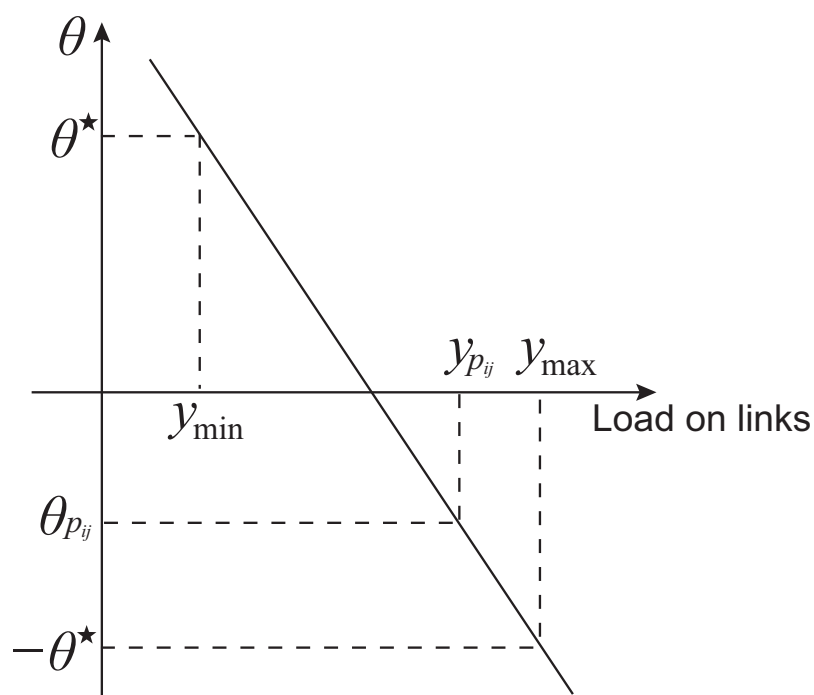


Figure 4.4: Sigmoid function

that has a high control value than a node pair that has a low control value. Function $f(z_{p_{ij}} - \theta_{p_{ij}})$, where $z_{p_{ij}} = \sum_{p_{sd}} W(p_{ij}, p_{sd}) \cdot x_{p_{sd}}$, has its center at $z_{p_{ij}} = \theta_{p_{ij}}$ and exhibits rapid growth near $\theta_{p_{ij}}$, as shown in Figure 4.4. With smaller $\theta_{p_{ij}}$, the curve of $f(z_{p_{ij}} - \theta_{p_{ij}})$ is shifted in the negative direction, and therefore $f(z_{p_{ij}} - \theta_{p_{ij}})$ increases. This increases $dx_{p_{ij}}/dt$, and this then leads to an increase in $x_{p_{ij}}$. This is equivalent to increasing the number of lightpaths between p_{ij} in our layered traffic engineering method. In the same way, a larger $\theta_{p_{ij}}$ leads to a decrease in $x_{p_{ij}}$ and then decreases the number of lightpaths between p_{ij} . Therefore, in our layered traffic engineering method, we control the number of lightpaths by adjusting $\theta_{p_{ij}}$ depending on the load on the link. To reduce the influence from fluctuations of the measured link load on layered traffic engineering, we use the exponential moving average of the link load, $y_{p_{ij}}$, with a smoothing factor of 0.5. To assign more lightpaths to a node pair that has a highly loaded link, we decrease $\theta_{p_{ij}}$ for node pair p_{ij} that has high $y_{p_{ij}}$. As seen in Figure 4.5, we determine $\theta_{p_{ij}}$ by using $\theta_{p_{ij}} = -(y_{p_{ij}} - y_{\min}) / (y_{\max} - y_{\min}) \times 2\theta^* - \theta^*$, where θ^* is the constant value that represents the range of $\theta_{p_{ij}}$, and y_{\max} and y_{\min} correspond to the maximum and minimum load in the network. If node pair p_{ij} has no links, we use y_{\min} as $y_{p_{ij}}$ to gradually modify the VNT.

Figure 4.5: Mapping $y_{p_{ij}}$ to $\theta_{p_{ij}}$

4.2.4 Regulatory Matrix

The regulatory matrix is an important parameter since the deterministic behavior of our layered traffic engineering method is dominated by this matrix. Each element in the regulatory matrix, which is denoted as $W(p_{ij}, p_{sd})$, represents the relation between node pair p_{ij} and p_{sd} . The value of $W(p_{ij}, p_{sd})$ is a positive number α_A , zero, or a negative number α_I , corresponding to activation, no relation, and inhibition of the control unit on p_{ij} by the control unit on p_{sd} . If the control unit on p_{ij} is activated by that on p_{sd} , increasing $x_{p_{sd}}$ leads to increasing p_{ij} . That is, node pair p_{sd} increases the number of lightpaths on p_{ij} in our layered traffic engineering method.

Let us consider three motivations for setting up or tearing down lightpaths for defining the regulatory matrix, i.e., establishing lightpaths for detouring traffic, increasing the number of lightpaths for the effective transport of traffic on the IP network, and decreasing the number of lightpaths due to a certain fiber being shared with other node pairs. First, for detouring traffic on the route from node i to j to other lightpaths, new lightpaths should be set up between node pair p_{ij} . Therefore, we interpret this motivation as the activation of the control unit on p_{ij} by the control units on each

node pair along the route of the lightpath between p_{ij} . Let us next consider the situation where a path on the IP network uses the lightpaths on p_{ij} and p_{sd} . In this case, a certain amount of traffic on p_{ij} is also transported on p_{sd} . Thus, if the number of lightpaths on p_{ij} is increased, the number of lightpaths on p_{sd} should also be increased for IP traffic to be effectively transported. Therefore, the control units on p_{ij} and p_{sd} activate each other. Finally, let us consider the relation between node pairs that share a certain fiber. Here, if the number of lightpaths on one node pair increases, the number of lightpaths on the other node pairs should decrease because of limitations on wavelengths. Therefore, the control unit on p_{ij} is inhibited by the control unit on p_{sd} if lightpaths between these node pairs share the same fiber. To achieve a more effective layered traffic engineering method in terms of optimal performance, other motivations such as the relation between adjacent node pairs should be considered. Since the main purpose in this research is to achieve an adaptive layered traffic engineering method, we consider these three motivations mentioned above.

The positive number, α_A , and the negative number, α_I , represent the strength of activation and inhibition. The total regulatory input to each control unit, $z_{p_{ij}} = \sum_{p_{sd}} W(p_{ij}, p_{sd})x_{p_{sd}}$, is inherent in Eq. (4.4) and should be independent of the number of control units since the appropriate regulatory input is determined by the sigmoid function, $f(z_{p_{ij}})$. To achieve a layered traffic engineering method that flexibly adapts to various environmental changes, Eq. (4.4) must have a sufficient number of equilibrium points, which are potential attractors depending on the surrounding environments. In [53], the authors evaluated their attractor selection model under a scenario where the gene regulatory network had 36 genes and each gene was activated or inhibited by other genes with a probability of 0.03. They demonstrated that the attractor selection model was extremely adaptable against environmental changes. We determine α_A and α_I on the basis of their results. Since $z_{p_{ij}}$ cannot be retrieved prior to calculating Eq. (4.4), we use $z'_{p_{ij}}{}^A = \sum_{p_{sd}} W^A(p_{ij}, p_{sd})$, and $z'_{p_{ij}}{}^I = \sum_{p_{sd}} W^I(p_{ij}, p_{sd})$, where $W^A(p_{ij}, p_{sd})$ and $W^I(p_{ij}, p_{sd})$ are the binary variables. The variable, $W^A(p_{ij}, p_{sd})$ takes 1 if the control unit on p_{ij} is activated by that on p_{sd} , and otherwise 0. To obtain the relation of inhibition, $W^I(p_{ij}, p_{sd})$ is defined in the same way as $W^A(p_{ij}, p_{sd})$. The two metrics, $z'_{p_{ij}}{}^A$ and $z'_{p_{ij}}{}^I$, indicate the total amount of activation or inhibition on the control unit, p_{ij} , from the other control units. Each gene in [53] had $z'^A = 0.03 \times 36 = 1.08$ since each gene was activated from 36 genes, including itself, with a probability of 0.03. In our layered traffic engineering method, each control unit has an average of $z'_{p_{ij}}{}^A = (\sum_{p_{ij}} \sum_{p_{sd}} \alpha_A W^A(p_{ij}, p_{sd}))/N$, where N is the number of control units. Thus, we define α_A as $\alpha_A = 1.08N / \sum_{p_{ij}} \sum_{p_{sd}} W^A(p_{ij}, p_{sd})$. In the same way, α_I is

defined as $\alpha_I = 1.08N / \sum_{p_{ij}} \sum_{p_{sd}} W^I(p_{ij}, p_{sd})$.

4.2.5 Activity

The growth rate is the value that indicates the conditions of the metabolic reaction network, and the gene regulatory network seeks to optimize the growth rate. In our layered traffic engineering method, we use the maximum link utilization, which is the total amount of traffic on a link normalized by its capacity, on the IP network as a metric that indicates the conditions of the IP network. To retrieve the maximum link utilization, we collect the traffic volume on all links and select their maximum values. This information is easily and directly retrieved by SNMP. To avoid confusion, we will refer to the growth rate defined in our layered traffic engineering method as *activity* after this. This activity must be an increasing function for the goodness of the conditions of the target system, i.e., the IP network in our case, as mentioned in Section 4.1. Therefore, we convert the maximum link utilization on the IP network, u_{\max} , into the activity, v_g , as

$$v_g = \begin{cases} \frac{\gamma}{1 + \exp(\delta \cdot (u_{\max} - \zeta))} & \text{if } u_{\max} \geq \zeta \\ \frac{\gamma}{1 + \exp(\delta/5 \cdot (u_{\max} - \zeta))} & \text{if } u_{\max} < \zeta \end{cases}, \quad (4.5)$$

where γ is the parameter that scales v_g and δ represents the gradient of this function. The constant number, ζ , is the threshold for the activity. One example curve for this activity function is plotted in Figure 4.6. If the maximum link utilization is more than threshold ζ , the activity rapidly approaches 0 due to the poor conditions of the IP network. Then, the dynamics of our layered traffic engineering method is governed by noise and the search for a new attractor. Where the maximum link utilization is less than ζ , we increase the activity slowly with decaying gain in the activity to improve the maximum link utilization. Since improving the maximum link utilization from a higher value has a greater impact on the IP network than that from a lower value, even if the degree of improvement is the same, we differentiate the gain of the activity as depending on the current maximum link utilization. Moreover, by retaining the incentive for improving maximum link utilization, our layered traffic engineering method continuously attempts to improve the conditions of the IP network. Parameter γ is set to 100, which is shown in [53] as the enough large value for the gene regulatory network to strongly converge attractors despite the existence of noise. We set the target maximum link utilization, ζ , to 0.5 and the gradient, δ , to 50 to achieve quick responses to changes in u_{\max} .

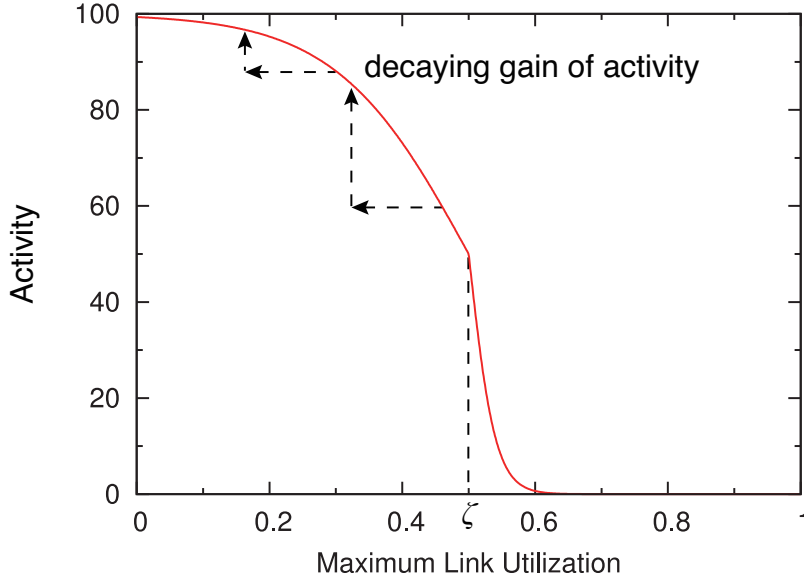


Figure 4.6: A sample curve of activity

4.2.6 Virtual Network Topology Construction

The number of lightpaths between node pair p_{ij} is calculated on the basis of $x_{p_{ij}}$. However, since a fixed amount of noise has a constant influence on our layered traffic engineering method even when the IP network has good conditions and activity is high, $x_{p_{ij}}$ keep fluctuating. Thus, it leads to fluctuations in VNTs to construct VNTs by using $x_{p_{ij}}$ directly. To achieve stable layered traffic engineering, we introduce hysteresis, which is often used for avoiding routing fluctuations [30]. We use $x'_{p_{ij}}$ as the hysteresis applied on expression level. We set $x'_{p_{ij}}$ to $x_{p_{ij}}$ when $|x_{p_{ij}} - x'_{p_{ij}}| > \Delta$, and keep its current value otherwise. We determine the hysteresis threshold as $\Delta = v_g \cdot \varepsilon$, where ε is a constant value. Since low activity means a poor condition of the IP network, VNTs must be reconfigured to recover. Thus, in the case of low activity, we encourage reconfigurations of VNTs by using a small hysteresis threshold. In contrast, we use a large hysteresis threshold in the case of high activity to improve the stability of our layered traffic engineering method. To achieve stable layered traffic engineering in the case of high activity, we set ε to 0.0025, which makes Δ slightly larger than the variance of noise, η .

To simplify the model of our layered traffic engineering method, we assume that the number of wavelengths on optical fibers will be sufficient and the number of transmitters and receivers of optical signals will restrict the number of lightpaths between node pairs. Each node has P_R receivers

and P_T transmitters. We assign transmitters and receivers to lightpaths between p_{ij} based on $x_{p_{ij}}$ normalized by the total control values for all the node pairs that use the transmitters or the receivers on node i or j . The number of lightpaths between p_{ij} , $G_{p_{ij}}$, is determined as

$$G_{p_{ij}} = \min\left(\lfloor P_R \cdot \frac{x_{p_{ij}}}{\sum_s x_{p_{sj}}} \rfloor, \lfloor P_T \cdot \frac{x_{p_{ij}}}{\sum_d x_{p_{id}}} \rfloor\right). \quad (4.6)$$

Since we adopt the floor function for converting real numbers to integers, each node has residual transmitters and receivers. We assign one lightpath in descending order of $x_{p_{ij}}$ while the constraint on the number of transmitters and receivers is satisfied. Note that other constraints such as the number of wavelengths on a fiber can easily be considered. For instance, restrictions on the number of wavelengths on a fiber are satisfied by adding $x_{p_{ij}}$ normalized by the total control values for all the node pairs that use the same fiber to Eq. (4.6).

4.3 Performance Evaluation

4.3.1 Simulation Conditions

We use the European Optical Network (EON) topology shown in Figure 4.7 for the physical topology. The EON topology has 19 nodes and 39 bidirectional links. Each node has eight transmitters and eight receivers. We use randomly generated traffic demand matrices in the evaluations that followed.

We focus on changes in traffic demand in the IP network and fiber failures as the environmental changes. We consider two types of changes in traffic demand; the first included gradual and periodic changes and the second included sudden and sharp changes. By using Fourier series, traffic demand from node i to j at time t , $d_{ij}(t)$, changes gradually and periodically as

$$d_{ij}(t) = \beta_{ij} \cdot \left(a + \sum_{h=1}^H \left(b_{ij}^h \cos\left(\frac{2\pi th}{T}\right) + c_{ij}^h \sin\left(\frac{2\pi th}{T}\right) \right) \right), \quad (4.7)$$

where T is the cycle of changes in traffic demand; we use 24 hours as a cycle in this simulation. The constant parameters a , b_{ij}^h , and c_{ij}^h define the curve of $d_{ij}(t)$, and β_{ij} scales $d_{ij}(t)$. Since our main objective is to achieve adaptability against changes in traffic demand and not to optimize the

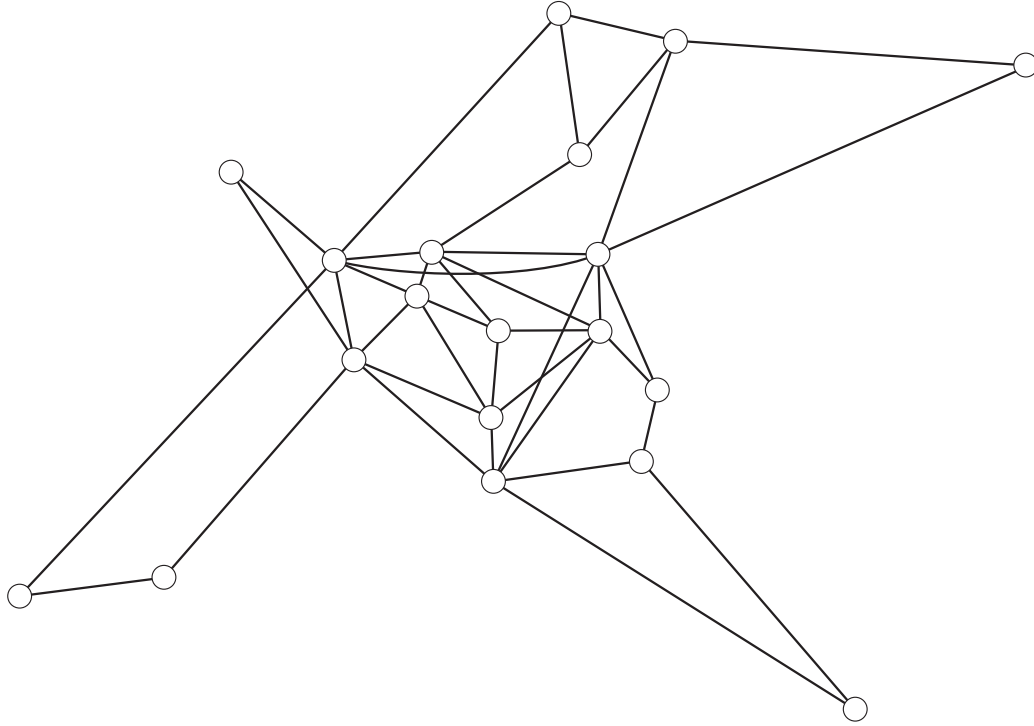


Figure 4.7: European Optical Network topology

performance of the layered traffic engineering method for realistic traffic patterns, we simply generate the parameters as follows. Parameters b_{ij}^h and c_{ij}^h are uniformly distributed random numbers in a range from 0 to 1. We set the constant value a to $\sqrt{2}$ to ensure that $d_{ij}(t)$ is non-negative. The scale factor of traffic demand β_{ij} follows a log-normal distribution with variance in the variable's logarithm, σ^2 , according to the observation in [63]. We set H to 1. For sudden and abrupt changes in traffic demand, we randomly change β_{ij} at certain intervals while keeping the expected value of total traffic demand in the network constant.

4.3.2 Behaviors of Layered Traffic Engineering Based on Attractor Selection

This section explains the basic behaviors of our layered traffic engineering method. In the simulation experiments, we assume that our layered traffic engineering method will collect information about the load on links every 5 minutes.

We evaluate our layered traffic engineering method with the maximum link utilization in Figure 4.8. The horizontal axis plots the time in hours and the vertical axis plots the maximum link

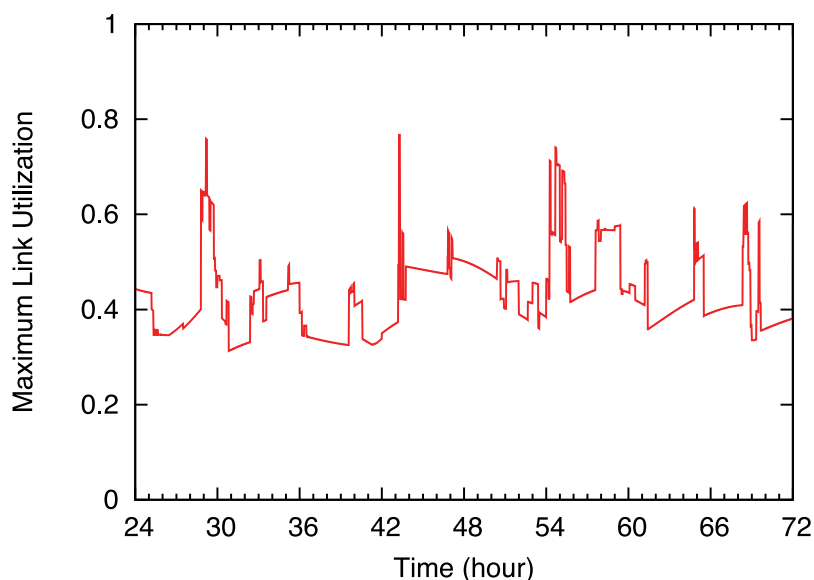


Figure 4.8: Maximum link utilization

utilization. The results for the first 24 hours have been omitted to disregard the transient phase during the simulation. In this section, we only focus on changes in traffic demand as environmental changes to highlight the basic behavior of our proposed method. Abrupt traffic changes occur every 3.6 hours and traffic demand continuously and gradually changes in the time between these abrupt traffic changes. Maximum link utilization degrades drastically every 3.6 hours due to the abrupt changes in traffic, but the maximum link utilization recovers shortly after this degradation.

To illustrate the adaptation mechanism of our layered traffic engineering method more clearly, we will present the control values, which determine the number of lightpaths between node pairs, and the activity, which is fed back to the our layered traffic engineering method and controls stochastic and deterministic behaviors, in Figures 4.9 and 4.10, respectively. In Figure 4.9, we selected ten control units out of 342 on all node pairs and have plotted the control values for these control units. When there are only periodic and gradual changes in traffic demand, our proposed method adjusts the control values depending on the changes in traffic demand. When maximum link utilization is degraded due to sharp changes in traffic demand, this degradation is reflected as a decrease in activity as shown in Figures 4.8 and 4.10. As the result of the decreases in activity, stochastic behavior dominates over deterministic behavior in our layered traffic engineering method. This is observed as fluctuations in the control values in Figure 4.9. Our method searches for a new VNT that is suitable

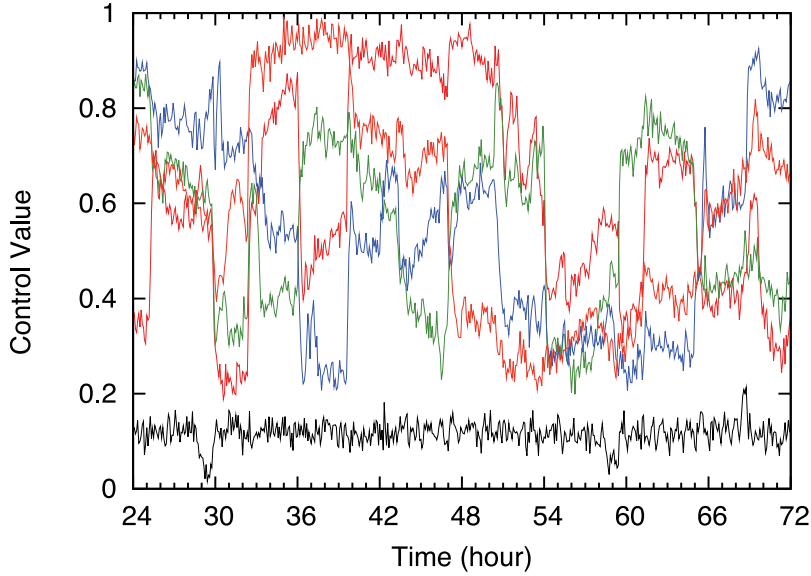


Figure 4.9: Control values

for the changed traffic demand while stochastic behavior dominates deterministic behavior. After the new VNT is constructed and the maximum link utilization is recovered, activity increases, and then deterministic behavior again dominates in the layered traffic engineering method. In this way, our method adapts to both abrupt and gradual changes in traffic demand by controlling deterministic and stochastic behavior with activity.

To observe the adaptation mechanism in terms of the VNT reconfiguration, we next investigate the ratio of changed lightpaths to the total number of lightpaths, as shown in Figure 4.11. Our layered traffic engineering method constructs a new VNT on the basis of the current VNT and the difference between these two VNTs is given by Eq. (4.4). The high degree of activity means that the current system state, $x_{p_{ij}}$, is near the attractor, which is one of the equilibrium points in Eq. (4.4), and therefore, the difference given by this equation is close to zero. Consequently, our layered traffic engineering method makes small changes to VNT enabling adaptation to changes in traffic demand. Where there is a low degree of activity due to poor conditions in the IP network, stochastic behavior dominates deterministic behavior. Here, the control values, $x_{p_{ij}}$, fluctuate randomly due to noise η to search for a new VNT that has lower maximum link utilization. To discover a suitable VNT efficiently from the huge number that are possible, our layered traffic engineering method makes large changes to the VNT. In this way, our proposed scheme modifies VNTs depending on

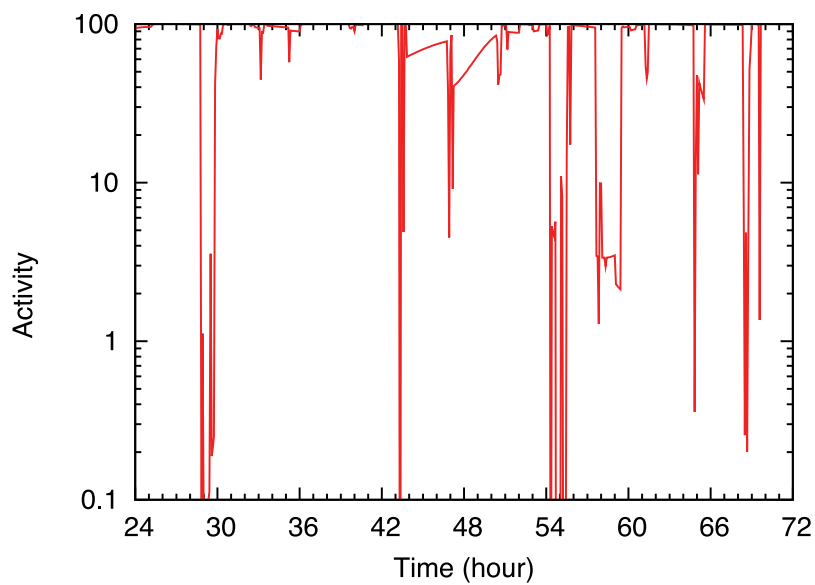


Figure 4.10: Activity

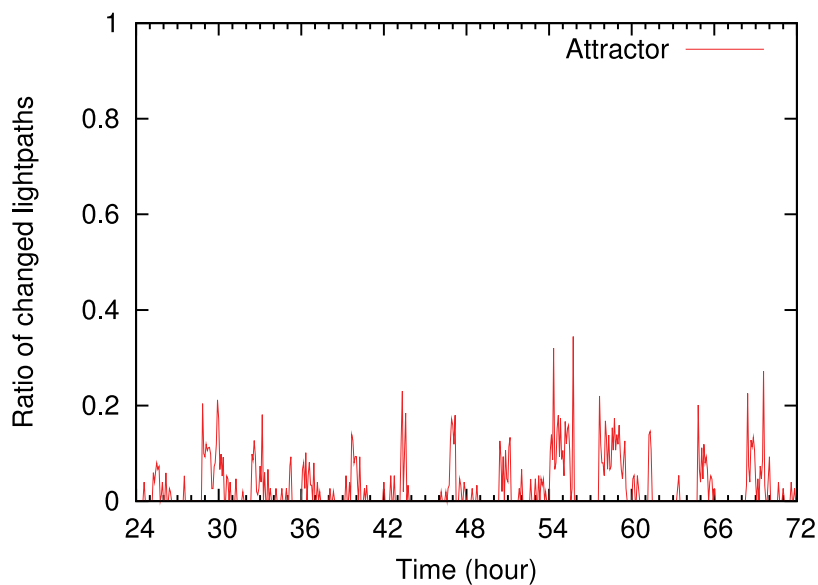


Figure 4.11: Ratio of number of changed lightpaths to total number of lightpaths

the maximum link utilization on IP networks and adapts to changes in traffic demand.

4.3.3 Adaptability to Changes in Traffic Demand

We evaluate the adaptability of our layered traffic engineering method to changes in traffic demand. For purposes of comparison, we use two existing heuristic layered traffic engineering methods. The MLDA (Minimum delay Logical topology Design Algorithm) [8] constructs VNTs on the basis of a given traffic demand matrix. The main objective of MLDA is to minimize the maximum link utilization. The basic idea behind MLDA is to place lightpaths between nodes in order of descending traffic demand. We use another layered traffic engineering method, which is introduced in [34]. After this, we will refer to this layered traffic engineering method as “ADAPTATION.” ADAPTATION aims at achieving adaptability against changes in traffic demand. This method reconfigures VNTs according to the load on links and the traffic demand matrix. ADAPTATION measures the actual load on links every 5 minutes and adds a new lightpath to the current VNT when congestion occurs. This method places a new lightpath on the node pair with the highest traffic demand among all node pairs that use the congested link. This decision is made according to the traffic demand matrix. However, to measure the traffic demand on all node pairs directly and in real-time is generally difficult due to the large overhead in collecting information. Therefore, we use the traffic demand matrix estimated with the method in [64] as the input parameter for ADAPTATION. In the simulation experiment, ADAPTATION reconfigures VNTs every 5 minutes using the measured load on links and the estimated traffic demand matrix. To simplify our evaluations, MLDA reconfigures VNTs every 60 minutes using the actual traffic demand matrix. For the all layered traffic engineering methods, we use the minimum hop routing of lightpaths on the wavelength-routed network.

The maximum link utilization over time is shown in Figure 4.12. The simulation conditions are the same as those discussed in Section 4.3.2. It is obvious that the maximum link utilization of MLDA continues to be high until the next reconfiguration is performed. Thus, degradation due to unsuitable VNT for changed traffic demand is retained for prolonged periods depending on the timing for the VNT reconfiguration. The recovery time, which is defined as the period until maximum link utilization is recovered, for our approach is much shorter than that for ADAPTATION, although both methods reconfigure VNTs every 5 minutes. The recovery time for ADAPTATION is approximately the same as that for MLDA. Errors between estimated and actual traffic demand lead to incorrect decisions on selecting the node pair on which a new lightpath is placed. Thus, the efficiency of setting up lightpaths is degraded. In contrast with ADAPTATION, our method uses

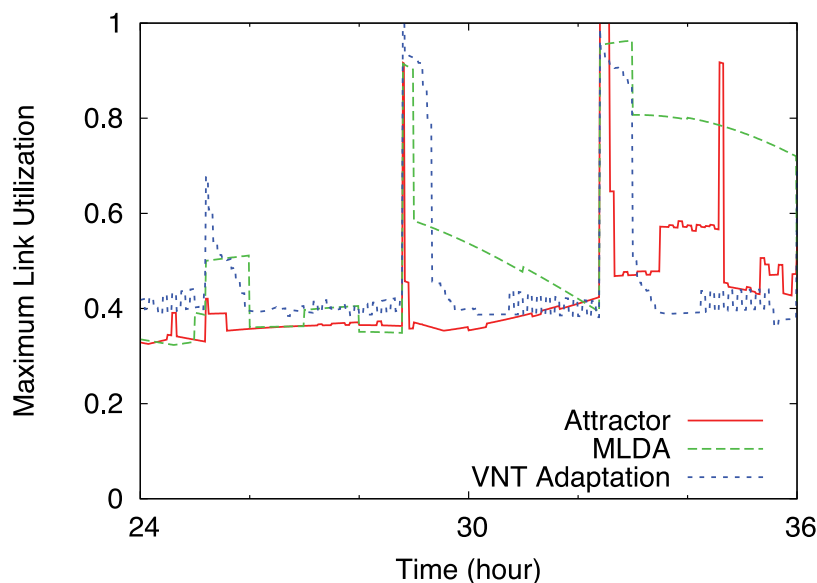


Figure 4.12: Adaptability of layered traffic engineering methods against changes in traffic demand

actual information, i.e., the measured load on links, and therefore quickly adapts to changes in traffic demand. This figure also shows that our proposed method achieves almost the same maximum link utilization as MLDA and ADAPTATION.

A fixed amount of noise has a constant influence on our layered traffic engineering method even when the IP network has good conditions and activity is high. The effect of noise plays an important role in achieving adaptability against changes in traffic demand, as explained in Section 4.3.2. However, noise does not always have a beneficial effect on our proposed scheme due to its random nature. At time 35, the maximum link utilization with our layered traffic engineering method increases drastically even though abrupt changes in traffic demand do not occur. However, this degradation in maximum link utilization is immediately reflected as a decrease in activity, and maximum link utilization quickly recovers due to the adaptation mechanism described in Section 4.3.2.

We next investigate how our layered traffic engineering method recovers maximum link utilization efficiently after abrupt changes in traffic demand occur. To evaluate its efficiency, we introduce a recovery ratio, which is defined as the ratio of recovered maximum link utilization after the i -th VNT reconfiguration to maximum link utilization after abrupt changes in traffic demand occur. More specifically, abrupt changes in traffic demand occur at time t_0 and the i -th VNT reconfiguration after that traffic change is performed at time t_i . The recovery ratio, R_i , is defined as

$(u_{\max}(t_0) - u_{\max}(t_i)) / u_{\max}(t_0)$, where $u_{\max}(t)$ is the maximum link utilization at time t . We evaluate the recovery ratio under different patterns of traffic demand by changing the variance in traffic demand σ , i.e., the standard deviation of β_{ij} in Eq. (4.7). By increasing σ , not only the variance in traffic demand but also the intensity of changes in traffic demand increases.

The recovery ratio for the first VNT reconfiguration depending on the variance in traffic demand is plotted in Figure 4.13. We plotted the average recovery ratio over two thousand samples for all variances in traffic demand. In these simulations, we used the same traffic patterns for both layered traffic engineering methods. This figure shows that our method recovers more maximum link utilization than ADAPTATION by one VNT reconfiguration. In the case of small σ , the differences in traffic demands on different node pairs are small, and thus the abrupt changes in traffic demand cause little degradation in maximum link utilization. Therefore, the adaptation mechanisms for both our proposed method and ADAPTATION do not need to work and the recovery ratios for both methods are low. As σ increases, the impact that the abrupt changes in traffic demand have on maximum link utilization increases. The recovery ratio with our proposal approaches reaches approximately 0.3 while that of ADAPTATION reaches 0.1. Moreover, the recovery ratio with our method saturates at $\sigma = 2.0$, whereas that of ADAPTATION saturates at $\sigma = 1.0$. By using stochastic behavior and controlling it appropriately depending on the activity, our proposed method adapts to various changes in traffic demand.

To demonstrate the adaptability of our method in terms of time, we show the recovery ratio depending on the number of VNT reconfigurations in Figure 4.14. We set σ to 1.0 at which the recovery ratio of ADAPTATION begins to saturate. Almost all recovery with our proposed approach occurs by the first VNT reconfiguration while it takes a long time for ADAPTATION to recover maximum link utilization. These results indicate that our method has capabilities for adapting to severe changes in traffic demand, and can adapt to these changes quickly.

4.3.4 Adaptability to Link Failures

We next show the behavior of our layered traffic engineering method when link failures and abrupt changes in traffic demand occur simultaneously. We select 10 out of 78 optical fibers randomly, which fail at time 30 and recover at time 42. While fibers fail, two abrupt changes in traffic demand occur at time 36 and 39. The main purpose in this experiment is to investigate the adaptability of our proposed method, which is performed on the WDM network. To observe the adaptability of our

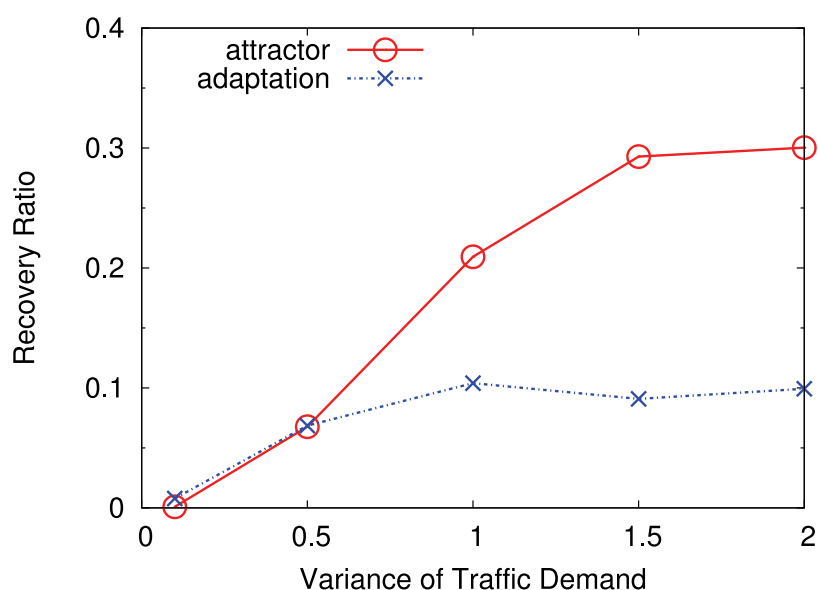


Figure 4.13: Recovery ratio of first VNT reconfiguration over variance in traffic demand

proposed method more clearly, we assume that the IP network reroutes its traffic shortly after the occurrence of fiber failures.

The maximum link utilization over time is shown in Figure 4.15. At time 30, it degrades due to fiber failures but recovers shortly after this degradation. Note that our proposed method has no mechanism to detect fiber failures and knows the condition of the IP network only through the activity. Therefore, the layered traffic engineering method based on attractor selection recovers from the degradation in the maximum link utilization due to fiber failures through the activity and the stochastic behavior as described in Section 4.3.2. Fiber failures and changes in traffic demand occur simultaneously at time 36 and 39, and this leads to the degradation in the maximum link utilization. However, our proposed method again recovers from this degradation in the same way as shown in Section 4.3.2.

4.4 Summary

We proposed a layered traffic engineering method that is adaptive to changes in traffic demand. It is based on attractor selection, which models the behaviors of biological systems that adapt to environmental changes and recover their conditions. Our new approach is extremely adaptable

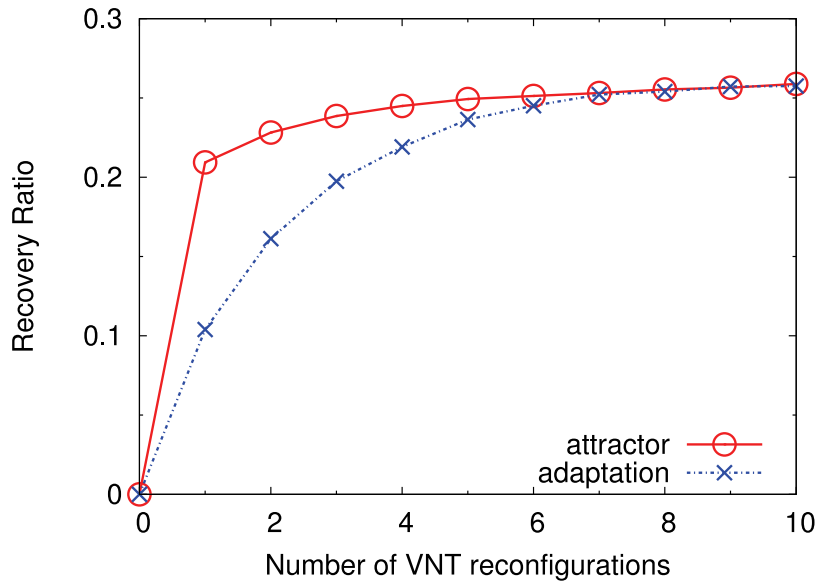


Figure 4.14: Recovery ratio over number of VNT reconfigurations with variance in traffic demand of 1.5

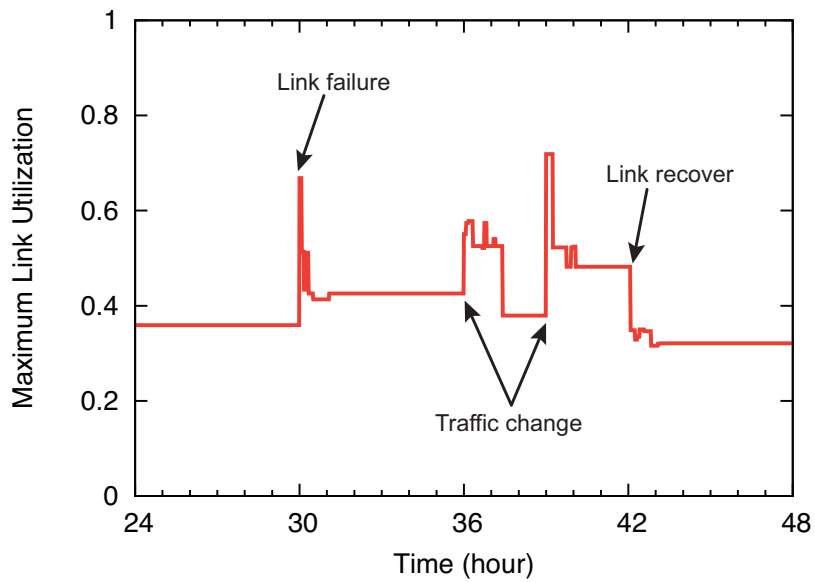


Figure 4.15: Robustness against changes in traffic demand and link failures

to changes in traffic demand by appropriately controlling deterministic and stochastic behaviors depending on the activity, which is simple feedback of the conditions on the IP network. Our proposed method only uses load information on links to determine the activity. Since the load on links is directly retrieved within short intervals, our proposed method quickly and adaptively responds to changes in traffic demand. The simulation results indicated that our layered traffic engineering method quickly responds and adapts to changes in traffic demand. By using stochastic behavior and controlling it appropriately depending on the activity, our new approach adapts to various changes in traffic demand.

In our approach, stochastic behavior, i.e., noise, plays an important role in achieving adaptability against changes in traffic demand. In this thesis, we defined the noise according to the observation in [53]. A future direction is to investigate a suitable type of the noise and its amplitude for layered traffic engineering methods to achieve more efficient search for a new VNT.

Chapter 5

Conclusion and Future Work

WDM networks offer flexible network infrastructures by using wavelength-routing capabilities. In such wavelength-routed networks, lightpaths are established between nodes via OXCs. One approach to accommodating Internet traffic on a wavelength-routed network is to configure a VNT, which consists of lightpaths and routers. To achieve effective transport of traffic, layered traffic engineering, which configures a VNT on the basis of characteristics of upper layer's traffic, has been investigated in many papers.

It is an essential issue to accommodate IP traffic, which is the majority of Internet traffic, effectively on wavelength-routed networks. In Chapter 2, we proposed an integrated routing mechanism for IP and wavelength-routed networks to achieve effective transport of IP traffic. The key idea is to prepare a set of virtual-links representing the lightpaths that can be established by the WDM network. We assigned cost values to those virtual-links aiming at maximizing network throughput by reducing load on IP routers. Then, we calculate the minimum cost route on an IP network including the virtual-links. In our method, since necessary lightpaths for transporting IP traffic are decided by the IP routing mechanism, the IP network always uses those lightpaths. Through simulations, we have shown that in the case that traffic patterns do not change, the throughput of our method is almost the same as that of a VNT optimally designed for a given traffic demand. In the case that traffic patterns change, the throughput of our method is about 50% higher than that of the VNTs generated by existing heuristic approaches.

However, it is insufficient only to accommodate IP traffic effectively since various traffic in addition to the legacy IP traffic such as web flows on Internet. In Chapter 3, we discussed the selfish

behavior of overlay routing on top of a VNT. We revealed that the dynamics of overlay routing cause high fluctuations in traffic demand, which lead to a significant layered traffic engineering instability. To overcome the traffic demand fluctuation and to make layered traffic engineering more stable, we applied demand hysteresis and utilization hysteresis to layered traffic engineering. We found that demand hysteresis improves the stability in terms of the number of changed lightpaths, but does not provide the stable maximum link utilization, especially when the overlay traffic ratio is large. We also found that utilization hysteresis improves the stability, but cannot always improve the maximum link utilization. Because of this, we proposed a two-state utilization hysteresis method that applies utilization hysteresis only when the maximum link utilization is sufficiently low. Simulation results show that two-state utilization hysteresis improves both the stability and the maximum link utilization. However, the convergence time becomes longer. To achieve faster convergence, we introduced a filtering method to the layered traffic engineering method with two-state utilization hysteresis. Through simulations, we showed that the filtering method reduces the convergence time. Both the hysteresis method and filtering method aim at improving the layered traffic engineering stability by reducing unnecessary changes in the VNT. In general, these types of approaches degrade the adaptability for changes in the traffic demand since the two methods tend to continue using the VNT designed for the old traffic demand. Although the layered traffic engineering method with two-state utilization hysteresis and filtering do not always follow extremely heavy changes in the traffic demand, it follows almost all the changes.

The interaction between layered traffic engineering and overlay routing brings out not only difficulties in the effective accommodation of traffic on wavelength-routed networks but also the large fluctuations in the network environments such as traffic demand and link load. Hence, adaptability against changes in environments becomes a more important issue to achieve effective wavelength-routed networks. In Chapter 4, we proposed a layered traffic engineering method that is adaptive to changes in traffic demand. It is based on attractor selection, which models the behaviors of biological systems that adapt to environmental changes and recover their conditions. Our new approach is extremely adaptable to changes in traffic demand by appropriately controlling deterministic and stochastic behaviors depending on the activity, which is simple feedback of the conditions on the IP network. Our proposed method only uses load information on links to determine the activity. Since the load on links is directly retrieved within short intervals, our proposed method quickly and adaptively responds to changes in traffic demand. The simulation results indicated that our layered

traffic engineering method quickly responds and adapts to changes in traffic demand. By using stochastic behavior and controlling it appropriately depending on the activity, our new approach adapts to various changes in traffic demand.

We have addressed the instability of layered traffic engineering due to the interaction between layered traffic engineering and single overlay routing in Chapter 3, and have proposed an adaptive layered traffic engineering against changes in environments in Chapter 4. One of our future directions is to prove that our approach proposed in Chapter 4 accommodates largely fluctuating traffic due to overlay routing adaptively. Another future direction is to find an approach to accommodating several overlay routing mechanisms on a single wavelength-routed network.

Finally, we believe that those above discussions contribute to the design and management of future wavelength-routed networks widespread around the world.

Bibliography

- [1] A. M. Odlyzko, “Internet traffic growth: sources and implications,” in *Proceedings of SPIE*, vol. 5247, pp. 1–15, 2003.
- [2] K. Cho, K. Fukuda, H. Esaki, and A. Kato, “The impact and implications of the growth in residential user-to-user traffic,” in *Proceedings of ACM SIGCOMM*, pp. 207–218, Sept. 2006.
- [3] M. Dischinger, A. Haeberlen, K. P. Gummadi, and S. Saroiu, “Characterizing residential broadband networks,” in *Proceedings of the 7th ACM SIGCOMM conference on Internet measurement*, pp. 43–56, Oct. 2007.
- [4] C. S. R. Murthy and M. Gurusamy, *WDM optical networks: Concepts, Design, and Algorithms*. NJ, USA: Prentice Hall PTR, Nov. 2001.
- [5] J. Zheng and H. T. Mouftah, *Optical WDM Networks: Concepts and Design Principles*. NJ, USA: Wiley-IEEE Press, Aug. 2004.
- [6] B. Mukherjee, *Optical WDM Networks*. NY, USA: Springer, Jan. 2006.
- [7] R. Dutta and G. N. Rouskas, “A survey of virtual topology design algorithms for wavelength routed optical networks,” *Optical Network Magazine*, vol. 1, pp. 73–89, Jan. 2000.
- [8] R. Ramaswami and K. N. Sivarajan, “Design of logical topologies for wavelength-routed optical networks,” *IEEE Journal on Selected Areas in Communications*, vol. 14, pp. 840–851, June 1996.
- [9] B. Mukherjee, D. Banerjee, S. Ramamurthy, and A. Mukherjee, “Some principles for designing a wide-area WDM optical network,” *IEEE/ACM Transactions on Networking*, vol. 4, no. 5, pp. 684–696, 1996.

- [10] M. S. Kodialam, T. V. Lakshman, J. B. Orlin, and S. Sengupta, "Preconfiguring IP-over-optical networks to handle router failures and unpredictable traffic," *IEEE Journal on Selected Areas in Communications*, vol. 25, pp. 934–948, June 2007.
- [11] Y. Fukushima, S. Arakawa, M. Murata, and H. Miyahara, "Design of logical topology with effective waveband usage in IP over WDM networks," *Photonic Network Communications*, vol. 11, pp. 151–161, Mar. 2006.
- [12] G. Agrawal and D. Medhi, "Lightpath topology configuration for wavelength-routed IP/MPLS networks for time-dependent traffic," in *Proceedings of GLOBECOM*, pp. 1–5, Nov. 2006.
- [13] S. Koo, G. Sahin, and S. Subramaniam, "Dynamic LSP provisioning in overlay, augmented, and peer architectures for IP/MPLS over WDM networks," in *Proceedings of IEEE INFOCOM*, pp. 514–523, Mar. 2004.
- [14] J. Li, G. Mohan, E. C. Tien, and K. C. Chua, "Dynamic routing with inaccurate link state information in integrated IP over WDM networks," *Computer Networks*, vol. 46, pp. 829–851, Dec. 2004.
- [15] T. Ye, Q. Zeng, Y. Su, L. Leng, W. Wei, Z. Zhang, W. Guo, and Y. Jin, "On-line integrated routing in dynamic multifiber IP/WDM networks," *IEEE Journal on Selected Areas in Communications*, vol. 22, pp. 1681–1691, Nov. 2004.
- [16] J. Comellas, R. Martinez, J. Prat, V. Sales, and G. Junyent, "Integrated IP/WDM routing in GMPLS-based optical networks," *IEEE Network Magazine*, vol. 17, pp. 22–27, Mar./Apr. 2003.
- [17] J. Katou, S. Arakawa, and M. Murata, "A design method for logical topologies with stable packet routing in IP over WDM networks," *IEICE Transactions on Communications*, vol. E86-B, pp. 2350–2357, Aug. 2003.
- [18] K. H. Liu, *IP over WDM*. NJ, USA: John Wiley & Sons, Nov. 2002.
- [19] M. Kodialam and T. V. Lakshman, "Integrated dynamic IP and wavelength routing in IP over WDM networks," in *Proceedings of IEEE INFOCOM*, pp. 358–366, Apr. 2001.

- [20] S. Arakawa, M. Murata, and H. Miyahara, "Functional partitioning for multi-layer survivability in IP over WDM networks," *IEICE Transactions on Communications*, vol. E83-B, pp. 2224–2233, Oct. 2000.
- [21] N. Ghani, S. Dixit, and T.-S. Wang, "On IP-over-WDM integration," *IEEE Communications Magazine*, vol. 38, pp. 72–84, Mar. 2000.
- [22] D. G. Andersen, H. Balakrishnan, M. F. Kaashoek, and R. Morris, "Resilient overlay networks," in *Proceedings of SOSP*, pp. 131–145, Oct. 2001.
- [23] S. Savage, T. Anderson, A. Aggarwal, D. Becker, N. Cardwell, A. Collins, E. Hoffman, J. Snell, A. Vahdat, G. Voelker, and J. Zahorjan, "Detour: a case for informed internet routing and transport," *IEEE Micro*, vol. 19, pp. 50–59, Jan. 1999.
- [24] R. Keralapura, N. Taft, C.-N. Chuah, and G. Iannaccone, "Can ISPs take the heat from overlay networks?," in *Proceedings of ACM Workshop on Hot Topics in Networks (HotNets-III)*, Nov. 2004.
- [25] Y. Liu, H. Zhang, W. Gong, and D. Towsley, "On the interaction between overlay routing and underlay routing," in *Proceedings of IEEE INFOCOM*, pp. 2543–2553, Mar. 2005.
- [26] S. Seetharaman and M. Ammar, "On the interaction between dynamic routing in the native and overlay layers," in *Proceedings of IEEE INFOCOM*, pp. 1–12, Apr. 2006.
- [27] T. Roughgarden and E. Tardos, "How bad is selfish routing?," *Journal of the ACM*, vol. 49, pp. 236–259, Mar. 2002.
- [28] L. Qiu, Y. R. Yang, Y. Zhang, and S. Shenker, "On selfish routing in internet-like environments," in *Proceedings of ACM SIGCOMM*, pp. 151–162, Aug. 2003.
- [29] R. Keralapura, C.-N. Chuah, N. Taft, and G. Iannaccone, "Race conditions in coexisting overlay networks," *IEEE/ACM Transactions on Networking*, vol. 16, pp. 1–14, Feb. 2008.
- [30] M. Seshadri and R. H. Katz, "Dynamics of simultaneous overlay network routing," Tech. Rep. UCB/CSD-03-1291, EECS Department, University of California, Berkeley, Nov. 2003.
- [31] W. Jiang, D.-M. Chiu, and J. C. S. Lui, "On the interaction of multiple overlay routing," *Performance Evaluation*, vol. 62, pp. 229–246, Oct. 2005.

- [32] F. Ricciato, S. Salsano, A. Belmonte, and M. Listanti, "Off-line configuration of a MPLS over WDM network under time-varying offered traffic," in *Proceedings of IEEE INFOCOM*, vol. 1, pp. 57–65, June 2002.
- [33] B. Ramamurthy and A. Ramakrishnan, "Virtual topology reconfiguration of wavelength-routed optical WDM networks," in *Proceedings of GLOBECOM*, vol. 2, pp. 1269–1275, Nov. 2000.
- [34] A. Gençata and B. Mukherjee, "Virtual-topology adaptation for WDM mesh networks under dynamic traffic," *IEEE/ACM Transactions on Networking*, vol. 11, pp. 236–247, Apr. 2003.
- [35] S. F. Gieselmann, N. K. Singhal, and B. Mukherjee, "Minimum-cost virtual-topology adaptation for optical WDM mesh networks," in *Proceedings of IEEE ICC*, vol. 3, pp. 1787–1791, June 2005.
- [36] N. Sreenath and C. S. R. Murthy, "On-line reconfiguration of virtual topologies in wavelength-routed WDM networks," *Journal of High Speed Networks*, vol. 12, pp. 141–169, July 2003.
- [37] I. Alfouzan and A. Jayasumana, "Dynamic reconfiguration of wavelength-routed WDM networks," in *Proceedings of IEEE LCN*, pp. 477–485, Nov. 2001.
- [38] N. Sreenath, B. Gurucharan, G. Mohan, and C. S. R. Murthy, "A two-stage approach for virtual topology reconfiguration of WDM optical networks," *Optical Networks Magazine*, vol. 2, pp. 58–71, May/June 2001.
- [39] A. Lakhina, K. Papagiannaki, M. Crovella, C. Diot, E. D. Kolaczyk, and N. Taft, "Structural analysis of network traffic flows," in *Proceedings of ACM Sigmetrics*, pp. 61–72, June 2004.
- [40] Y. Koizumi, S. Arakawa, and M. Murata, "An integrated routing mechanism for cross-layer traffic engineering in IP over WDM networks," *IEICE Transactions on Communications*, vol. E90-B, pp. 1142–1151, May 2007.
- [41] Y. Koizumi, S. Arakawa, and M. Murata, "On the integration of IP routing and wavelength routing in IP over WDM networks," in *Proceedings of SPIE Asia-Pacific Optical Communications (APOC 2005) Network Architectures, Management, and Applications III*, vol. 6022, 602205, (Shanghai, China), Nov. 2005.

- [42] Y. Koizumi, S. Arakawa, and M. Murata, "On the integration of IP routing and wavelength routing in IP over WDM networks," *Technical Reports of IEICE (PN2005-24)*, vol. 105, pp. 25–30, Aug. 2005. (*in Japanese*).
- [43] N. Tsutsui, Y. Koizumi, S. Arakawa, and M. Murata, "Implementation and evaluation of integrated routing mechanism in IP over WDM networks," *Technical Reports of IEICE (PN2007-80)*, vol. 107, pp. 35–40, Mar. 2008. (*in Japanese*).
- [44] Y. Koizumi, T. Miyamura, S. Arakawa, E. Oki, K. Shiimoto, and M. Murata, "Stability of virtual network topology control for overlay routing services," *OSA Journal of Optical Networking*, vol. 7, pp. 704–719, July 2008.
- [45] Y. Koizumi, T. Miyamura, S. Arakawa, E. Oki, K. Shiimoto, and M. Murata, "On the stability of virtual network topology control for overlay routing services," in *Proceedings of IEEE Fourth International Conference on Broadband Communications, Networks, and Systems (IEEE Broadnets 2007)*, (Raleigh, NC, USA), pp. 810–819, Sept. 2007.
- [46] Y. Koizumi, T. Miyamura, S. Arakawa, E. Oki, K. Shiimoto, and M. Murata, "On the stability of virtual network topology control for overlay routing services," *Technical Reports of IEICE (PN2007-27)*, vol. 107, pp. 33–38, Oct. 2007.
- [47] Y. Koizumi, T. Miyamura, S. Arakawa, E. Oki, K. Shiimoto, and M. Murata, "Application of attractor selection to adaptive virtual network topology control," in *Proceedings of ACM 3rd International Conference on Bio-Inspired Models of Network, Information, and Computing Systems (BIONETICS 2008)*, (Hyogo, Japan), Nov. 2008.
- [48] Y. Koizumi, T. Miyamura, S. Arakawa, E. Oki, K. Shiimoto, and M. Murata, "Adaptive virtual network topology control based on attractor selection," *Technical Reports of IEICE (PN2008-14)*, vol. 108, pp. 1–6, Aug. 2008.
- [49] Y. Koizumi, T. Miyamura, S. Arakawa, E. Oki, K. Shiimoto, and M. Murata, "Robust virtual network topology control based on attractor selection," submitted to *13th Conference on Optical Network Design and Modeling (ONDM 2009)*, Feb. 2009.

- [50] Y. Koizumi, T. Miyamura, S. Arakawa, E. Oki, K. Shiimoto, and M. Murata, "Adaptive virtual network topology control based on attractor selection," re-submitted to *IEEE/OSA Journal of Lightwave Technology*, 2008.
- [51] K. Kaneko, *Life: An introduction to complex systems biology*. Understanding Complex Systems, New York: Springer, 2006.
- [52] A. Kashiwagi, I. Urabe, K. Kaneko, and T. Yomo, "Adaptive response of a gene network to environmental changes by fitness-induced attractor selection," *PLoS ONE*, vol. 1, p. e49, Dec. 2006.
- [53] C. Furusawa and K. Kaneko, "A generic mechanism for adaptive growth rate regulation," *PLoS Computational Biology*, vol. 4, p. e3, Jan. 2008.
- [54] K. Leibnitz, N. Wakamiya, and M. Murata, "Biologically-inspired self-adaptive multi-path routing in overlay networks," *Communications of the ACM, Special Issue on Self-Managed Systems and Services*, vol. 49, pp. 62–67, Mar. 2006.
- [55] E. Mannie, "Generalized multi-protocol label switching (GMPLS) architecture." RFC 3945 (Proposed Standard), Oct. 2004.
- [56] "OPNET." <http://www.opnet.com/>.
- [57] "The network simulator - ns-2." <http://www.isi.edu/nsnam/ns/>.
- [58] C. Kiddle, R. Simmonds, C. L. Williamson, and B. Unger, "Hybrid packet/fluid flow network simulation," in *Proceedings of the 17th Workshop on Parallel and Distributed Simulation*, pp. 143–152, June 2003.
- [59] F. Baccelli and D. Hong, "Flow level simulation of large IP networks," in *Proceedings of IEEE INFOCOM*, pp. 1911–1921, Mar. 2003.
- [60] D. Bertsekas and R. Gallager, *Data Networks*. Englewood Cliffs, New Jersey: Prentice Hall, Inc., Englewood Cliffs, 1987.
- [61] E. Leonardi, M. Mellia, and M. A. Marsan, "Algorithms for the logical topology design in WDM all-optical networks," *Optical Networks Magazin*, vol. 1, pp. 35–46, Jan. 2000.

- [62] R. Gao, C. Dovrolis, and E. W. Zegura, “Avoiding oscillations due to intelligent route control systems,” in *Proceedings of IEEE INFOCOM*, Apr. 2006.
- [63] A. Nucci, A. Sridharan, and N. Taft, “The problem of synthetically generating IP traffic matrices: initial recommendations,” *Computer Communication Review*, vol. 35, no. 3, pp. 19–32, 2005.
- [64] Y. Zhang, M. Roughan, N. Duffield, and A. Greenberg, “Fast accurate computation of large-scale IP traffic matrices from link loads,” in *Proceedings of ACM Sigmetrics*, vol. 31, pp. 206–217, June 2003.